

Abiological Catalysis by Artificial Heme Proteins Containing Noble Metals in Place of Iron

Contents

Materials and Methods	pages 2-18
Supplementary Figures 1 - 29	pages 19-33
Supplementary Tables 1 - 16	pages 34-79
NMR Spectra	pages 80-102
References	page 101

I. Protein Expression, Purification, and Characterization

a. General Methods

Unless otherwise noted, the chemicals, salts, and solvents used were reagent grade and used as received from commercial suppliers without further purification. All expression media and buffers were prepared using ddH₂O (MilliQ A10 Advantage purification system, Millipore). All expression media were sterilized using either an autoclave (45 min, 121°C) or a sterile syringe filter (0.22 µm). To maintain sterile conditions, sterile materials and *E. coli* cells were manipulated near a lit Bunsen burner. TEV protease was obtained from the UC Berkeley Macrolab.

b. Cloning

A double mutant of the gene encoding sperm whale myoglobin (Y103C, S108C) was purchased from GenScript with codon optimization for *E. coli* (Table 2). The gene was cloned into the expression vectors 2-BT (6xHis-TEV-ORF; AddGene #29666) and 2OT (6xHis-TEV-mOCR-ORF; AddGene 29710) at the QB3 Macrolab at UC Berkeley.

c. Media Preparation

Preparation of optimized minimal expression media: Salts (15 g Na₂HPO₄, 7.5 g K₂HPO₄, 0.3 g NaH₂PO₄, 0.3 g KH₂PO₄, 1.5 g NaCl, 5 g NH₄Cl) were dissolved in 2 L ddH₂O and autoclaved to give a media with pH ~8.0 - 8.2. Solutions of glucose (20%), casamino acids (BD Company, low Fe, 20%), and MgSO₄ (1 M), were autoclaved separately. Solutions of ampicillin (100 mg/ mL) and CaCl₂ (1 M) were sterilized by syringe filter. The following amounts of the listed solutions were added per 2 L of sterile salt solution: 40 mL glucose, 20 mL casamino acids, 4 mL MgSO₄, 100 µL CaCl₂, 2 mL ampicillin. Stock solutions were stored for several weeks; prepared media was stored for less than 1 day. Minimal media plates were prepared from the same media with the addition of 17 g agar/L media. In this case, agar was autoclaved in 1 L ddH₂O, and salts were autoclaved separately as a 20X solution, after which they were added to the agar solution.

Preparation of rich expression media: LB media (10 g tryptone, 5 g yeast, 10 g NaCl, 1 L ddH₂O) was autoclaved and supplemented with MgSO₄ (2 mL, 1 M), glucose (20 mL, 20%), ampicillin (1 mL, 100 mg/mL), and M9 salts (50 mL, 20X). Minimal media plates were prepared from the same media with the addition of 17 g agar/L media.

d. Mutagenesis

Site-directed mutagenesis was performed using the QuickChange Lightning mutagenesis kit (Agilent); requisite double stranded DNA primers were designed according to the Agilent Primer Design Program and purchased from Integrated DNA Technology. PCR reactions were performed according to the manufacturer's directions. PCR reactions contained: 5 µL reaction buffer, 34 µL ddH₂O, 1.5 µL QuickSolution, 1 µL plasmids (50 ng/µL), 1.25 µL sense primer (100 ng/µL), 1.25 µL antisense primer (100 ng/ µL), 5 µL dNTPs (2 mM/base), and 1 µL polymerase.

PCR Program: Phase 1 (1 cycle): 95 °C, 1.5 min; Phase 2 (18 cycles): 95 °C, 20 sec, 60 °C, 10 sec, 68 °C, 3 min; Phase 3 (1 cycle): 68 °C, 3 min; Phase 4 (storage): 4 °C

Plasmid Preparation for Phase 1 of Directed Evolution: The general PCR method was used with degenerate primers encoding H93A, G and H64A, V, L, I.

Preparation of the Combinatorial Library of Mutants of Positions 43/68 (Phase 2): The general PCR method was used with degenerate primers encoding F43Y, W, L, I, T, H, V and V68A, G, F, Y, S, T.

Preparation of the Combinatorial Library of Mutants of Positions 32/33/97/99 (Phase 3): The general PCR method was used with degenerate primers encoding L32V, I, F, H, W, Y, F33V, L, I, H, W, Y, H97V, L, I, F, W, Y, and I99V, L, F, H, W, Y.

DNA Isolation and Storage: Following the completion of the above set of PCR procedures, 1.5 μ L DPN 1 was added to each reaction, and the reactions were further incubated (3 h, 37°C). The crude PCR mixture was used to transform XL-10 Gold Ultracompetent cells (45 μ L cells, 2 μ L PCR reactions). The mixture was incubated on ice (30 min), heat shocked (30 s, 42 °C), recovered with SOC media (1 h, 37 °C, 275 rpm), and plated on LB plates. Plates were grown (18 h, 37 °C), and individual colonies were used to inoculate 1 mL rich media cultures, which were grown in 96-well plates (13 h, 37 °C, 300 rpm). DNA was isolated from the 96-well cultures using magnetic bead technology at the UC Berkeley DNA Sequencing Facility. Alternatively, individual colonies were used to inoculate 4 mL rich media cultures and grown overnight (13 h, 37 °C, 300 rpm), and the plasmids were purified using a Qiagen DNA Miniprep kit according to the manufacturer's instructions.

e. Protein Expression

Optimized Expression of Apo Myoglobin: BL21 Star competent *E. coli* cells (50 μ L, QB3 Macrolab, UC Berkeley) were thawed on ice, transferred to 14 mL Falcon tubes, and transformed with the desired plasmid solution (2 μ L, 50-250 ng/ μ L). The cells were incubated on ice (30 min), heat shocked (20 sec, 42°C), re-cooled on ice (2 min), and recovered with SOC media (37 °C, 1 h, 250 rpm). Aliquots of the cultures were diluted (0.02X), plated on minimal media plates (expression media supplemented with 17 g agar/L), and incubated (20 h, 37 °C) to produce approximately 10-100 colonies per plate. Single colonies were used to inoculate starter cultures (3 mL, expression media), which were grown (6-8 hours, 37°C, 275 rpm) and used to inoculate 100 mL overnight cultures (minimal media, 37° C, 275 rpm). Each overnight culture was used to inoculate 750 mL of minimal media, which was further grown (9 h, 37°C, 275 rpm). Expression was induced with IPTG (800 μ L, 1M), and the cultures were further grown (15 h, 20° C, 275 rpm). Cells were harvested by centrifugation (5000 rpm, 15 min, 4° C), and the pellets were resuspended in 20 mL Ni-NTA lysis buffer (50 mM NaPi, 250 mM NaCl, 10 mM Imidazole, pH = 8.0) and stored at -80° C until purification.

Expression of Fe Myoglobin: Fe-myoglobin was expressed following a procedure modified from the literature¹. BL21 Star competent *E. coli* cells (50 μ L, QB3 Macrolab, UC Berkeley) were thawed on ice, transferred to 14 mL Falcon tubes, and transformed with the desired plasmid solution (2 μ L, 50-250 ng/ μ L). The cells were incubated on ice (30 min), heat shocked (20 sec, 42°C), re-cooled on ice (2 min), and recovered with SOC media (37°C, 1 h, 250 rpm). Aliquots of the cultures were diluted (0.02X), plated on minimal media (expression media supplemented with 17g agar/L), and incubated (20 h, 37°C) to produce approximately 10-100 colonies per plate. Single colonies were used to inoculate starter cultures (3 mL, expression media), which were grown (6-8 hours, 37°C,

275 rpm) and used to inoculate 100 mL overnight cultures (minimal media, 37° C, 275 rpm). A 5 mL portion of the overnight culture was used to inoculate 750 mL of LB media supplemented with 1X M9 salts, MgSO₄ (1.5 mL, 1M) and glucose (15 mL, 20% glucose), which was further grown (9 h, 37°C, 275 rpm). Expression was induced with IPTG (800 µL, 1M) and ALA (0.8 mL, 0.3 M) was added, and the cultures were further grown (15 h, 25° C, 250 rpm). Cells were harvested by centrifugation (5000 rpm, 15 min, 4° C), and the pellets were resuspended in 20 mL Ni-NTA lysis buffer (50 mM NaPi, 250 mM NaCl, 10 mM Imidazole, pH = 8.0) and stored at -80° C until purification.

Protein Purification: Cell suspensions were thawed in a room temperature ice bath, decanted to 50 mL glass beakers, and lysed on ice by sonication (3x30 sec on, 2x2 min off, 60% power). Crude lysates were transferred to 50 mL Falcon tubes, treated with triton X (100 µL, 2% in H₂O), and incubated on an end-over-end shaker (30 min, rt, 15 rpm). Cell debris was removed by centrifugation (10 000 rpm, 60 min, 4° C), and Ni-NTA (5 mL, 50% suspension per 850 mL cell culture) was added. The lysates were briefly incubated with Ni-NTA (30 min, 4° C, 20 rpm) and poured into glass frits (coarse, 50 mL). The resin was washed with Ni-NTA lysis buffer (3 x 35 mL), and the wash fractions were monitored using Bradford assay dye. The desired protein was eluted with 18 mL Ni-NTA elution buffer (50 mM NaPi, 250 mM NaCl, 250 mM Imidazole, pH = 8.0), dialyzed against Tris buffer (10 mM, pH = 8.0, 12 h, 4° C), concentrated to the desired concentration using a spin concentrator, and metallated within several hours. Apo protein was not stored for more than 8 hours.

Metallation of the Apo-Protein (General Method): Stock solutions of metal cofactors in DMF were added to solutions of apo protein (0.3-0.6 mM) at room temperature in the desired stoichiometry with a final DMF concentration of 2%. The proteins were briefly incubated at room temperature (5 minutes), and DMF was removed by using a NAP column, according to manufactures instructions.

Protein Storage: Glycerol was added to a solution of the protein (3:1 v:v protein solution: 50% glycerol), the solution was divided into 1.5 mL eppendorf tubes (0.5 mL per aliquot), and the tubes were flash frozen in liquid nitrogen and stored at -80 ° C until further use. Frozen aliquots of the protein were thawed in a room-temperature water bath.

f. Protein Characterization

Gel Electrophoresis: Protein purity was analyzed by sodium dodecyl sulfate-polyacrylamide (SDS-PAGE) gel electrophoresis using precast gels (polyacrylamide, 10-20% linear gradient, Biorad).

Mass Spectrometry: Apo-proteins were analyzed with an Agilent 1200 series liquid chromatograph connected in-line with an Agilent 6224 time-of-flight (TOF) LC/MS system using a Turbospray ion source. Metallated proteins were analyzed by native nanoelectrospray ionization mass spectrometry (nanoESI-MS) using a Waters Q-ToF Premier quadrupole time-of-flight mass spectrometer equipped with a nanoESI source (Milford, MA). Mass spectra were acquired in the positive ion mode and processed using MassLynx software (version 4.1, Waters). The instrument is located in the QB3/Chemistry Mass Spectrometry Facility at UC Berkeley.

UV-Vis Spectroscopy: Protein concentration was determined using a NanoDrop 2000 UV-Vis Spectrophotometer (Thermo Scientific). UV-Vis spectra of proteins were measured using a SpectraMax microplate reader (Molecular Devices) configured in the 96-well plate format.

CD Spectroscopy: CD spectra were acquired on a JASCO J-815 instrument in 3 mL quartz cuvettes using 2 mL of the appropriate protein solution (0.03 mg/ mL).

II. Organic Synthesis and Characterization

a. General methods and materials

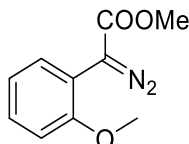
Unless stated otherwise, all reactions and manipulations were conducted on the laboratory bench in air with reagent grade solvents. Reactions under inert gas atmosphere were carried out in the oven dried glassware in a nitrogen-filled glovebox or by standard Schlenk techniques under nitrogen.

NMR spectra were acquired on 400 MHz, 500 MHz, 600 MHz, or 900 MHz Bruker instruments at the University of California, Berkeley. NMR spectra were processed with MestReNova 9.0 (Mestrelab Research SL). Chemical shifts are reported in ppm and referenced to residual solvent peaks². Coupling constants are reported in hertz. GC analyses were obtained on an Agilent 6890 GC equipped with either, an HP-5 column (25 m x 0.20 mm ID x 0.33 m film) for achiral analysis or Cyclosil-B column (30m x 0.25mm x 0.25 um film) for chiral analysis, and an FID detector. GC yields were calculated using dodecane as the internal standard and not corrected for response factors of minor isomers. High-resolution mass spectra and elemental analysis were obtained via the Micro-Mass/Analytical Facility operated by the College of Chemistry, University of California, Berkeley.

Unless noted otherwise, all reagents and solvents were purchased from commercial suppliers and used without further purification. If required, dichloromethane (DCM) and tetrahydrofuran (THF) were degassed by purging with argon for 15 minutes and dried with a solvent purification system containing a one-meter column of activated alumina; dried and degassed acetonitrile, 1,2-xylene, toluene, N,N-dimethylformamide (DMF), ethanol and methanol were purchased from commercial suppliers and used as received.

b. Substrates

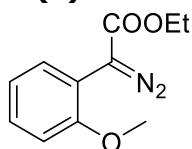
Methyl (2-methoxyphenyl)diazoacetate (**1**):



To a stirred solution of methyl (2-methoxyphenyl)acetate (3.2 ml, 20 mmol) and 4-acetamidobenzenesulfonyl azide (p-ABSA, 7.2 g, 30 mmol) in acetonitrile (40 ml) at 0 °C, 1,8-diazabicycloundec-7-ene (DBU, 4.8 ml, 32 mmol) was added dropwise. The cooling bath was removed, and the reaction was allowed to continue stirring overnight. The reaction mixture was diluted with dichloromethane (~60 ml), washed with water (2 x ~50 ml), dried over MgSO₄. After filtration, the volatile material from the filtrate was evaporated under reduced pressure. The crude product was purified by column chromatography on silica gel, with a mixture of hexanes and ethyl acetate (100:0 → 95:5 gradient) as the eluent. Fractions of the pure product were combined, and

the solvent evaporated, yielding 3.9 g (95%) of product. The NMR data match those of the reported molecule ³.

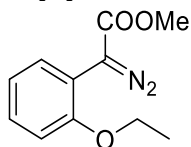
Ethyl (2-methoxyphenyl)diazoacetate (6):



In a closed vial, a solution of (2-methoxyphenyl)acetic acid (3.3 g, 20 mmol) in ethanol (20 ml), containing several drops of sulfuric acid, was stirred overnight at 80 °C. The volatile materials were evaporated under vacuum. The residue was dissolved in ethyl acetate (~40 ml), washed with NaHCO₃ sat. (40 ml) and water (40 ml), and dried over MgSO₄. After filtration, the volatile material from the filtrate was evaporated under reduced pressure. The resulting crude product was used in the next step without further purification.

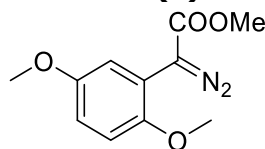
To a stirred solution of ethyl (2-methoxyphenyl)acetate and 4-acetamidobenzenesulfonyl azide (p-ABSA, 7.2 g, 30 mmol) in acetonitrile (40 ml) at 0 °C, 1,8-diazabicycloundec-7-ene (DBU, 4.8 ml, 32 mmol) was added dropwise. The cooling bath was removed, and the reaction was allowed to continue stirring overnight. The reaction mixture was diluted with dichloromethane (~60 ml), washed with water (2 x ~50 ml), and dried over MgSO₄. After filtration, the volatile material from the filtrate was evaporated under reduced pressure. The crude product was purified by column chromatography on silica gel, with a mixture of hexanes and ethyl acetate (100:0 → 95:5 gradient) as the eluent. Fractions of the pure product were combined, and the solvent evaporated, yielding 2.15 g (49%) of product. The NMR data match those of the reported molecule ⁴.

Methyl (2-ethoxyphenyl)diazoacetate (7):



To a solution of 2-ethoxyphenylacetic acid (3.8 g, 20 mmol) in toluene (40 ml) and methanol (20 ml), a solution of trimethylsilyldiazomethane in diethyl ether (15 ml, 2 M, 30 mmol) was added dropwise while stirring, and stirring was continued for 2 h. Upon evaporation of the volatile materials under vacuum, the product was obtained in quantitative yield without the need for further purification.

To a stirred solution of methyl 2-ethoxyphenylacetate (20 mmol) and 4-acetamidobenzenesulfonyl azide (p-ABSA, 7.2 g, 30 mmol) in acetonitrile (40 ml) at 0 °C, 1,8-diazabicycloundec-7-ene (DBU, 4.8 ml, 32 mmol) was added dropwise. The cooling bath was removed, and the reaction was allowed to continue stirring overnight. The reaction mixture was diluted with dichloromethane (~60 ml), washed with water (2 x ~50 ml), dried over MgSO₄ and evaporated. The crude product was purified by column chromatography on silica gel, with a mixture of hexanes and ethyl acetate (100:0 → 95:5 gradient) as the eluent. Fractions of the pure product were combined, and the solvent evaporated, yielding 2.6 g (59%) of product. The NMR data match those of the reported molecule ⁴.

Methyl (2,5-dimethoxyphenyl)diazoacetate (8):

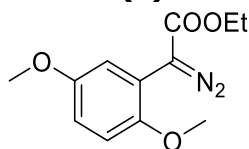
In a closed vial, a solution of (2,5-dimethoxyphenyl)acetic acid (3.8 g, 20 mmol) in methanol (20 ml) containing several drops of sulfuric acid, was stirred overnight at 80 °C. The volatile materials were evaporated under vacuum. The residue was dissolved in ethyl acetate (~40 ml), washed with NaHCO₃ sat. (40 ml) and water (40 ml), dried over MgSO₄ and evaporated. The crude product was used in the next step without further purification.

To a stirred solution of methyl (2,5-dimethoxyphenyl)acetate and 4-acetamidobenzenesulfonyl azide (p-ABSA, 7.2 g, 30 mmol) in acetonitrile (40 ml) at 0 °C, 1,8-diazabicycloundec-7-ene (DBU, 4.8 ml, 32 mmol) was added dropwise. The cooling bath was removed, and the reaction was allowed to continue stirring for 48 h (the reaction progress was followed by TLC). The reaction mixture was diluted with dichloromethane (~60 ml), washed with water (2 x ~50 ml), and dried over MgSO₄. After filtration, the volatile material from the filtrate was evaporated under reduced pressure. The crude product was purified by column chromatography on silica gel, with a mixture of hexanes and ethyl acetate (100:0 → 95:5 gradient) as the eluent. Fractions of the pure product were combined, and the solvent evaporated, yielding 4.1 g (87%) of product.

¹H NMR (900 MHz, CDCl₃): d = 7.14 (d, J = 3.0 Hz, 1H), 6.78 (d, J = 8.9 Hz, 1H), 6.75 (dd, J = 8.9 Hz, J = 3.0 Hz, 1H), 3.80 (s, 3H), 3.76 (s, 3H), 3.74 (s, 3H);

¹³C NMR (225 MHz, CDCl₃): d = 166.7, 154.1, 149.8, 115.2, 114.7, 114.0, 112.3, 56.4, 56.0, 52.2 (C=N₂ signal missing, as observed before for related molecules (4));

HR MS (EI): calcd. for C₁₁H₁₂N₂O₄ [M]⁺: 236.0797, found: 236.0801.

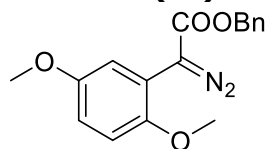
Ethyl (2,5-dimethoxyphenyl)diazoacetate (9):

To a stirred solution of ethyl (2,5-dimethoxyphenyl)acetate (4.3 g, 19.2 mmol) and 4-acetamidobenzenesulfonyl azide (p-ABSA, 7.2 g, 30 mmol) in acetonitrile (40 ml) at 0 °C, 1,8-diazabicycloundec-7-ene (DBU, 4.8 ml, 32 mmol) was added dropwise. The cooling bath was removed, and the reaction was allowed to continue stirring for 48 h (the reaction progress was followed by TLC). The reaction mixture was diluted with dichloromethane (~60 ml), washed with water (2 x ~50 ml), and dried over MgSO₄. After filtration, the volatile material from the filtrate was evaporated under reduced pressure. The crude product was purified by column chromatography on silica gel, with a mixture of hexanes and ethyl acetate (100:0 → 95:5 gradient) as the eluent. Fractions of the pure product were combined, and the solvent evaporated, yielding 3.9 g (81%) of product.

¹H NMR (900 MHz, CDCl₃): d = 7.16 (d, J = 3.0 Hz, 1H), 6.78 (d, J = 9.0 Hz, 1H), 6.74 (dd, J = 9.0 Hz, J = 3.0 Hz, 1H), 4.27 (q, J = 7.2 Hz, 2H, OCH₂), 3.77 (s, 3H), 3.74 (s, 3H), 1.28 (t, J = 7.2 Hz, 3H, CH₂CH₃);

¹³C NMR (225 MHz, CDCl₃): d = 166.3, 154.1, 149.8, 115.0, 114.9, 114.0, 112.3, 61.1, 56.4, 56.0, 14.8 (C=N₂ signal missing, as observed before for related molecules (4));

HR MS (EI): calcd. for C₁₂H₁₄N₂O₄ [M]⁺: 250.0954, found: 250.0957.

Benzyl (2,5-dimethoxyphenyl)diazoacetate (10):

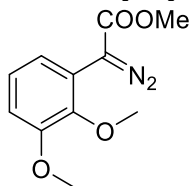
To a solution of (2,5-dimethoxyphenyl)acetic acid (0.95 g, 5 mmol) in dichloromethane (20 ml) thionyl chloride (2 ml) was added dropwise and the reaction mixture was stirred under reflux for 1 h. The volatile materials were evaporated under vacuum. The residue was dissolved in dichloromethane (40 ml), benzyl alcohol (1 ml) was added, followed by slow addition of trimethylamine (1 ml), and the reaction mixture was stirred for 48 h (the reaction progress was followed by TLC). The reaction mixture was washed with HCl (0.5 M, 40 ml) and water (40 ml), dried over MgSO₄ and evaporated. The crude product was purified by column chromatography on silica gel, with a mixture of hexanes and ethyl acetate (100:0 → 95:5 gradient) as the eluent. Fractions of the product were combined, and the solvent evaporated, yielding 1.43 g (quantitative) of benzyl (2,5-dimethoxyphenyl)acetate.

To a stirred solution of benzyl (2,5-dimethoxyphenyl)acetate (1.43 g, 5 mmol) and 4-acetamidobenzenesulfonyl azide (p-ABSA, 1.8 g, 7.5 mmol) in acetonitrile (20 ml) at 0 °C, 1,8-diazabicycloundec-7-ene (DBU, 1.2 ml, 8 mmol) was added dropwise. The cooling bath was removed, and the reaction was allowed to continue stirring overnight. The reaction mixture was diluted with dichloromethane (~50 ml), washed with water (2 x ~50 ml), dried over MgSO₄ and evaporated. The crude product was purified by column chromatography on silica gel, with a mixture of hexanes and ethyl acetate (100:0 → 80:20 gradient) as the eluent. Fractions of the pure product were combined, and the solvent evaporated, yielding 0.94 g (60%) of product.

¹H NMR (900 MHz, CDCl₃): δ = 7.37–7.32 (m, 4H), 7.31–7.28 (m, 1H), 7.16 (bs, 1H), 6.78 (d, J = 9.0 Hz, 1H), 6.75 (dd, J = 9.0 Hz, J = 3.0 Hz, 1H), 5.26 (s, 2H), 3.76 (s, 3H), 3.71 (s, 3H);

¹³C NMR (225 MHz, CDCl₃): δ = 166.1, 154.1, 149.8, 136.3, 128.8, 128.4, 115.0, 114.6, 114.2, 112.3, 66.6, 56.4, 56.0 (C=N₂ signal missing, as observed before for related molecules (4));

HR MS (EI): calcd. for C₁₇H₁₆N₂O₄ [M]⁺: 312.1110, found: 312.1111.

Methyl (2,3-dimethoxyphenyl)diazoacetate (11):

In a closed vial, a solution of (2,3-dimethoxyphenyl)acetic acid (1.5 g, 7.9 mmol) in methanol (20 ml) containing several drops of sulfuric acid, was stirred overnight at 80 °C. The volatile materials were evaporated under vacuum. The residue was dissolved in ethyl acetate (~40 ml), washed with NaHCO₃ sat. (40 ml) and water (40 ml), dried over MgSO₄ and evaporated. The crude product was used in the next step without further purification.

To a stirred solution of methyl (2,3-dimethoxyphenyl)acetate and 4-acetamidobenzenesulfonyl azide (p-ABSA, 2.9 g, 12 mmol) in acetonitrile (30 ml) at 0 °C, 1,8-diazabicycloundec-7-ene (DBU, 1.9 ml, 13 mmol) was added dropwise. The cooling bath was removed, and the reaction was allowed to continue stirring for 48 h (the reaction progress was followed by TLC). The reaction mixture was diluted with dichloromethane (~50 ml), washed with water (2 x ~50 ml), and dried over MgSO₄. After filtration, the volatile material from the filtrate was evaporated under reduced pressure. The crude product was purified by column chromatography on silica gel, with a mixture

of hexanes and ethyl acetate (100:0 → 80:20 gradient) as the eluent. Fractions of the pure product were combined, and the solvent evaporated, yielding 1.55 g (83%) of product.

¹H NMR (900 MHz, CDCl₃): d = 7.19 (d, J = 7.9 Hz, 1H), 7.05 (dd, J = 8.1 Hz, J = 8.1 Hz, 1H), 6.79 (d, J = 8.2 Hz, 1H), 3.83 (s, 3H), 3.81 (s, 3H), 3.79 (s, 3H);

¹³C NMR (225 MHz, CDCl₃): d = 166.6, 152.9, 145.3, 124.5, 121.3, 120.0, 111.4, 60.8, 56.0, 52.2 (C=N₂ signal missing, as observed before for related molecules (4));

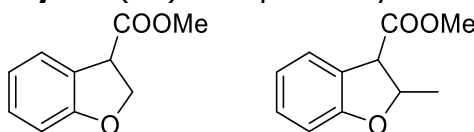
HR MS (EI): calcd. for C₁₁H₁₂N₂O₄ [M]⁺: 236.0797, found: 236.0800.

c. Authentic Products

General procedure for synthesis of dihydrobenzofurans

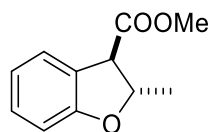
To 5 ml of a solution of a derivative of methyl (2-methoxyphenyl)diazoacetate (~50 mM) in toluene 60-300 ul of a solution of Ir(Me)-PIX (8 mM, 0.2-1 mol%) in DMF was added, and the reaction mixture was vigorously stirred. The reaction progress was monitored by TLC. Upon completion, the volatile materials were removed, and the residue was purified by column chromatography on silica gel, with a mixture of hexanes and ethyl acetate (100:0 → 80:20 gradient) as eluent. Fractions of the pure product were combined, and the solvent evaporated, yielding 20-90% of desired product.

Methyl 2,3-dihydrobenzofuran-3-carboxylate (2) and **methyl 2-methyl-2,3-dihydrobenzofuran-3-carboxylate (P7)** were previously characterized^{3,5}.



The absolute configurations of enantiomers of **2** were assigned on the basis of a previous report.⁵ In the previous report, the samples were analyzed by HPLC using the following method: Chiralcel OD-H (Daicel), flow rate= 0.5 mL/min; solvent= n-hexane/2-PrOH (98:2)); using this method, the R enantiomer eluted prior to the S enantiomer. We analyzed a racemic sample of **2** using the same HPLC column and method; the first enantiomer – assigned (*R*)-**2** eluted at 17.3 minutes and the second enantiomer – assigned as (*S*)-**2** eluted at 20.9 minutes. We then analyzed an enantioenriched sample and determined that the major enantiomer present was enantiomer (*S*)-**2**, eluting at 20.9 minutes. The same enantioenriched sample was then analyzed by chiral gc by the method reported in Table 15. In this case, the major enantiomer (identified as (*S*)-**2** by HPLC) eluted at 14.0 minutes, while the minor enantiomer eluted at 13.8 minutes. Further samples were characterized by chiral GC according to these assigned retention times: $t_{(R)-2} = 13.8$ min and $t_{(S)-2} = 14.0$ min.

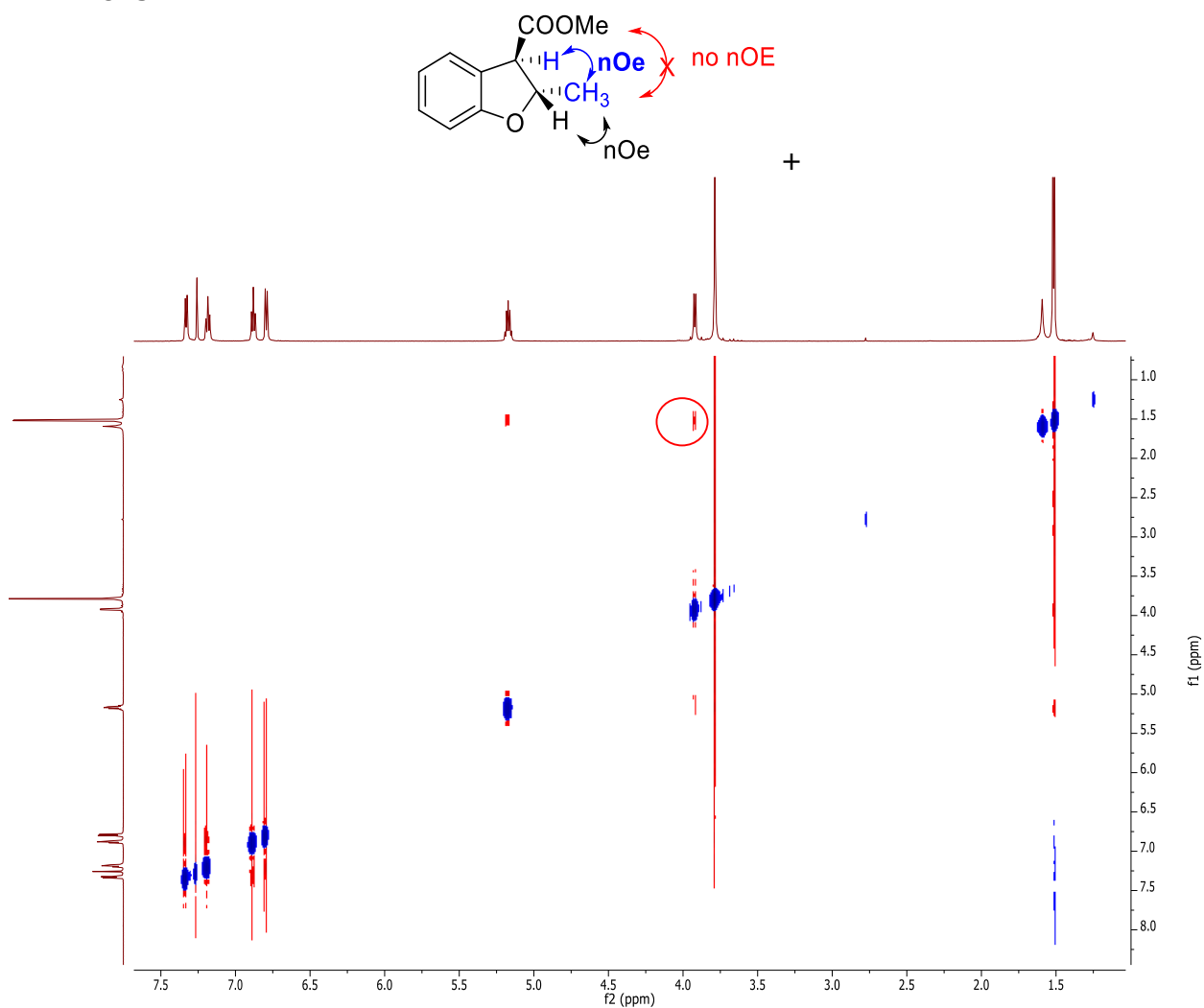
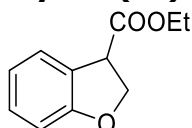
Trans-methyl 2-methyl-2,3-dihydrobenzofuran-3-carboxylate (P7):



¹H NMR (900 MHz, CDCl₃): d = 7.29 (d, J = 7.7 Hz, 1H), 7.15 (dd, J = 7.8 Hz, J = 7.6 Hz, 1H), 6.84 (dd, J = 7.6 Hz, J = 7.6 Hz, 1H), 6.76 (d, J = 7.9 Hz, 1H), 5.13 (dq, J = 7.5 Hz, J = 6.5 Hz, 1H), 3.88 (d, J = 7.5 Hz, 1H), 3.75 (s, 3H), 1.48 (d, J = 6.5 Hz, 3H);

¹³C NMR (225 MHz, CDCl₃): d = 171.7, 159.4, 129.7, 125.6, 124.4, 120.7, 110.1, 81.5, 54.5, 52.7, 21.4;

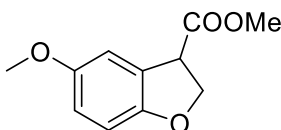
HR MS (EI): calcd. for C₁₁H₁₂O₃ [M]⁺: 192.0786, found: 192.0784.

^1H - ^1H NOESY NMR:**Ethyl 2,3-dihydrobenzofuran-3-carboxylate (P6):**

^1H NMR (900 MHz, CDCl_3): d = 7.34 (d, J = 7.5 Hz, 1H), 7.14 (dd, J = 7.9 Hz, J = 7.9 Hz, 1H), 6.85 (dd, J = 7.5 Hz, J = 7.5 Hz, 1H), 6.78 (d, J = 8.0 Hz, 1H), 4.90 (dd, J = 9.0 Hz, J = 6.8 Hz, 1H), 4.63 (dd, J = 9.4 Hz, J = 9.4 Hz, 1H), 4.29 (dd, J = 9.7 Hz, J = 6.8 Hz, 1H), 4.19 (dq, J = 13.3 Hz, J = 7.1 Hz, 2H), 1.27 (t, J = 7.1 Hz, 3H);

^{13}C NMR (225 MHz, CDCl_3): d = 173.9, 162.6, 132.2, 128.1, 127.1, 123.4, 112.7, 75.2, 64.3, 49.9, 17.0;

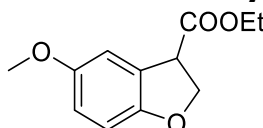
HR MS (EI): calcd. for $\text{C}_{11}\text{H}_{12}\text{O}_3$ $[\text{M}]^+$: 192.0786, found: 192.0782.

Methyl 5-methoxy-2,3-dihydrobenzofuran-3-carboxylate (P8):

¹H NMR (900 MHz, CDCl₃): d = 6.91 (s, 1H), 6.71-6.68 (m, 2H), 4.86 (dd, J = 9.1 Hz, J = 6.7 Hz, 1H), 4.61 (dd, J = 9.5 Hz, J = 9.3 Hz, 1H), 4.27 (dd, J = 9.5 Hz, J = 6.7 Hz, 1H), 3.74 (s, 3H), 3.73 (s, 3H);

¹³C NMR (225 MHz, CDCl₃): d = 171.7, 154.4, 154.1, 125.2, 114.9, 111.5, 110.1, 72.9, 56.3, 52.8, 47.8;

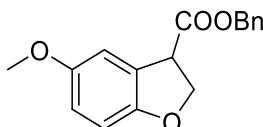
HR MS (EI): calcd. for C₁₁H₁₂O₄ [M]⁺: 208.0736, found: 208.0740.

Ethyl 5-methoxy-2,3-dihydrobenzofuran-3-carboxylate (P9):

¹H NMR (900 MHz, CDCl₃): d = 6.92 (s, 1H), 6.70-6.68 (m, 2H), 4.86 (dd, J = 9.0 Hz, J = 6.9 Hz, 1H), 4.61 (dd, J = 9.6 Hz, J = 9.1 Hz, 1H), 4.26 (dd, J = 9.5 Hz, J = 7.0 Hz, 1H), 4.19 (dq, J = 19.2 Hz, J = 7.1 Hz, 2H), 3.72 (s, 3H), 1.27 (t, J = 7.1 Hz, 3H);

¹³C NMR (225 MHz, CDCl₃): d = 171.2, 154.3, 154.2, 125.3, 114.9, 111.4, 110.1, 61.7, 56.3, 47.8, 14.5;

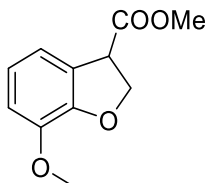
HR MS (EI): calcd. for C₁₂H₁₄O₄ [M]⁺: 222.0892, found: 222.0893.

Benzyl 5-methoxy-2,3-dihydrobenzofuran-3-carboxylate (P10):

¹H NMR (900 MHz, CDCl₃): d = 7.35-7.29 (m, 5H), 6.86 (s, 1H), 6.70-6.68 (m, 2H), 5.17 (dd, J = 43.3 Hz, J = 12.2 Hz, 2H), 4.88 (dd, J = 9.1 Hz, J = 6.8 Hz, 1H), 4.62 (dd, J = 9.5 Hz, J = 9.2 Hz, 1H), 4.31 (dd, J = 9.6 Hz, J = 7.0 Hz, 1H), 3.66 (s, 3H);

¹³C NMR (225 MHz, CDCl₃): d = 171.0, 154.3, 154.1, 135.7, 128.9, 128.7, 128.6, 125.0, 115.4, 111.1, 110.2, 72.9, 67.5, 56.2, 47.8;

HR MS (EI): calcd. for C₁₇H₁₆O₄ [M]⁺: 284.1049, found: 284.1053.

Methyl 7-methoxy-2,3-dihydrobenzofuran-3-carboxylate (P11):

¹H NMR (900 MHz, CDCl₃): d = 6.95 (d, J = 7.7 Hz, 1H), 6.81 (dd, J = 7.9 Hz, J = 7.7 Hz, 1H), 6.76 (d, J = 8.2 Hz, 1H), 4.95 (dd, J = 9.2 Hz, J = 6.8 Hz, 1H), 4.69 (dd, J = 9.7 Hz, J = 9.3 Hz, 1H), 4.33 (dd, J = 9.7 Hz, J = 6.9 Hz, 1H), 3.83 (s, 3H), 3.73 (s, 3H);

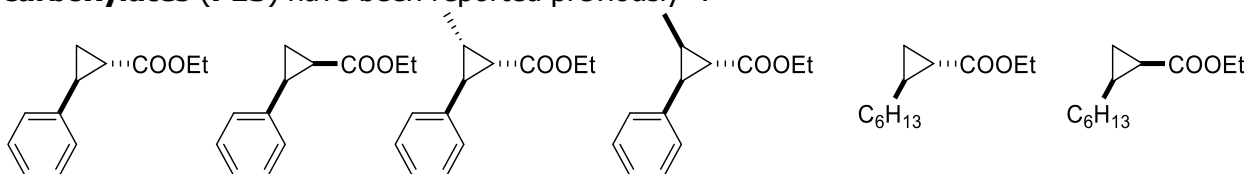
¹³C NMR (225 MHz, CDCl₃): d = 171.7, 148.6, 145.1, 125.2, 121.5, 117.6, 112.6, 73.4, 56.2, 52.8, 47.9;

HR MS (EI): calcd. for C₁₁H₁₂O₄ [M]⁺: 208.0738, found: 208.0740.

General procedure for synthesis of cyclopropanes

To a vial charged with the alkene (5-10 mmol, 5-10 equiv.) in toluene (10 ml), was added 100 μ l of an 8 mM solution of Ir(Me)-PIX (0.0008 equiv.) in DMF. A solution of ethyl diazoacetate (1 mmol, 1 equiv.) in toluene (1 ml) was then added slowly while the reaction mixture was vigorously stirred. After complete addition of EDA, the reaction was stirred for 30-60 min, after which time the evolution of nitrogen stopped, indicating full consumption of EDA. Then, the volatile materials were removed, and the residue was purified by column chromatography on silica gel, with a mixture of hexanes and ethyl acetate (100:0 \rightarrow 95:5 gradient) as the eluent. Fractions of the pure product(s) were combined, and the solvent evaporated, yielding cyclopropanation products.

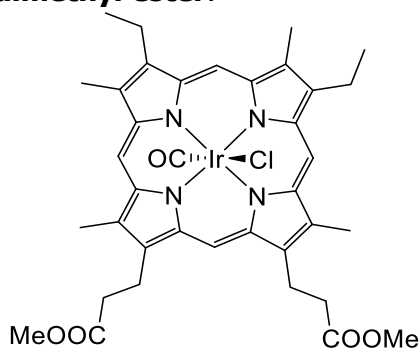
Cis- and trans- ethyl 2-phenylcyclopropane-1-carboxylates (P12), ethyl syn-2-methyl-anti-3-phenylcyclopropane-1-carboxylate (5), ethyl syn-2-methyl-syn-3-phenylcyclopropane-1-carboxylate and cis- and trans-ethyl 2-hexylcyclopropane-1-carboxylates (P13) have been reported previously ⁶.



The absolute configurations of cis- and trans- ethyl 2-phenylcyclopropane-1-carboxylates, and cis- and trans-ethyl 2-hexylcyclopropane-1-carboxylate were assigned on the basis of reported retention times,^{7,8} conducting analysis according to literature methods (Table 15).

d. Metal cofactors

Ir(CO)Cl-Mesoporphyrin IX dimethyl ester:



Under an air atmosphere, a solution of mesoporphyrin IX dimethyl ester (270 mg, 0.45 mmol) and [Ir(COD)Cl]₂ (410 mg, 0.61 mmol) in 1,2-xylene (250 ml) was refluxed. The conversion of the substrate was followed by TLC, with a hexane and ethyl acetate mixture (1:1) as the eluent. Upon completion (\sim 3.5 h), the volatile materials were evaporated, and the solid residue was purified by column chromatography on silica gel. The organic material was first eluted with a mixture of hexanes and ethyl acetate (100:0 \rightarrow 75:25 gradient) to remove the impurities. Then it was eluted with a mixture of hexanes and ethyl acetate (75:25 \rightarrow 50:50 gradient) to collect the product. Fractions containing the product were combined, and the solvent evaporated. The solid material was dissolved in DCM (10 ml) and hexane (100 ml). The mixture was concentrated (\sim 10 ml) under vacuum, resulting in precipitation of the pure product, which was isolated by filtration yielding 151 mg (39%) of a deep red solid.

¹H NMR (500 MHz, CDCl₃): δ = 10.33–10.28 (m, 4H), 4.53–4.41 (m, 4H), 4.20–4.01 (m, 4H), 3.75–3.71 (m, 6H), 3.71–3.67 (m, 9H), 3.64 (s, 3HH), 3.38 (t, J = 7.8 Hz, 4H), 1.95 (t, J = 7.6 HZ, 6H);

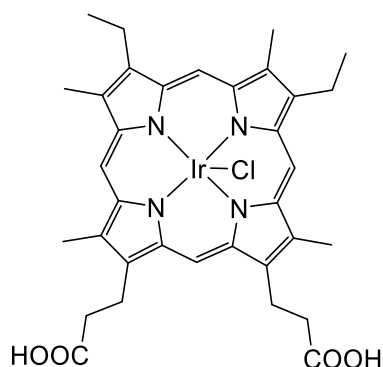
^{13}C NMR (225 MHz, CDCl_3): δ = 173.83, 173.82, 143.2, 143.1, 140.0, 139.8, 139.4, 139.23, 139.20, 139.19, 138.9, 138.5, 138.45, 138.4, 137.38, 137.35, 136.4, 136.3, 135.0, 99.2, 99.1, 99.0, 98.9, 51.99, 51.96, 37.05, 37.04, 22.07, 22.01, 20.10, 20.09, 17.85, 17.83, 12.02, 11.98, 11.85, 11.81;

HR MS (ESI): calcd. for $\text{C}_{36}\text{H}_{40}\text{IrN}_4\text{O}_4$ $[\text{M}-\text{Cl}-\text{CO}]^+$: 785.2673, found: 785.2715;

IR (neat): 2031, 1735 cm^{-1} ;

UV/Vis (DMF, $\text{C}=5\cdot 10^{-6}$ M): λ_{max} ($\log \epsilon$) 327 (4.23), 393 (5.29), 510 (4.02), 540 nm (4.27).

Ir(Cl)-Mesoporphyrin IX:



A solution of Ir(CO)Cl-mesoporphyrin IX dimethyl ester (25 mg, 0.03 mmol) and LiOH (100 mg) in THF (3 ml), methanol (1 ml) and water (1 ml) was stirred at rt for 2 h. The reaction mixture was concentrated (~ 1 ml) under vacuum, diluted with sodium phosphate buffer (4 ml, 0.1 M, pH = 5) and slowly acidified with HCl (0.5 M) to \sim pH = 5. The red precipitate was separated from the liquid by centrifugation (2000 rpm, 15 min, 4 $^{\circ}\text{C}$) and subsequent decanting of the liquid. The red solid residue was suspended in water (15 ml), the mixture was centrifuged, and the liquid was decanted. The resulting solid was dried for overnight under high vacuum at rt, yielding 21 mg (88%) of dark red powder.

(Alternatively, the precipitate can be isolated by filtration, followed by washing with water and drying).

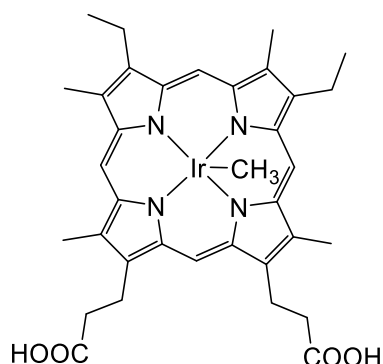
^1H NMR (600 MHz, $\text{D}_2\text{O}+0.5\%$ NaOD): δ = 10.22 (bs, 1H), 9.98 (bs, 3H), 4.35 (bs, 4H), 4.08 (bs, 4H), 3.67 (bs, 12H), 3.12 (bs, 4H), 1.84 (bs, 6H);

^{13}C NMR (225 MHz, $\text{D}_2\text{O}+0.5\%$ NaOD): δ = 185.7, 145.8, 145.6, 145.16, 145.10, 145.07, 145.0, 144.09, 144.08, 144.05, 143.9, 142.53, 142.51, 139.74, 139.71, 138.7, 138.5, 102.37, 102.14, 101.99, 101.96, 43.7, 25.4, 21.5, 19.95, 19.94, 13.12, 13.10, 12.88;

HR MS (ESI): calcd. for $\text{C}_{34}\text{H}_{36}\text{IrN}_4\text{O}_4$ $[\text{M}-\text{Cl}]^+$: 757.2360, found: 757.2393;

IR (neat): 1706 cm^{-1} ;

UV/Vis (DMF, $\text{C}=5\cdot 10^{-6}$ M): λ_{max} ($\log \epsilon$) 326 (4.40), 393 (5.26), 510 (4.15), 540 nm (4.37).

Ir(Me)-Mesoporphyrin IX:

Under a nitrogen atmosphere, to a suspension of Ir(CO)Cl-mesoporphyrin IX dimethyl ester (110 mg, 0.13 mmol) in degassed ethanol (10 ml), a degassed solution of NaBH₄ (25 mg) and NaOH (1 M) in water (3 ml) was added. The mixture was stirred at 50 °C for 1 h in the dark. Subsequently, the reaction mixture was cooled to rt, methyl iodide (10 ml) was added, and the obtained solution was stirred overnight at rt. The reaction mixture was concentrated (~3 ml) under vacuum (NOTE: Evaporation of unreacted methyl iodide is important), followed by addition of LiOH (200 mg). The reaction mixture was stirred at rt for 1h, diluted with sodium phosphate buffer (8 ml, 0.1 M, pH = 5) and slowly acidified with HCl (0.5 M) to ~ pH = 5. The red precipitate was separated from the liquid by centrifugation (2000 rpm, 15 min, 4 °C) and subsequent decanting of the liquid. The red solid residue was suspended in water (15 ml), the mixture was centrifuged, and the liquid was decanted. The resulting solid was dried for overnight under high vacuum at rt, yielding product quantitatively; dark red powder. (Alternatively, the precipitate can be isolated by filtration, followed by washing with water and drying).

¹H NMR (900 MHz, DMF-*d*₇): δ = 12.56 (bs, 2H), 9.93 (s, 1H), 9.78 (s, 3H), 4.38–4.33 (m, 2H), 4.29–4.24 (m, 2H), 4.03–3.98 (m, 4H), 3.61 (s, 6H), 3.58 (s, 3H), 3.57 (s, 3H), 3.28 (q, J = 7.5 Hz, 6H), 1.83 (t, J = 7.5 Hz, 6H), -7.61 (s, 3H);

¹³C NMR (225 MHz, DMF-*d*₇): δ = 175.40, 175.39, 143.5, 143.2, 143.0, 142.91, 142.88, 142.79, 142.4, 142.0, 141.83, 141.82, 139.82, 139.76, 136.95, 136.90, 135.9, 135.7, 101.0, 100.9, 100.7, 100.5, 38.34, 38.32, 22.50, 22.49, 20.09, 20.06, 18.59, 18.55, 11.63, 11.61, 11.48, 11.44, -45.0;

HR MS (ESI): calcd. for C₃₅H₄₀IrN₄O₄ [M+H]⁺: 773.2673, found: 773.2708;

IR (neat): 1706 cm⁻¹;

UV/Vis (DMF, C=5·10⁻⁶ M): λ_{max} (log ε) 341 (4.39), 392 (5.07), 530 (4.24).

III. Preparation of the Multi-Dimensional Catalyst Array

In a nitrogen-atmosphere glove box, stock solutions of 9 metal cofactors (8.3 μL per well, 6 mM, DMF) were distributed down the columns of a 96-well plate containing 1.2 mL glass vials (Table 2). Eight mutants (Table 2) of apo-mOCR-myo were expressed and purified according to the procedure in Section I.e. Each mutant was concentrated to 0.6 mM and degassed on a Schlenk line (3 cycles vacuum/refill), and the mutants were distributed across the rows of the same 96-well plate (166 μL protein per vial) to generate 72 unique catalysts formed from different combinations of cofactors and mutants. The prepared portion of each catalyst was evenly divided among 4 separate 96-well reaction plates of the same type (42 μL per well), and each well was diluted to 250 μL with 10 mM tris buffer, pH = 8.0.

IV. Design of a Size-Selective Inhibitor for Deactivating Free Cofactor Released During Reactions

To facilitate the screening process, we sought a size-selective inhibitor that would bind to any free cofactor released in the event of protein denaturation during the reaction, but that would be excluded from the porphyrin binding due to steric interactions with the protein scaffold. Such an inhibitor would enable a more direct comparison of the inherent selectivities of different mutants. Several classes of molecules are known to be potent inhibitors of Fe-PPIX-proteins, including imidazoles, pyridines, and isonitriles⁹.

To ascertain whether size-selective inhibition could be realized, an assay was developed based on the enantioselective cyclopropanation of 4-OMe-styrene with EDA catalyzed by Fe-PPIX-Myo. The reaction catalyzed by the mutant Fe-PPIX-Myo-V68A occurs in 90% ee, whereas the reaction catalyzed by the combination of Fe-Myo-V68A and Ir(Me)-PPIX (free cofactor) occurs in lower ee (30%), due to competing reaction catalyzed by the achiral Ir-PPIX cofactor. Therefore, we expected that reactions catalyzed by this combination of catalysts in the presence of a size-selective inhibitor would occur with ee's reflecting that of the Fe-PPIX-Myo-V68A protein. Using this assay, a series of inhibitors based on pyridines, imidazoles, and isocyanides were evaluated. Each reaction was set up on a 250 μL scale with Tris/MeCN (10 mM Tris, pH 8.0, containing 8 vol% MeCN) as solvent (Fig. S10). Each 250 μL reaction contained 10 mM 4-OMe styrene, 30 mM EDA, 0.5 mM total catalyst, and one potential inhibitor. A summary of the results of the evaluation can be found in Figure 10. The cyclopropanation of 4-OMe styrene with EDA by the combination of 0.05 mM Fe-Myo-V68A and 0.05 mM Ir(Me)-PPIX in the presence of 4-morpholino pyridine occurred with the highest yield (53%) and enantioselectivity (74% ee) (Figure 10-S11). Therefore, this inhibitor was chosen for inclusion in the directed evolution studies due to its effectiveness as a selective inhibitor of the free Ir-porphyrin and its high water solubility.

Catalytic Experiments

- a. *General Methods:* Unless otherwise noted, catalytic reactions were performed in 4 mL individually-capped vials or in 1.2 mL vials as part of a 96-well array fitted with a screw on cover. Reactions were either (1) assembled in a nitrogen atmosphere glove box or (2) assembled on the bench. In the latter case, the headspace of the vial purged with nitrogen through a septum cap. Solutions of Ir(Me)-PIX-mOCR-Myo were gently degassed on a Schlenk line (3 cycles vacuum/refill) before being pumped into a glove box in sealed vials. Organic reagents were added as stock solutions in

MeCN, such that the final amount of MeCN in the reaction was approximately 8% by volume. Protein catalysts were diluted to reaction concentration in Tris buffer (10 mM, pH = 8.0) before being added to reaction vials. Unless otherwise noted, all reactions were performed with catalysts generated from a 1:2 ratio of [M]-cofactor : apo protein, with 0.5% catalyst loading with respect to [M] cofactor and limiting reagent, if not noted otherwise. All reactions were conducted in a shaking incubator (20 °C, 16 h, 275 rpm).

b. Reaction Setup and Composition for Each Transformation Class

The catalyst stock solution: The Ir(Me)-myoglobin stock solution was prepared, by addition of Ir(Me)-PIX (1 equiv. 8 mM) in DMF to the solution of the apo-protein (2 equiv., 0.2 mM) in Tris buffer (10 mM, pH = 8). The 2 : 1 ratio of the apo-protein to Ir(Me)-PIX was used to ensure that all Ir-PIX was bound. The mixture was incubated for 10 min, and desalted with the NAP-10 desalting column equilibrated with Tris buffer (10 mM, pH = 8). The protein mixture was diluted to the required reaction concentration with Tris buffer (10 mM, pH = 8.0).

Cyclopropanation: 240 ul of the catalyst stock solution (0.125 umol of [Ir]) was added to a vial. A stock solution of the appropriate olefin (2.5 umol in 10 uL MeCN) was added, followed by a stock solution of the appropriate diazo compound (15 umol in 10 uL MeCN).

Intramolecular C-H Insertion: 240 ul of the catalyst stock solution (0.125 umol of [Ir]) was added to a vial, followed by addition of a stock solution of the appropriate diazo compound (2.5 umol in 20 uL MeCN).

c. Evaluation of the Activity of Catalysts in the Array:

Plates containing the catalyst array were prepared as described in Section III. Reactions were assembled in a nitrogen atmosphere glove box according to the general methods described in Sections Va,b using multichannel pipets. Plates were sealed before being removed from the glove box.

d. Mutant Screening (directed evolution)

Mutants were evaluated for C-H insertion reactions in 96 well plates with the reaction conditions described in the general method (Section Va,b). Twelve mutants were analyzed per 96 well plate. Seven aliquots of each Ir(Me)-Myo mutant were distributed down the columns of a 96 well plate. Next, 2.5 uL of a solution of 4-(pyridin-4-yl)morpholine (100 mM stock solution in water) was added to each well, giving a final inhibitor concentration of 1 mM. Finally, aliquots of 7 substrates for C-H insertion were added to each of the rows (A-G) to generate 84 unique reactions. The most selective mutants were subsequently evaluated without the size selective inhibitor (4-(pyridin-4-yl)morpholine). The same enantioselectivities and similar yields were measured in both sets of experiments. The results reported in Figures 3 and 4 (main text) are from the reactions conducted without the inhibitor.

e. Procedure for typical catalytic experiments

240 ul of the catalyst stock solution (0.125 umol of [Ir]) – prepared as in section Vb – was added to a vial. For the intramolecular C-H insertion reactions, the appropriate diazo compound (2.5 umol

in 20 μL MeCN) was then added. For the cyclopropanation reactions, the appropriate olefin (2.5 μmol in 10 μL MeCN) and EDA (15 μmol in 10 μL MeCN) were added subsequently. For experiments with higher substrate concentration (> 50 mM), the substrate was added directly to a vial, followed by the appropriate organic solvent and 240 μL of the catalyst stock solution. The vial was sealed with a cap, removed from a glovebox and shaken (20 $^{\circ}\text{C}$, 275 rpm). Upon completion, the reaction mixture was analyzed in the general method described in section VI.

f. Experiments with slow addition of EDA

960 μL of the catalyst stock solution (0.5 μmol of [Ir]) – prepared as in section Vb – was added to a vial equipped with a magnetic stirring bar. A stock solution of the appropriate olefin (10 μmol in 40 μL MeCN) was added. The vial was sealed with a septum-cap and removed from a glovebox. The stock solution of EDA (60 μmol in 40 μL MeCN) was added slowly from a gas-tight syringe (a needle extending into the reaction mixture) over ~ 8 h, using a syringe pump, with slow stirring (100 rpm). Upon completion, the reaction mixture was incubated for additional 1 h and analyzed by the general method described in section VI.

g. Reaction on a synthetic scale

12 ml of the catalyst stock solution (6 μmol of [Ir]) – prepared as in described section Vb, using mOCR-myo-93A,64A,43W,68A mutant) – was added to a Schlenk flask and gently degassed on a Schlenk line (3 cycles vacuum/refill). A solution of substrate **11** (28.3 mg, 0.12 mmol in 0.96 mL acetonitrile) was added. The flask was sealed and gently shaken (120 rpm) at 20 $^{\circ}\text{C}$ for 72 h. The reaction was diluted with brine (30 ml) and extracted with ethyl acetate (3 \times 50 ml). If required, the phase separation was achieved by centrifuging (2000 rpm, 3 min) the mixture. The combined organic fractions were washed with brine (30 ml) and dried over MgSO_4 . After filtration, the volatile material from the filtrate was evaporated under reduced pressure. The residue was purified by column chromatography on silica gel, with a mixture of hexanes and ethyl acetate (100:0 \rightarrow 90:10 gradient) as the eluent. Fractions of the pure product were combined, and the solvent evaporated, yielding 20.1 mg (80%) of product **P11**. Er: 90:10, $[\alpha]_{\text{D}}^{20} = -52^{\circ}$ ($c = 0.8$, CHCl_3).

V. Analysis of Yield and Enantiomeric Ratio (er)

Yields were determined by achiral or chiral GC using dodecane as an internal standard (Figures 12-20). Enantiomeric ratios were determined either by chiral GC or chiral SFC (Figures 21-29). Achiral GC was used to determine the yields for reactions analyzed by SFC, while the yields for reactions analyzed by chiral GC were determined concurrently with that analysis. The methods used to determine the er of each product are summarized in Table 15. Representative traces can be found in Figures 21-29. Samples for analysis were prepared as follows, depending on the analysis method:

SFC/achiral GC: Saturated NaCl (200 μL) was added to each reaction vial, followed by a solution of dodecane (500 μL , 1 $\mu\text{L}/\text{ml}$) in EtOAc. The contents of the vial were mixed by pipet, and the phases were allowed to separate. A portion (250 μL) of the organic layer was removed from the top of the vial by pipet, transferred to a new vial, evaporated and redissolved in MeOH for analysis by SFC. An additional portion of EtOAc (250 μL) was added to the original reaction vial, and the reaction was quenched by the addition of HBr (40 μL , 50% in water). After separation of the

layers, approximately 400 μL of the aqueous phase was removed from the bottom of the vial by pipet. The remaining contents of the vial were neutralized by the addition of sat. NaHCO_3 (200 μL), and the organic layer was further diluted with EtOAc (500 μL). The organic layer was then transferred to a separate vial for GC analysis. In the case of experiments performed in a 96-well array, all manipulations were performed using a multichannel pipet.

Chiral GC: Saturated NaCl (200 μL) was added to each reaction vial, followed by a solution of dodecane (500 μL , 1 $\mu\text{L}/\text{ml}$) in EtOAc. The contents of the vial were mixed by pipet and the phases were allowed to separate. The reaction was then quenched by the addition HBr (40 μL , 50% in water). After separation of the layers, approximately 400 μL of the aqueous phase was removed from the bottom of the vial by pipet. The remaining contents of the vial were neutralized by the addition of sat. NaHCO_3 (200 μL), and the organic layer was further diluted with EtOAc (500 μL). The organic layer was then transferred to a separate vial for GC analysis. In the case of experiments performed in a 96-well array, all manipulations were performed using a multichannel pipet.

Control extraction studies: 240 μL of the a stock solution of mOCR-myo-93A,64A,43W,68A (0.125 μmol of $[\text{Ir}]$) – prepared as in section Vb – was added to a vial, followed by addition of the stock solution of product **2** (2.5 μmol in 20 μL MeCN). Saturated NaCl (200 μL) was added, followed by a solution of dodecane (500 μL , 1 $\mu\text{L}/\text{ml}$) in EtOAc. To this mixture HBr (40 μL , 50% in water) was added. The content of the vial was mixed by pipet. After separation of the layers, approximately 400 μL of the aqueous phase was removed from the bottom of the vial by pipet. The remaining contents of the vial were neutralized by the addition of sat. NaHCO_3 (200 μL), and the organic layer was further diluted with EtOAc (500 μL). The organic layer was then transferred to a separate vial for GC analysis. As a control, a 20 μL aliquot of the stock solution of product **2** (2.5 μmol in 20 μL MeCN) was diluted with a solution of dodecane (500 μL , 1 $\mu\text{L}/\text{ml}$) in EtOAc and analyzed with GC. All measurements were performed triplicate. These experiments showed that the product was extracted nearly quantitatively from the catalyst solution mixture – Table 16. These experiments confirmed the accuracy of the method.

VI. Supplementary Figures

Figure 1. Characterization of purified apo myoglobin (A), mOCR-myoglobin (B), and P411-CIS (C) proteins by SDS-PAGE gel electrophoresis. Protein samples are shown in comparison to a standard protein ladder (D)

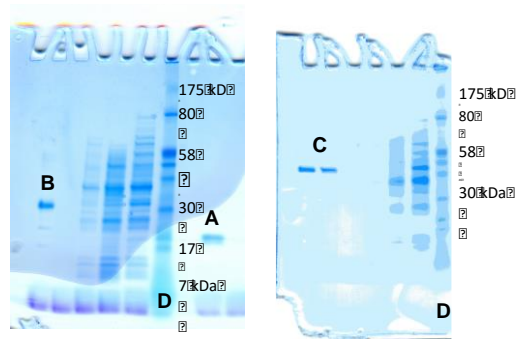


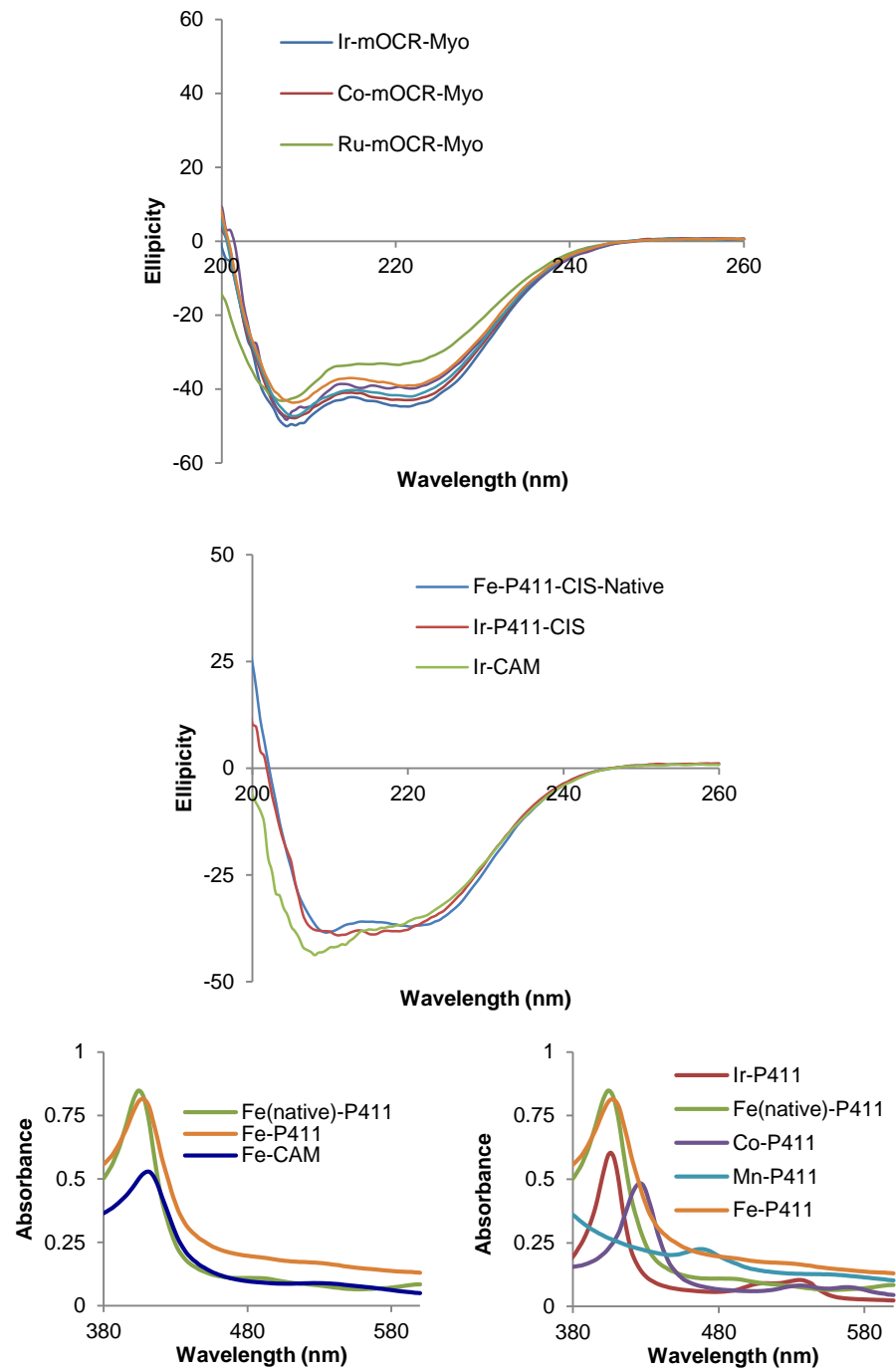
Figure 2. CD and UV spectra of native and artificially metallated myoglobins and P450s.

Figure 3. Native NS-ESI-MS showing the binding of hemin (top) and Ir(Me)-PIX (middle) to apo-Myo (bottom) in a 1:1 stoichiometry to the apo protein.

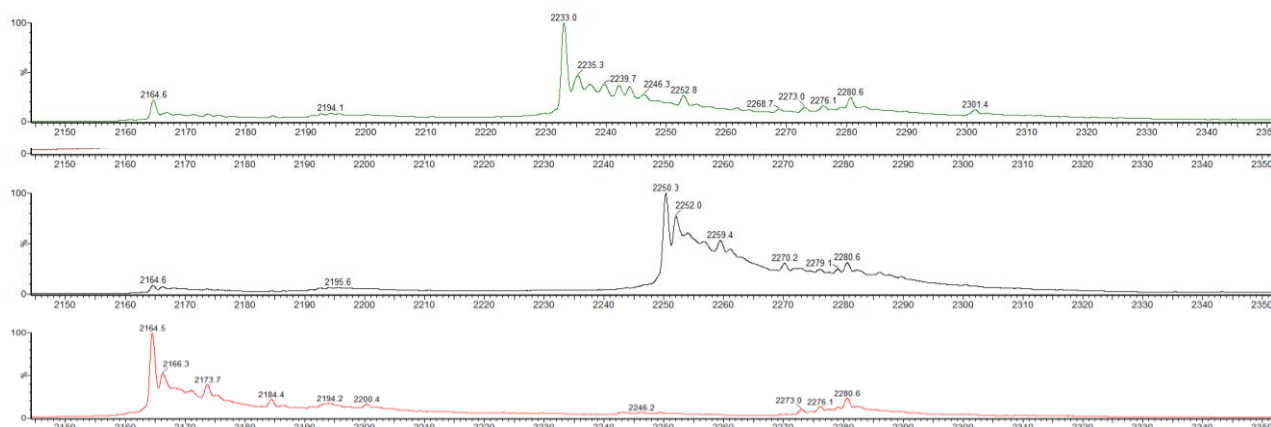
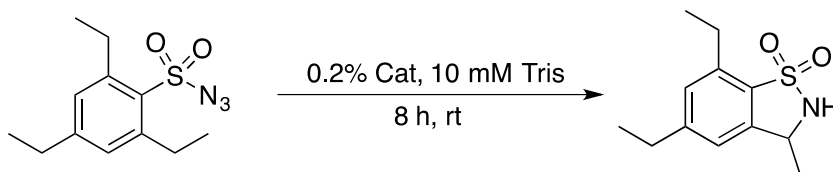
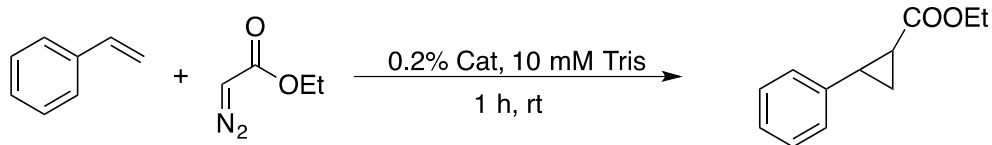


Figure 4. Selectivities of reactions catalyzed by native Fe and reconstituted Fe-PIX-proteins.

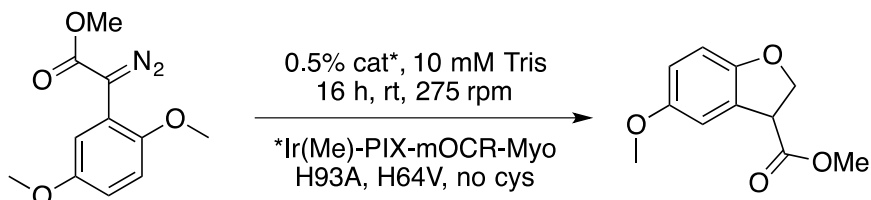


Native Fe-P411-CIS: 95 : 5 er
 Reconstituted Fe-P411-CIS: 95 : 5 er



Native Fe-Myo-F43V: 64 : 36 er
 Reconstituted Fe-Myo-F43V: 65 : 35 er

Figure 5. Selectivities of reactions of Ir(Me)-PIX-H93A/H64V upon storage under various conditions.



Catalyst Preparation

Freshly prepared	85:15 er
Frozen (12.5% glycerol), thawed	
Glycerol removed (NAP column)	85:15 er
Glycerol not removed	83:17 er
Lyophilized and redissolved	83:17 er

Figure 6. Comparison of activities and selectivities for C-H insertion reactions catalyzed by the same Ir(Me)-PIX-mOCR-Myo mutant (H93A/H64V) for substrates varied at the arene, ester, and alkoxy-functionalities. TON determined by GC.

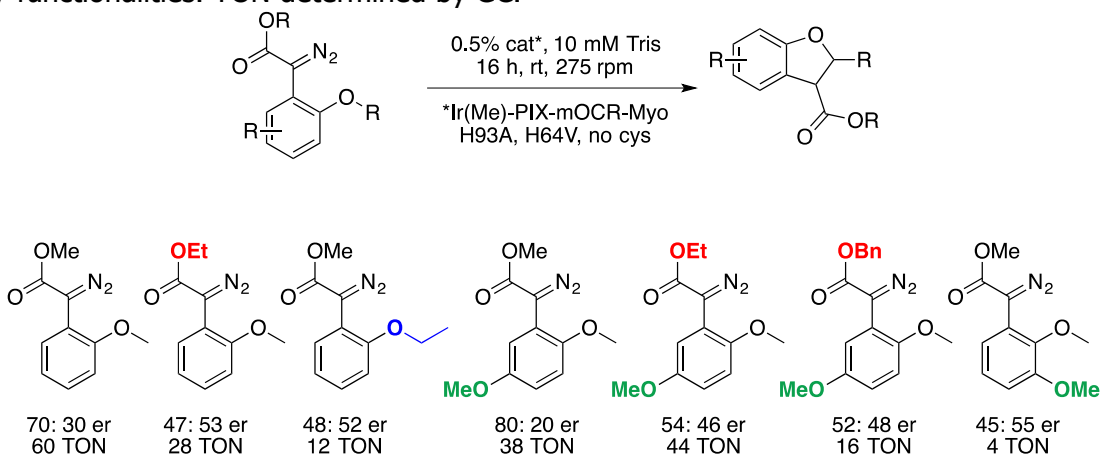


Figure 7. Directed evolution trees showing the progression toward the most selective catalysts for several substrates.

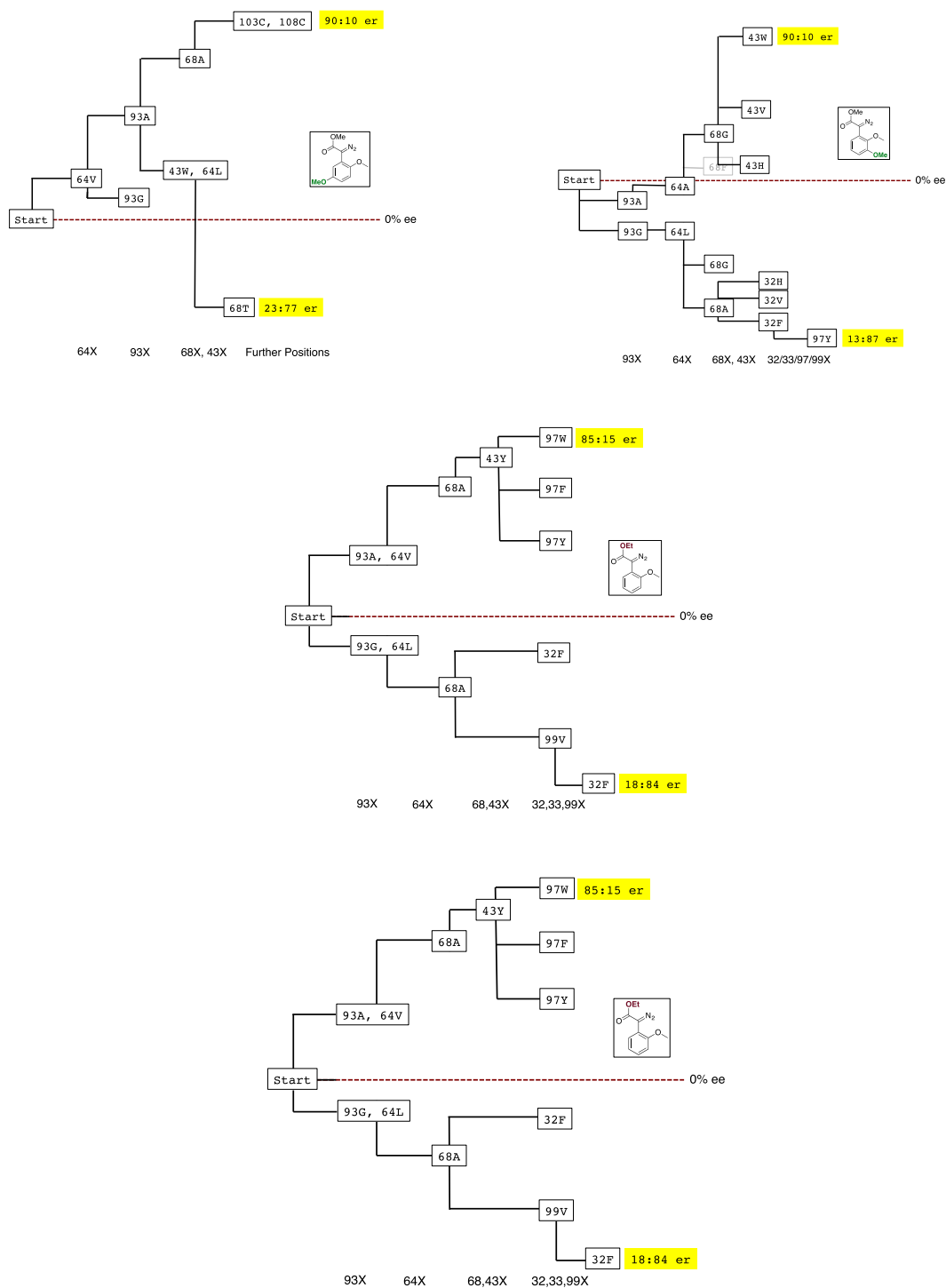


Figure 8. Infrared spectra (neat) of porphyrin complexes; from the top: Ir(CO)Cl-Mesoporphyrin IX dimethyl ester, Ir(Cl)-Mesoporphyrin IX, Ir(Me)-Mesoporphyrin IX.

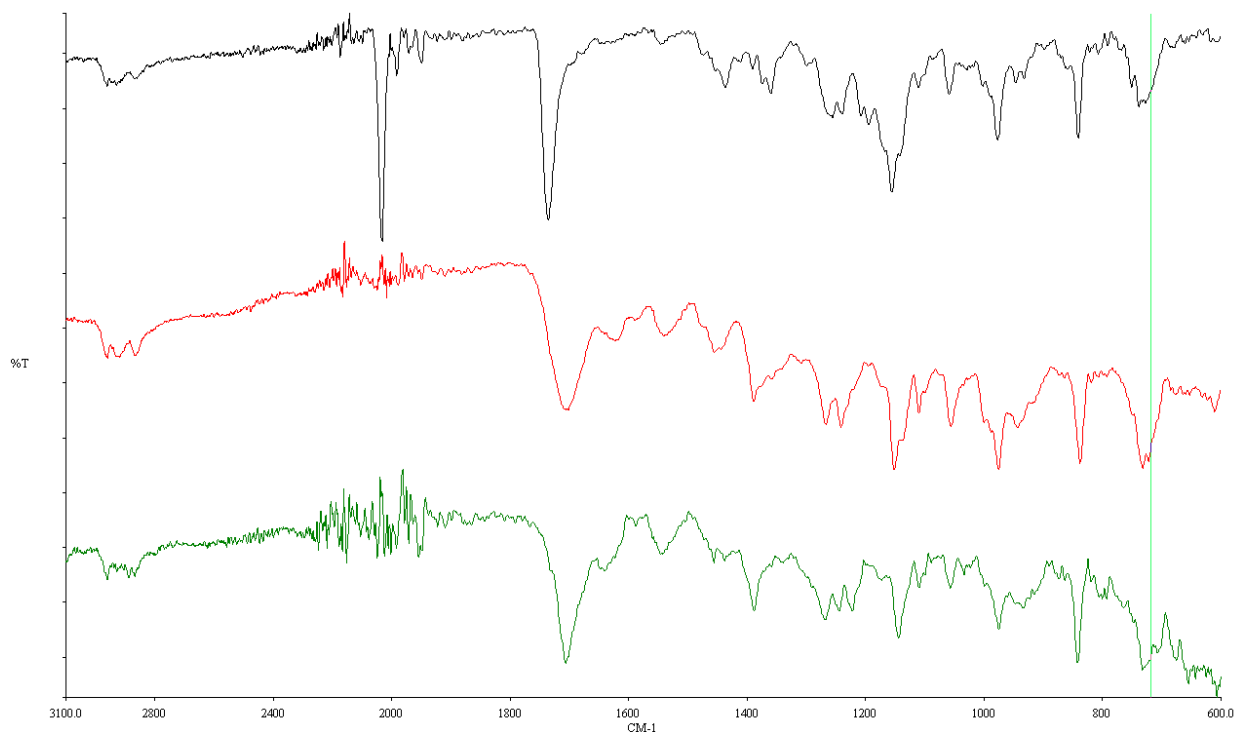


Figure 9. UV-Vis spectra (DMF, $C = 5 \cdot 10^{-6}$ M) of Ir(CO)Cl-Mesoporphyrin IX dimethyl ester, Ir(Cl)-Mesoporphyrin IX, Ir(Me)-Mesoporphyrin IX.

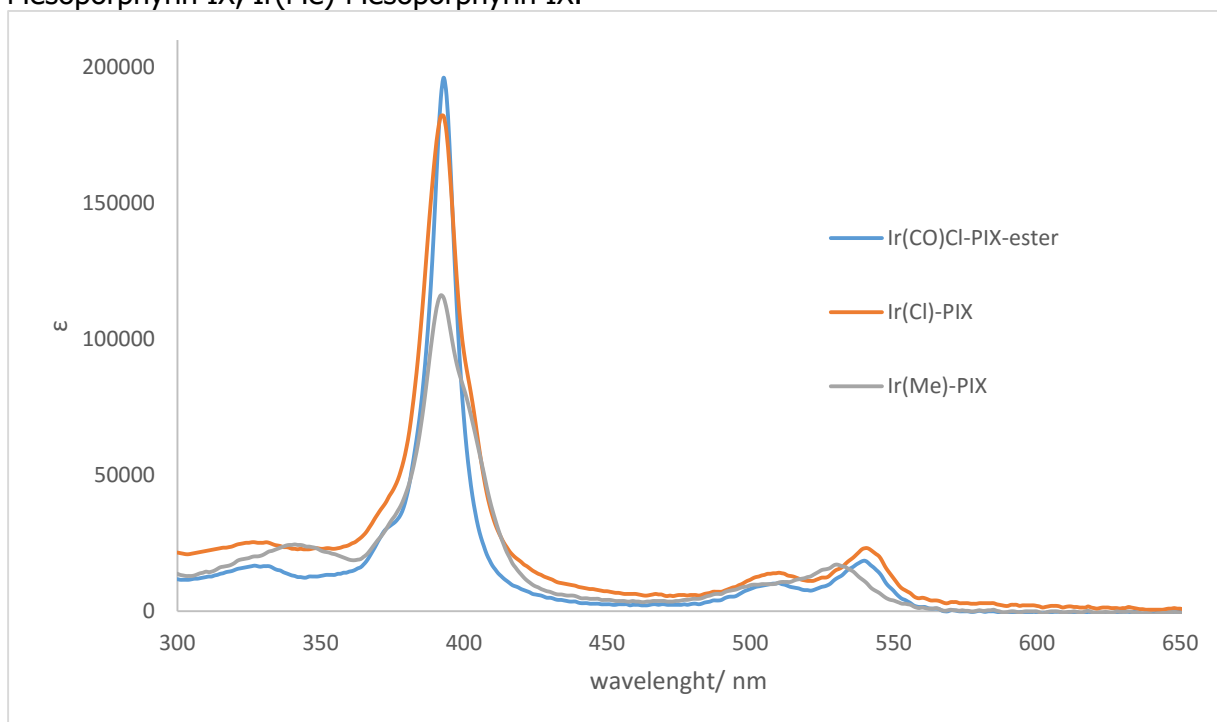


Figure 10. Scheme of the cyclopropanation reaction used to assay for size-selective inhibitors of free Ir(Me)-PIX not bound within the porphyrin-binding site of myoglobin. The assay is described fully in section IV and the results can be found in Figure 11.

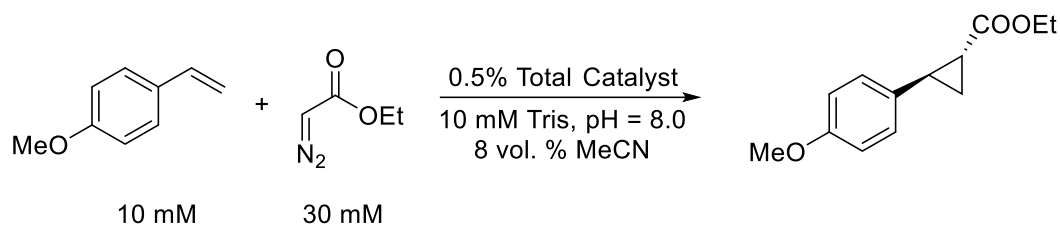


Figure 11. Results of the assay the cyclopropanation reactions (Figure 10) co-catalyzed by Fe-myoglobin and free Ir(Me)-PIX in the presence of putative size-selective inhibitors (experiment described in section IV. Pyr = pyridine, Mor-Pyr = 4-morpholino pyridine. Mor-Isocy = 2-(4-Morpholino)ethyl isocyanide).

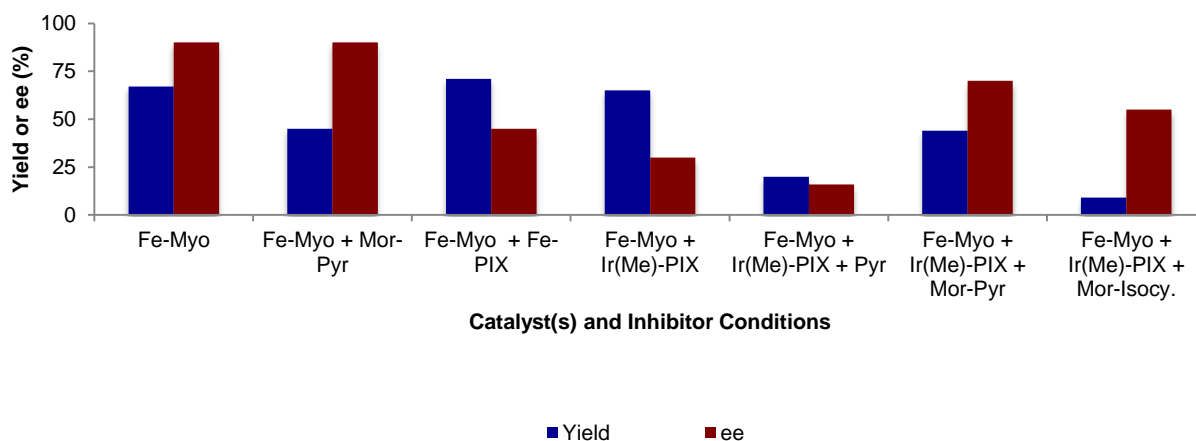


Figure 12. Calibration curve for product 2.

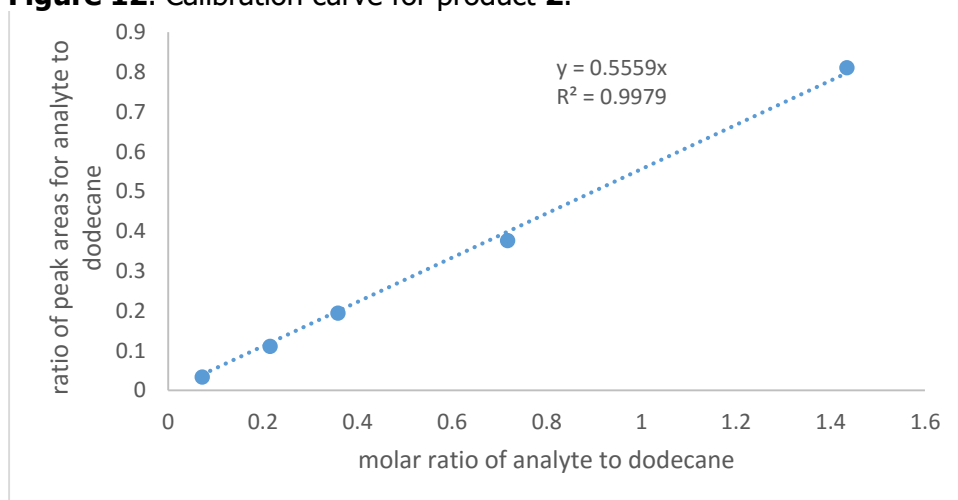


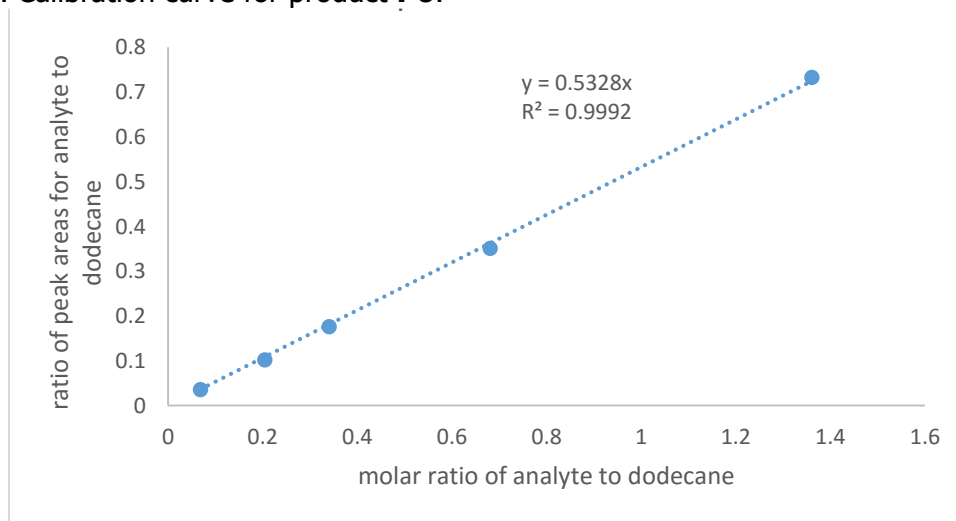
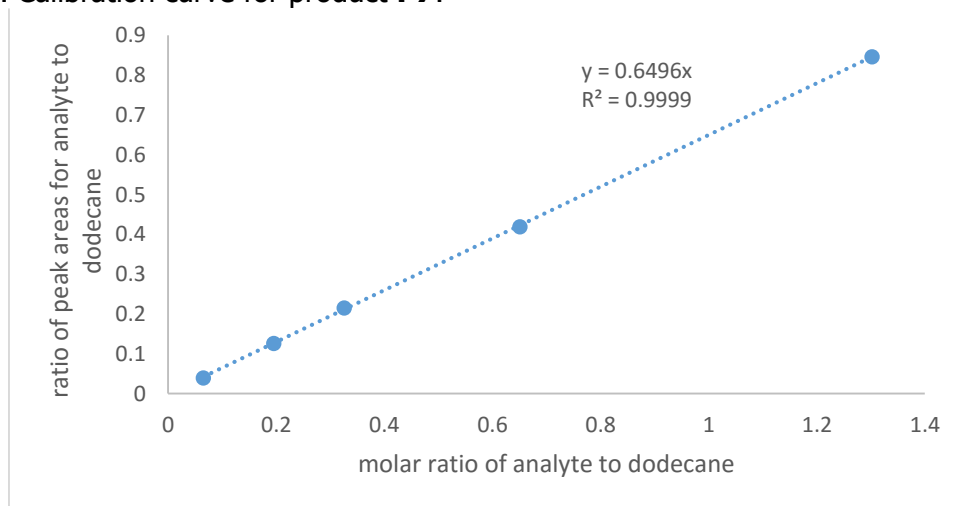
Figure 13. Calibration curve for product **P6**.**Figure 14.** Calibration curve for product **P7**.

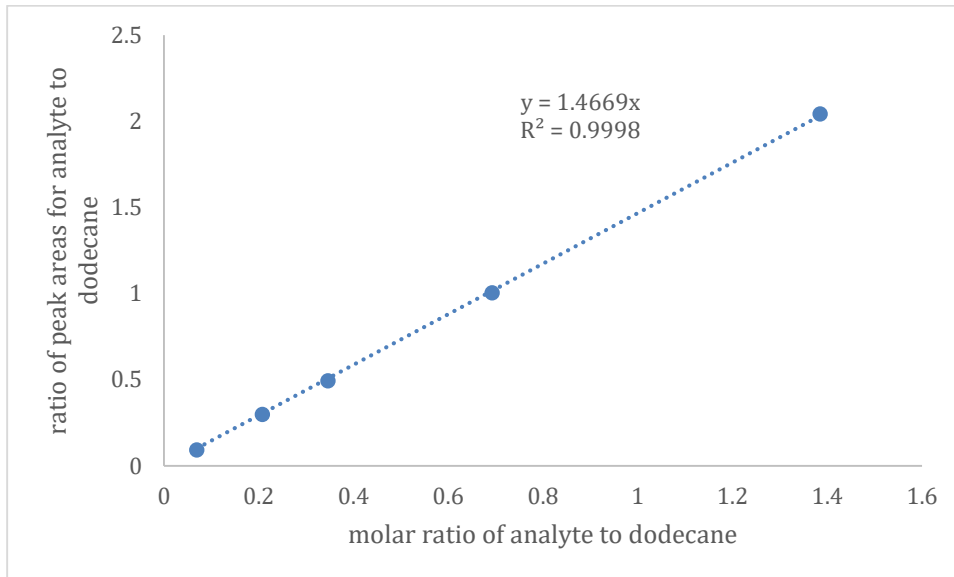
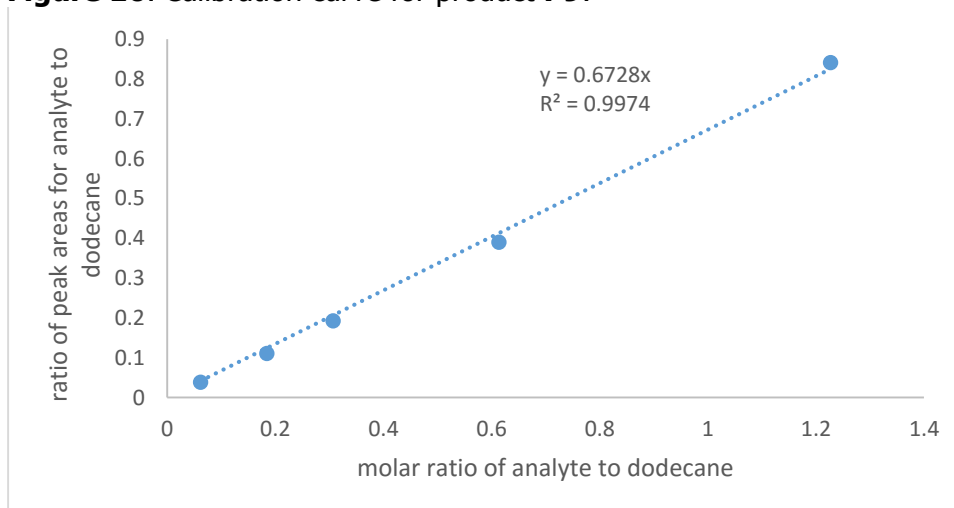
Figure 15. Calibration curve for product **P8**.**Figure 16.** Calibration curve for product **P9**.

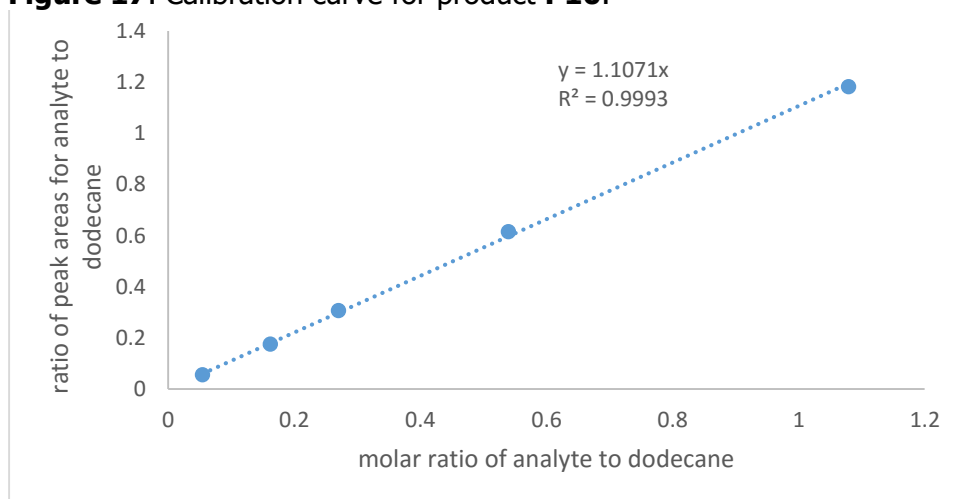
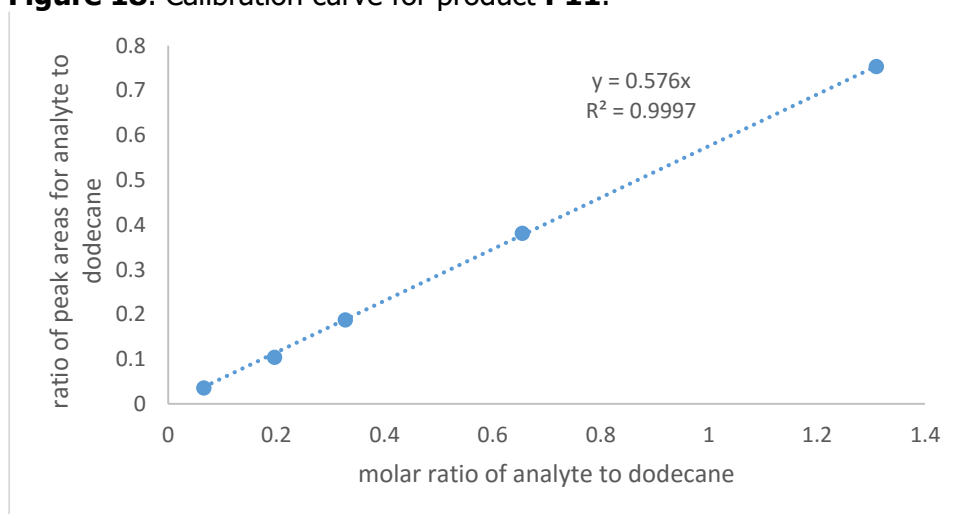
Figure 17. Calibration curve for product **P10**.**Figure 18.** Calibration curve for product **P11**.

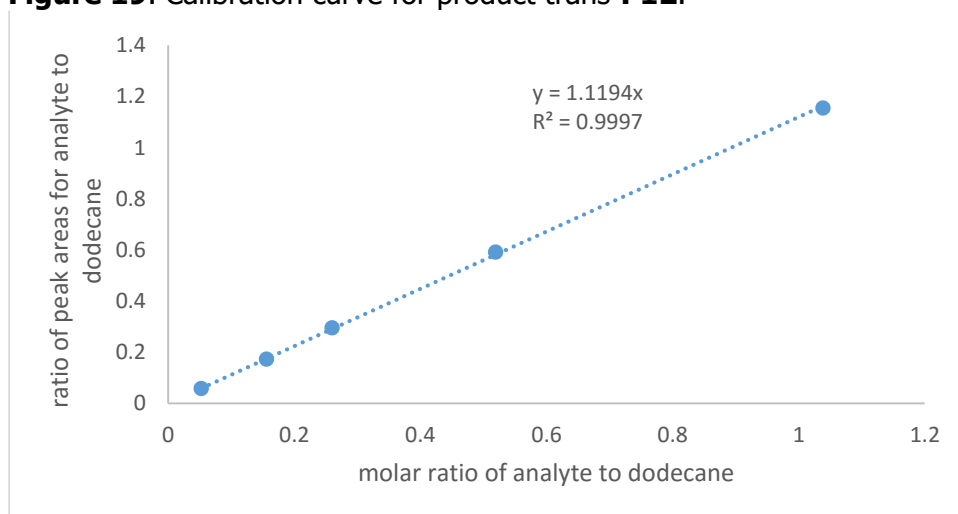
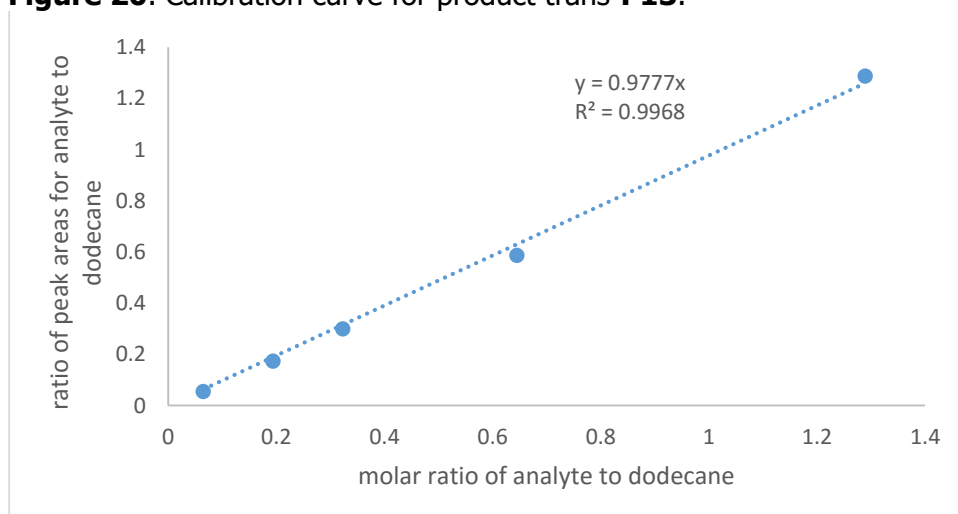
Figure 19. Calibration curve for product trans-P12.**Figure 20.** Calibration curve for product trans-P13.

Figure 21. Chiral GC traces for product **2**; racemate (above) and enantioenriched samples (below).

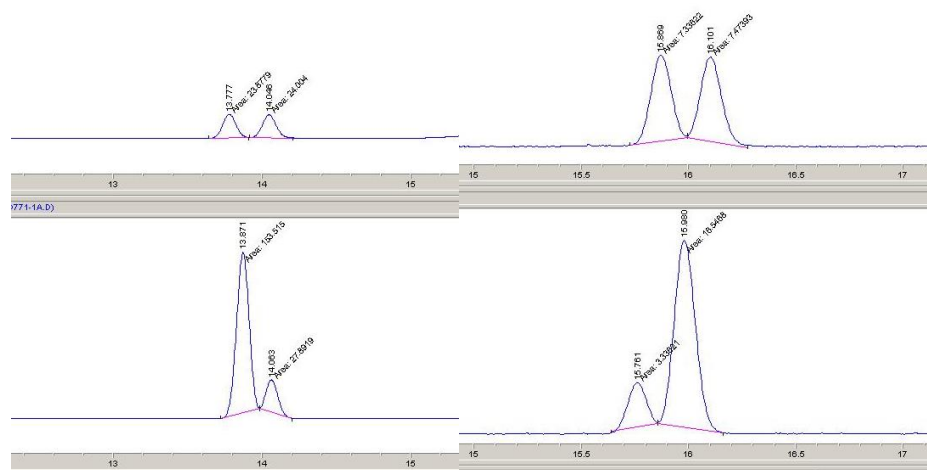


Figure 22. Chiral GC traces for product **P7**; racemate (above) and enantioenriched samples (below).

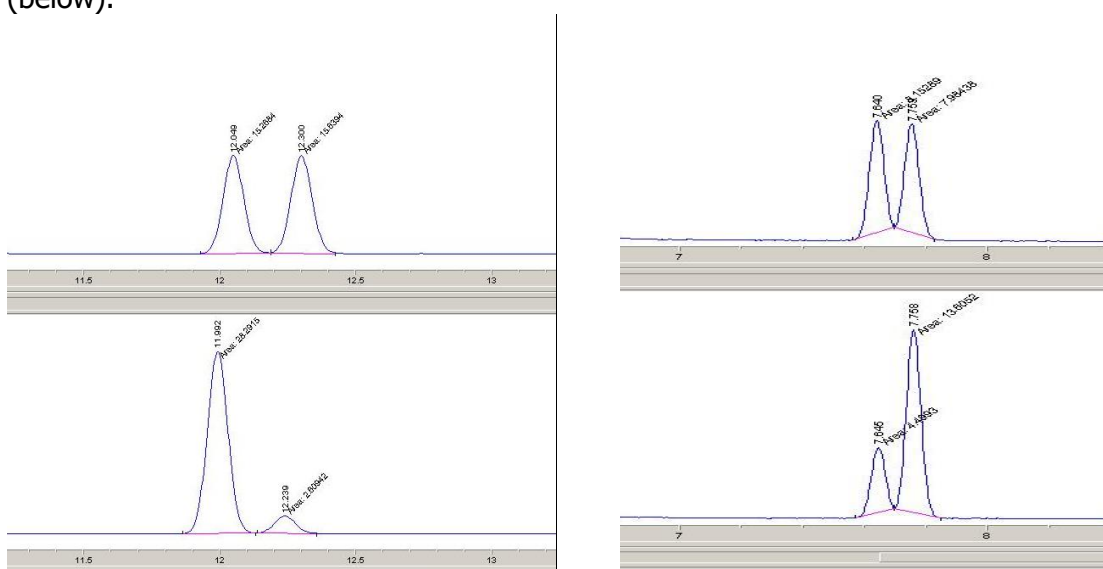


Figure 23. Chiral GC traces for product **P8**; racemate (above) and enantioenriched samples (below).

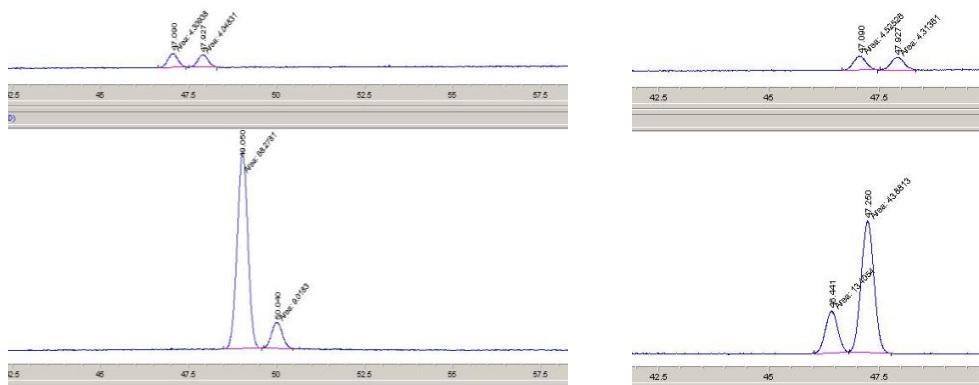


Figure 24. Chiral GC traces for product **P11**; racemate (above) and enantioenriched samples (below).

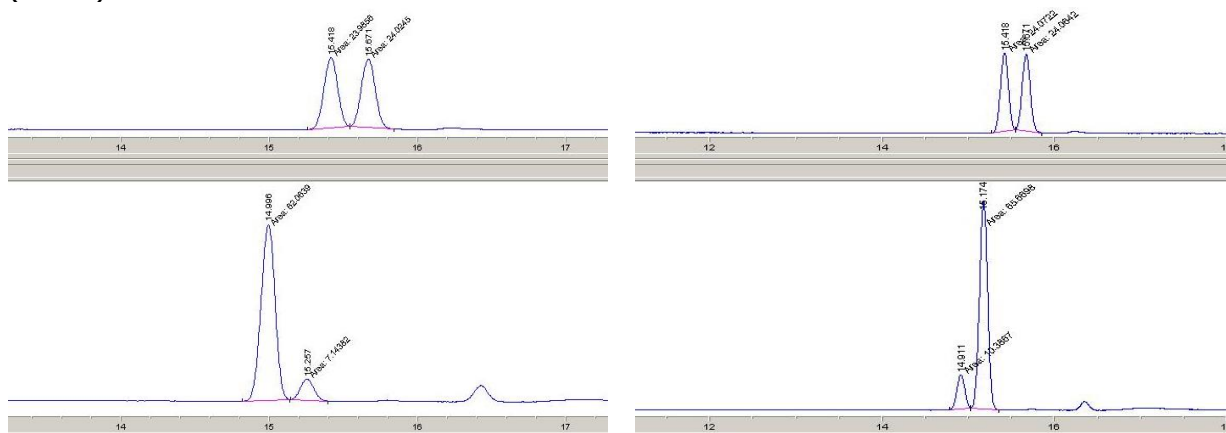


Figure 25. Chiral GC traces for ethyl syn-2-methyl-anti-3-phenylcyclopropane-1-carboxylate (**5**) (product of cyclopropanation of trans- β -methylstyrene with EDA); racemate (above) and enantioenriched sample (below). ($D_r > 50$).

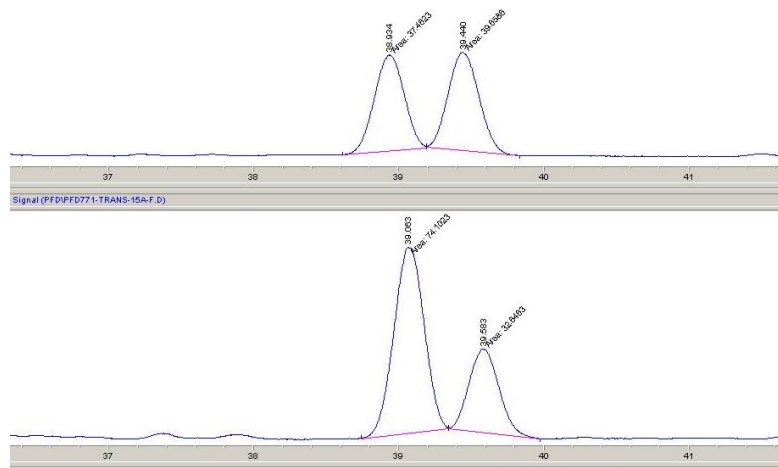


Figure 26. Chiral GC traces for cis- and trans-ethyl 2-hexylcyclopropane-1-carboxylates (**P13**) (products of cyclopropanation of 1-octene with EDA); racemate (above) and enantioenriched sample (below).

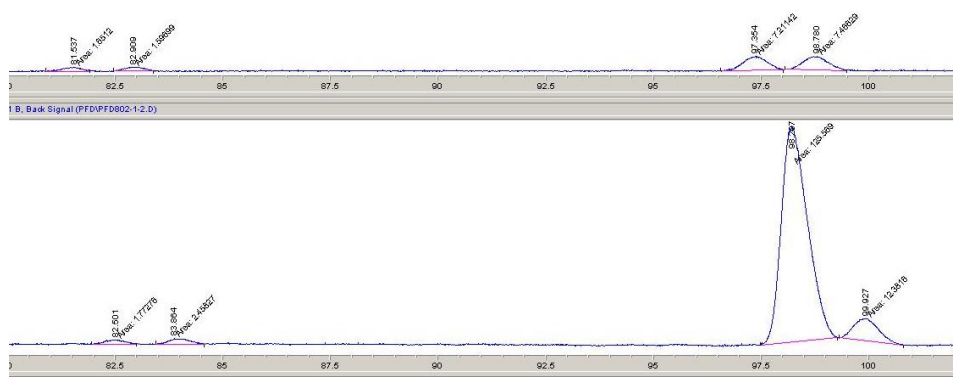


Figure 27. Chiral SFC traces for product **P6**; racemate (left) and enantioenriched samples (center, right).

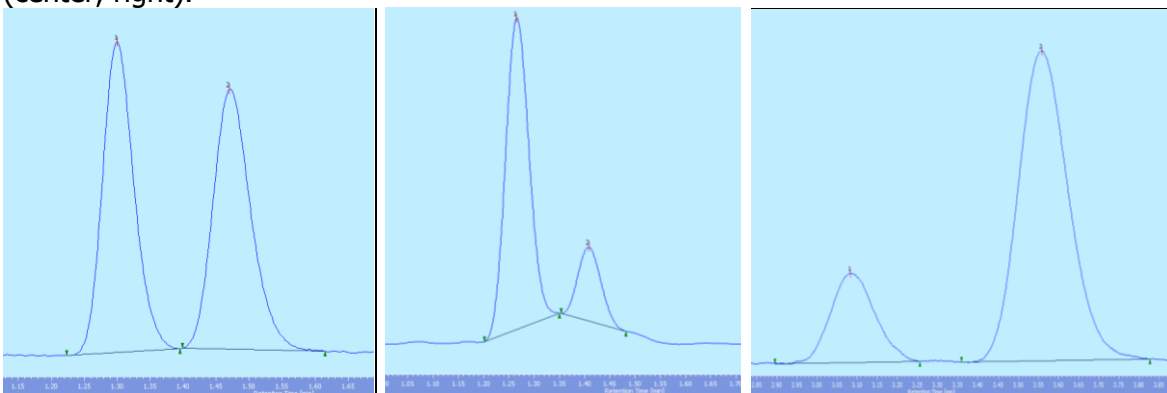


Figure 28. Chiral SFC traces for product **P9**; racemate (left) and enantioenriched samples (center, right).

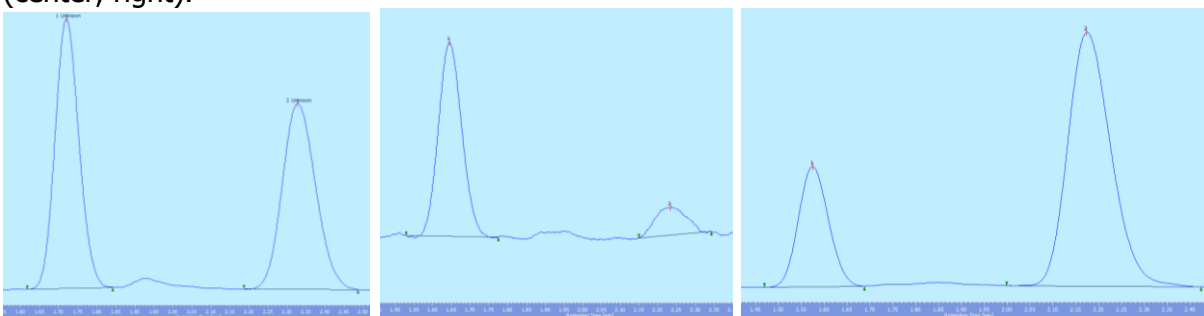
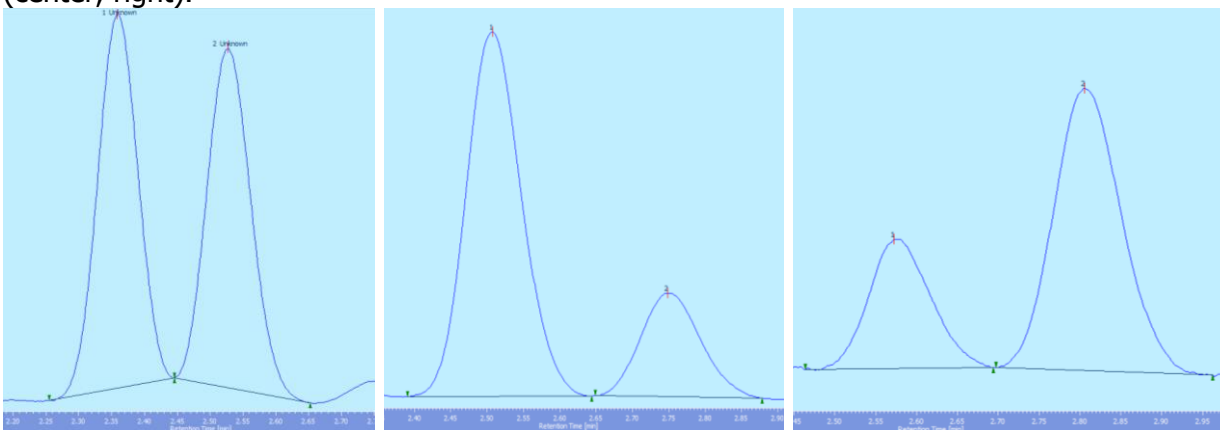


Figure 29. Chiral SFC traces for product **P10**; racemate (left) and enantioenriched samples (center, right).



VII. Supplementary Tables

Table 1. Selected expression conditions evaluated in the optimization of the direct expression of apo-Myo (103C/108C)

Expression Condition	Induction Method	OD at Induction	Induction Time	Induction Temp	Media pH	Isolated Protein Yield (Per liter expression)
A	IPTG	0.61	16 h	30 °C	7.2	5 mg
B	Auto	---	24 h	30 °C	7.2	5 mg
C	IPTG	0.82	16 h	30 °C	7.2	3 mg
D	IPTG	0.98	16 h	30 °C	7.2	3 mg
E	IPTG	0.98	16 h	30 °C	8.2	20 mg
F	IPTG	1.4	16 h	15 °C	8.2	16 mg
G	IPTG	1.4	16 h	20 °C	8.2	40 mg
H	IPTG	1.4	16 h	25 °C	8.2	15 mg
I	IPTG	1.4	16 h	30 °C	8.2	18 mg

Table 2. Heme proteins and metal cofactors used in this study

A. Amino acid sequences of proteins evaluated in this study

Protein	Organism	Construction	Vector	Sequence
Myo-globin	<i>Physeter macrocephalus</i>	6xHis-TEV-Myo	2BT	EGDIHMKSSHHHHHHENLYFQSNVASEGEWQLVHLVWAKVEADVAGHGQDILIRLFKSHPETLEKFDRFKHLKTEAEMKASEDLKKHGVTVLTALGAILKKKGHHEAELKPLAQSHATKHKIPIKYLEFISEAIIHVLHSRHPGDFGADAQGAMNKALELFRKDIAAKYKELGYQG
mOCR-Myo-globin	<i>Physeter macrocephalus</i>	6xHis-TEV-mOCR-Myo	2BT	EGDIHMKSSHHHHHHENLYFQSNMNSNMTYNNVFDHAYEMLKENIRYDDIRDTDDLHD AIHMAADNAVPHYYADIRSVMASEGIDLEFEDSGLMPDTKDDIRILQARIYEQLTIDLWEDAEDLLNEYLEEVEEYEEDEEGTSETPGTSESVLSEGEWQLVHLVWAKVEADVAGHGQDILIRLFKSHPETLEKFDRFKHLKTEAEMKASEDLKKHGVTVLTALGAILKKKGHHEAELKPLAQSHATKHKIPIKYLEFISEAIIHVLHSRHPGDFGADAQGAMNKALELFRKDIAAKYKELGYQG
P450 BM3	<i>Bacillus megaterium</i>	P450-BM3-6xHis	pcWori	MTIKEMPQPKTFGELKNLPLLNTDKPVQALMKIADDELGEIFKFEAPGRVTRYLSSQRLIKEACDESFRDKNLSQALKFARDFAGDGLVTSWTHEKNWKKAHNILLPSFSQQAMKGYHAMMVDIAVQLVQKWERLNADEHIEVSEDMTRLTLDITGLCGFNRYRFNSFYRDQPHFPIISMVRALDEVNKLQRANPDDPAYDENKRQFQEDIKVMNDLVDKIIADRKARGEQSDDLTLQMLNGKDPETGEPLDDGNIRYQIITFLIAGHEATSGLLSFALYFLVKNPHVLQKVAEEAARVLVDPVPSYKQVKQLKYVGMVLNEALRLWPTAPAFSLYAKEDTVLGGEYPLEKGDEVMVLI PQLHRDKTVWGDDVEEFRPERFENPSAIPQHAFKPFNGGQRASIGQQFALHEATLV LGMMLKHFD FEDHTNYELD IKETLTLKPKGFVVKAKSKKI PLGGIPSPSTHHHHHH

B. Metal cofactors used in this study

Cofactor Abbreviation	Metal	Axial Ligand	Porphyrin Ligand	Source
Fe(Cl)-PIX	Iron	Chloride	Protoporphyrin IX	Commercial (Aldrich)
Co(Cl)-PIX	Cobalt	Chloride	Protoporphyrin IX	Commercial (Frontier Scientific)
Cu-PIX	Copper	None	Protoporphyrin IX	Commercial (Frontier Scientific)
Mn(Cl)-PIX	Manganese	Chloride	Protoporphyrin IX	Commercial (Frontier Scientific)
Rh-PIX	Rhodium	None	Protoporphyrin IX	Commercial (Frontier Scientific)
Ir(Cl)-PIX	Iridium	Chloride	Mesoporphyrin IX	Synthetic (Section II d, Page 12)
Ir(Me)-PIX	Iridium	Methyl	Mesoporphyrin IX	Synthetic (Section II d, Page 12)
Ru(CO)-PIX	Ruthenium	Carbon monoxide	Protoporphyrin IX	Commercial (Frontier Scientific)
Ag-PIX	Silver	None	Protoporphyrin IX	Commercial (Frontier Scientific)

Table 3. Most selective mutants obtained for substrates for C-H insertion in the second phase of directed evolution.

TON and selectivities obtained

Substrate	Mutant Providing (-) enantiomer					Mutant Providing (+) enantiomer				
	H93X	H64X	F43X	V68X	er (TON)	H93X	H64X	F43X	V68X	er (TON)
1	A	V	--	F	79:21 (42)	G	L	--	A	23:77 (50)
6	G	L	L	A	80:20 (68)	G	L	V	G	31:69 (46)
7	G	I	V	--	84:16 (62)	A	L	Y	G	31:69 (36)
8	A	V	--	A	90:10 (98) ^a	A	L	W	T	23:77 (164)
9	G	L	Y	--	84:16 (100)	A	V	I	T	25:75 (138)
10	A	V	H	S	77:23 (44)	G	L	L	G	33:67 (42)
11	A	A	W	G	90:10 (52)	G	L	--	A	20:80 (10)

^a Y103C, S108C as additional mutations**Table 4.** Most selective mutants obtained for substrates for C-H insertion in the directed evolution of Ir(Me)-PIX-mOCR-myo as a catalyst.

Substrate	Mutations Providing (-) enantiomer				Mutations Providing (+) enantiomer			
	H93/H64	F43/V68	Additional Mutations	er (TON)	H93/H64	F43/V68	Additional Mutations	er (TON)
1	93A, 64L	43L	33V	85:15 (134) ^a	93G, 64L	68A	32F, 99V	16:84 (62)
6	93A, 64V	43Y, 68A	97W	81:19 (128)	93G, 64L	68A	99V	20:80 (26) ^a
7	93G, 64L	43L	99F	92:8 (92)	93A, 64L	68A, 43W	97Y	25:75 (68)
8	93A, 64V	68A	103C, 108C	90:10 (98)	93A, 64L	43W, 68T	--	23:77 (164)
9	93A, 64L	43W, 68A	33I	85:15 (86)	93A, 64V	43I, 68T	--	25:75 (138)
10	93A, 64V	43H, 68S	--	77:23 (44)	93A, 64V	68A	33V, 97Y	17:83 (42)
11	93A, 64A	43W, 68G	--	90:10 (52) 90:10 (160) ^b 84:16 (7260) ^c	93G, 64L	68A	32F, 97Y	13:87 (144)

^a Reaction performed under modified conditions: 10 mM NaPi, pH = 7.5, no inhibitor^b Reaction on a synthetic scale (Section V.g): 0.12 mmol of substrate, no inhibitor, TON based on the isolated yield of the product (80%)^c Reaction performed under modified conditions: [substrate] = 0.2 M, [catalyst] = 0.005 mM, 72 h, no inhibitor

Table 5A-BB. Complete, tabulated results for the directed evolution of Ir(Me)-PIX-mOCR-Myo for the C-H insertion of substrate **1** under the standard, screening reactions conditions. Mutants are designated by the substitutions listed in the table header plus additional mutations indicated in the row and column headers of each table. Data are presented as: enantiomeric ratio (GC yield).

mOCR-Myo. H93G, H64A- 2-OMe, COOMe							
6A	68V	V68A	V68G	V68F	V68Y	V68S	V68T
43F	35 : 65 (12)	32 : 68 (8)	35 : 65 (20)	39 : 61 (16)		39 : 61 (21)	41 : 59 (14)
F43Y	49 : 51 (14)	61 : 39 (22)	59 : 41 (41)			50 : 50 (17)	
F43W	49 : 51 (12)	55 : 45 (24)	62 : 38 (38)	52 : 48 (19)			
F43L	47 : 53 (14)	67 : 33 (20)	50 : 50 (41)	50 : 50 (23)	51 : 49 (24)	58 : 42 (18)	
F43I	48 : 52 (13)	59 : 41 (28)	49 : 51 (57)	49 : 51 (19)			
F43T					46 : 54 (24)		
F43H	49 : 51 (13)	51 : 49 (12)		58 : 42 (15)	49 : 51 (13)	48 : 52 (14)	
F43V			49 : 51 (21)	44 : 56 (24)		50 : 50 (13)	

mOCR-Myo. H93G, H64V- 2-OMe, COOMe							
6B	68V	V68A	V68G	V68F	V68Y	V68S	V68T
43F	30 : 70 (18)	45 : 55 NA	45 : 55 NA	42 : 58 (15)	47 : 53 NA	45 : 55 NA	44 : 56 NA
F43Y	49 : 51 NA						
F43W	49 : 51 NA	55 : 45 (29)					
F43L	47 : 53 NA	55 : 45 (21)					
F43I	50 : 50 NA	52 : 48 (43)					
F43T	51 : 49 NA		51 : 49 (54)				
F43H		57 : 43 (35)					
F43V							

mOCR-Myo. H93G, H64L- 2-OMe, COOMe							
6C	68V	V68A	V68G	V68F	V68Y	V68S	V68T
43F	26 : 74 (37)	23 : 77 (25)	29 : 71 NA	46 : 54 (12)	77 : 23 (20)		26 : 74 (22)
F43Y		40 : 60 (24)		38 : 62 NA			
F43W	43 : 57 (16)	52 : 48 (23)	51 : 49 NA		48 : 52 (14)	47 : 53 (22)	46 : 54 (15)
F43L	32 : 68 (31)	82 : 18 (55)	48 : 52 (34)	63 : 37 (15)	72 : 28 (46)		
F43I	50 : 50 (29)	42 : 58 NA		52 : 48 (13)			
F43T		54 : 46 NA		51 : 49 (15)			
F43H	63 : 37 (40)	50 : 50 NA	53 : 47 (18)	50 : 50 (15)			
F43V	77 : 23 (20)		24 : 76 (30)	48 : 52 (15)			

mOCR-Myo. H93G, H64I- 2-OMe, COOMe							
6D	68V	V68A	V68G	V68F	V68Y	V68S	V68T
43F	36 : 64 (17)	37 : 63 NA	34 : 66 (21)	47 : 53 NA			
F43Y		56 : 44 (49)					
F43W	46 : 54 (16)	56 : 44 NA					
F43L	53 : 47 (11)		65 : 35 NA				
F43I	46 : 54 (11)	55 : 45 (25)			49 : 51 (13)		
F43T		56 : 44 NA		48 : 52 (8)			
F43H	51 : 49 (14)	56 : 44 NA					
F43V	41 : 59 (24)		48 : 52 (18)				

Table 5A-BB continued from previous page.

mOCR-Myo. H93A, H64A- 2-OMe, COOMe							
6E	68V	V68A	V68G	V68F	V68Y	V68S	V68T
43F	64 : 36 (17)	44 : 56 (19)	48 : 52 (34)	62 : 38 (7)	58 : 42 (24)	55 : 45 (31)	61 : 39 (32)
F43Y	52 : 48 (12)	54 : 46 (28)		43 : 57 (15)	50 : 50 (20)	56 : 44 (24)	36 : 64 (36)
F43W			59 : 41 (51)	55 : 45 (12)	51 : 49 (24)		54 : 46 (25)
F43L							
F43I						43 : 57 (19)	
F43T	53 : 47 (11)	56 : 44 (23)					
F43H	58 : 42 (9)	60 : 40 (14)	63 : 37 (41)			58 : 42 (20)	
F43V	60 : 40 (18)	56 : 44 (42)	61 : 39 (24)		44 : 56 (31)		

mOCR-Myo. H93A, H64V- 2-OMe, COOMe							
6F	68V	V68A	V68G	V68F	V68Y	V68S	V68T
43F	70 : 30 (30)	76 : 24 (37)		79 : 21 (21)	76 : 24 (63)	69 : 31 (28)	
F43Y	52 : 48 (6)	76 : 24 (33)	53 : 47 (19)		56 : 44 (11)	65 : 35 (26)	50 : 50 (8)
F43W	56 : 44 (9)			52 : 49 (18)	51 : 50 (10)	66 : 34 (18)	54 : 46 (11)
F43L	53 : 48 (10)	72 : 28 (27)	59 : 41 (32)	58 : 43 (4)			
F43I	52 : 48 (9)	62 : 38 (22)	53 : 47 (28)	51 : 49 (5)			43 : 57 (11)
F43T	51 : 49 (9)					52 : 48 (9)	
F43H	61 : 39 (5)		68 : 32 (26)			66 : 34 (21)	50 : 50 (12)
F43V							

mOCR-Myo. H93A, H64L- 2-OMe, COOMe							
6G	68V	V68A	V68G	V68F	V68Y	V68S	V68T
43F	77 : 23 (50)	78 : 22 (27)	64 : 36 NA	76 : 24 (29)	65 : 35 (17)	55 : 45 (7)	36 : 64 (17)
F43Y	66 : 34 (26)	75 : 25 (52)	71 : 29 (43)		54 : 46 (10)	66 : 34 (32)	
F43W	57 : 43 (17)	71 : 29 NA	67 : 33 (25)	62 : 38 (18)	51 : 49 (14)	64 : 36 (20)	44 : 56 (17)
F43L		78 : 22 (32)	68 : 32 (46)	68 : 32 (42)			
F43I	49 : 51 (26)	76 : 24 (16)	55 : 45 (12)	69 : 31 (19)	60 : 40 (15)	49 : 51 (20)	
F43T	51 : 49 (21)	72 : 29 NA	50 : 50 (16)	50 : 50 (8)	50 : 50 (15)		
F43H	68 : 32 (17)		66 : 34 (27)	70 : 30 (17)	52 : 48 (12)		
F43V	57 : 43 (6)	65 : 35 (39)		55 : 45 (25)	64 : 37 (34)	63 : 37 (25)	

mOCR-Myo. H93G, H64A- 2-OMe, COOMe							
6H	68V	V68A	V68G	V68F	V68Y	V68S	V68T
43F	73 : 27 (40)	76 : 24 (49)	68 : 32 (48)	67 : 33 (19)	69 : 31 (24)		
F43Y	55 : 45 NA	34 : 66 (28)	65 : 35 (34)				
F43W	57 : 43 (11)						
F43L	47 : 53 (13)		60 : 40 (30)				
F43I	55 : 45 (7)	61 : 39 (26)			50 : 50 (11)		
F43T	44 : 56 (12)	78 : 22 (51)	59 : 41 NA	48 : 52 NA			
F43H	56 : 44 (8)	39 : 61 (42)	62 : 38 (30)	55 : 45 NA			
F43V	60 : 40 (8)	50 : 50 (25)	62 : 38 (30)	46 : 54 (10)			

Table 5A-BB continued from previous page.

mOCR-Myo 93A, 64L, 43Y, 68A				
6I	L32X	F33X	H97X	I99X
V		68:32 (23)		
L			59:41 (21)	
I				
F		70:30 (22)	68:32 (27)	
H				
W			72:28 (42)	
Y			73:27 (59)	

mOCR-Myo 93A, 64L, 43L, 68A				
6J	L32X	F33X	H97X	I99X
V		82:18 (30)	68:32 (43)	
L		82:18 (36)		
I	73:27 (42)	78:22 (25)	68:32 (30)	
F	74:26 (36)			
H	54:46 (14)			
W	56:44 (18)	69:31 (21)	77:23 (60)	
Y	65:35 (43)	76:24 (33)	78:22 (66)	

mOCR-Myo 93G, 64L, 68A				
6K	L32X	F33X	H97X	I99X
V	25:75 (30)	31:69 (11)		21:79 (14)
L		28:72 (29)	30:70 (24)	54:46 (17)
I		33:67 (15)	50:50 (38)	
F	26:74 (31)			46:54 (7)
H	41:59 (9)			46:54 (11)
W		27:73 (21)		
Y		26:74 (26)	46:54 0	50:50 (11)

mOCR-Myo 93G, 64L, 68A				
6L	L32X	F33X	H97X	I99X
V	40:60 (27)	42:58 (13)		
L		41:59 (24)		
I	46:54 (58)			
F	49:51 (46)			
H				
W				
Y	47:53 (18)	44:56 (14)		

mOCR-Myo 93A, 64L, 43W, 68A				
6M	L32X	F33X	H97X	I99X
V		67:33 (25)		
L			64:36 (54)	
I		68:32 (33)		
F			65:35 (54)	
H		67:33 (25)		
W		65:35 (29)	76:24 (97)	
Y		67:33 (22)	73:27 (64)	

mOCR-Myo 93A, 64V, 68A, 103C, 108C				
6N	L32X	F33X	H97X	I99X
V			67:33 (41)	67:33 (32)
L		67:33 (22)	61:39 (47)	
I	59:41 (35)		62:38 (42)	
F	58:42 (32)			
H		61:39 (9)		49:51 (10)
W	53:47 (12)	63:37 (25)	70:30 (72)	67:33 (11)
Y	72:28 (62)	65:35 (19)	73:27 (69)	51:49 (11)

mOCR-Myo 93G, 64L, 43V				
6P	L32X	F33X	H97X	I99X
V		46:54 (19)		28:72 (46)
L				
I				
F				
H				
W			43:57 (41)	
Y		42:58 (26)	38:62 (57)	

mOCR-Myo 93G, 64L, 43L				
6Q	L32X	F33X	H97X	I99X
V	39:61 (17)		45:55 (45)	19:81 (61)
L			37:63 (40)	42:58 (30)
I	41:59 (27)			
F	44:56 (14)		31:69 (37)	22:78 (32)
H	44:56 (12)			
W	49:51 (12)		36:64 (29)	
Y	49:51 (18)		29:71 (34)	

Table 5A-BB continued from previous page.

mOCR-Myo 93A, 64I, 43H, 68A				
6R	L32X	F33X	H97X	I99X
V		64:36 (33)	64:36 (18)	72:28 (37)
L			60:40 (17)	
I		70:30 (15)		
F	55:45 (103)		65:35 (33)	75:25 (107)
H				
W			78:22 (58)	
Y	68:32 (21)	73:27 (35)	76:24 (41)	

mOCR-Myo 93A, 64L, 68A				
6S	L32X	F33X	H97X	I99X
V		79:21 (38)	76:24 (98)	75:25 (74)
L			54:46 (92)	
I	72:28 (69)		74:26 (93)	
F			53:47 (26)	
H				
W			66:34 (91)	
Y		69:31 (87)		

mOCR-Myo 93A, 64V, 43Y, 68A				
6T	L32X	F33X	H97X	I99X
V	71:29 (52)	60:40 (89)	56:44 (45)	75:25 (56)
L		78:22 (80)	62:38 (72)	58:42 (11)
I	75:25 (68)	69:31 (28)	59:41 (67)	76:24 (58)
F	70:30 (57)		64:36 (62)	
H		70:30 (38)		
W	65:35 (21)	68:32 (48)	78:22 (92)	51:49 (6)
Y		79:21 (77)	61:39 (81)	

mOCR-Myo 93A, 64L, 43L, 33V				
6U	L32X	F33X	H97X	I99X
V			73:27 (45)	75:25 (37)
L				
I			66:34 (56)	
F			80:20 (76)	58:42 (8)
H				
W			79:21 (67)	
Y			80:20 (76)	

mOCR-Myo 93A, 64V, 68S				
6V	L32X	F33X	H97X	I99X
V	61:39 (72)			
L			73:27 (96)	
I			66:34 (103)	
F			58:42 (89)	
H				
W			59:41 (101)	
Y	56:44 (20)	72:28 (39)		

mOCR-Myo 93A, 64L, 43W, 68A, 97Y				
6W	L32X	F33X	H97X	I99X
V	72:28 (67)	72:28 (66)		
L		74:26 (71)		
I	71:29 (66)	75:25 (55)		
F	71:29 (70)			
H	72:28 (79)	68:32 (56)		
W	68:32 (59)			
Y	67:33 (74)	68:32 (66)		

mOCR-Myo 93A, 64V, 68A				
6X	L32X	F33X	H97X	I99X
V				63:37 (71)
L		60:40 (49)		
I				
F				
H				
W				
Y		70:30 (57)		

mOCR-Myo 93G, 64L, 68A, 32F				
6Y	L32X	F33X	H97X	I99X
V			51:49 (68)	16:84 (31)
L			34:66 (69)	56:44 (14)
I			51:49 (68)	
F				33:67 (30)
H				46:54 (11)
W			39:61 (91)	
Y			25:75 (99)	54:46 (58)

Table 5A-BB continued from previous page.

mOCR-Myo93G, 64L, 3L, 9V				
6Z	L32X	F33X	H97X	I99X
V	35:65 (30)	38:62 (22)		
L		27:73 (39)		
I	34:66 (50)	29:71 (36)		
F	40:60 (30)			
H	35:65 (33)			
W	44:56 (30)	33:67 (36)		
Y	45:55 (42)	27:73 (38)		

mOCR-Myo93G, 64L, 3L, 9F				
6AA	L32X	F33X	H97X	I99X
V	45:55 (25)	37:63 (10)		
L				
I	31:69 (27)			
F	27:73 (26)			
H	49:51 (17)	47:53 (11)		
W	49:51 (24)	36:64 (26)		
Y	48:52 (22)	33:67 (26)		

mOCR-Myo93A, 64V, 3Y, 8A, 32I				
6BB	L32X	F33X	H97X	I99X
V				70:30 (57)
L				58:42 (43)
I				
F				29:71 (45)
H				
W				
Y				50:50 (15)

Table 6A-BB. Complete, tabulated results for the directed evolution of Ir(Me)-PIX-mOCR-Myo for the C-H insertion of substrate **6** under the standard, screening reactions conditions. Mutants are designated by the substitutions listed in the table header plus additional mutations indicated in the row and column headers of each table. Data are presented as: enantiomeric ratio (GC yield).

mOCR-Myo. H93G, H64A- 2-OMe, COOMe							
7A	68V	V68A	V68G	V68F	V68Y	V68S	V68T
43F	54 : 46 (8)	59 : 41 (9)	57 : 43 (10)	56 : 44 (6)			
F43Y	52 : 48 (8)	43 : 57 (10)	46 : 54 (24)				
F43W	51 : 49 (9)		47 : 53 (22)	47 : 53 (7)			
F43L	52 : 48 (10)	39 : 61 (47)	51 : 49 (24)	53 : 47 (9)			
F43I	53 : 47 (9)			51 : 50 (9)			
F43T							
F43H	52 : 48 (9)	50 : 50 (6)		55 : 45 (7)			
F43V							

mOCR-Myo. H93G, H64V- 2-OMe, COOMe							
7B	68V	V68A	V68G	V68F	V68Y	V68S	V68T
43F	69 : 31 (9)	53 : 47 NA	53 : 47 NA	48 : 52 (15)	48 : 52 NA	48 : 52 NA	55 : 45 (1)
F43Y	52 : 48 NA						
F43W	51 : 49 NA	48 : 52 (20)					
F43L	57 : 43 (8)	54 : 46 (13)					
F43I	54 : 46 NA	53 : 47 (23)					
F43T	54 : 46 NA		51 : 49 (23)				
F43H		44 : 56 (23)					
F43V							

mOCR-Myo. H93G, H64L- 2-OMe, COOMe							
7C	68V	V68A	V68G	V68F	V68Y	V68S	V68T
43F	78 : 22 (26)	69 : 31 (10)	56 : 44 NA	51 : 49 NA	38 : 63 (10)		66 : 34 (11)
F43Y		56 : 44 (12)		55 : 45 (22)			
F43W	59 : 41 (10)	51 : 49 (10)	47 : 53 NA		52 : 48 (5)		
F43L	90 : 10 (40)	40 : 60 (23)	48 : 52 (19)	52 : 48 (8)	35 : 65 (26)	54 : 46 (8)	56 : 44 (6)
F43I	56 : 44 (19)	58 : 42 NA		46 : 54 (3)			
F43T		52 : 48 NA		46 : 54 (9)			
F43H	50 : 50 (24)	55 : 45 NA	47 : 53 (9)	53 : 47 (15)			
F43V	83 : 17 (60)		80 : 20 (16)	46 : 54 (8)			

mOCR-Myo. H93G, H64I- 2-OMe, COOMe							
7D	68V	V68A	V68G	V68F	V68Y	V68S	V68T
43F	60 : 40 (17)	58 : 42 (10)	57 : 43 (15)	50 : 50 NA			
F43Y		53 : 47 (23)					
F43W	61 : 39 (9)	47 : 53 NA					
F43L	50 : 50 (8)		45 : 55 NA				
F43I	66 : 34 (10)	53 : 47 (16)			49 : 51 (8)		
F43T		48 : 52 NA		49 : 51 (5)			
F43H	57 : 43 (11)	52 : 48 NA					
F43V	84 : 17 (31)		54 : 47 (8)				

Table 6A-BB continued from previous page.

mOCR-Myo. H93A, H64A- 2-OMe, COOMe							
7E	68V	V68A	V68G	V68F	V68Y	V68S	V68T
43F	53 : 47 (10)		49 : 51 (18)	57 : 44 (2)	62 : 38 (58)		
F43Y		35 : 65 (67)		46 : 54 (15)	51 : 49 (17)	42 : 58 (47)	48 : 52 (46)
F43W			38 : 62 (78)	40 : 60 (15)	48 : 52 (23)		46 : 54 (29)
F43L	49 : 51 (8)						
F43I						55 : 45 (36)	
F43T		48 : 52 (70)					
F43H		51 : 49 (27)	39 : 61 (68)			48 : 52 (37)	
F43V					49 : 51 (27)		

mOCR-Myo. H93A, H64V- 2-OMe, COOMe							
7F	68V	V68A	V68G	V68F	V68Y	V68S	V68T
43F	48 : 52 (6)	39 : 61 (19)		48 : 52 (5)		52 : 48 (14)	
F43Y	51 : 49 (4)	39 : 61 (19)	46 : 54 (11)		49 : 51 (7)	43 : 57 (29)	47 : 53 (6)
F43W	53 : 47 (4)			40 : 60 (3)	55 : 45 (6)	54 : 46 (13)	55 : 45 (6)
F43L	51 : 49 (6)	43 : 57 (13)	37 : 63 (18)	46 : 54 (2)			
F43I	49 : 51 (5)	45 : 55 (12)	40 : 60 (15)	46 : 54 (2)			53 : 47 (6)
F43T	51 : 49 (5)					53 : 47 (6)	
F43H	52 : 48 (5)		39 : 61 (13)			47 : 53 (13)	53 : 47 (7)
F43V							

mOCR-Myo. H93A, H64L- 2-OMe, COOMe							
7G	68V	V68A	V68G	V68F	V68Y	V68S	V68T
43F	39 : 61 (14)	41 : 59 (12)	44 : 56 NA	38 : 62 NA	49 : 51 (12)	41 : 59 (8)	48 : 52 (5)
F43Y	50 : 50 (8)	35 : 65 (21)	31 : 69 (18)		48 : 52 (10)	44 : 56 (16)	
F43W	49 : 51 (10)	33 : 68 NA	31 : 69 (13)	35 : 65 (8)	49 : 51 (8)	36 : 64 (5)	54 : 46 (5)
F43L		40 : 60 (19)	35 : 65 (21)	35 : 65 (18)			
F43I	52 : 48 NA	36 : 64 NA		31 : 69 (10)	37 : 63 (8)		
F43T	59 : 41 NA	38 : 62 NA	51 : 49 (8)		46 : 54 (8)		
F43H	41 : 59 (21)		37 : 63 (11)	35 : 65 (11)	49 : 51 (8)		
F43V	51 : 49 (3)	36 : 64 (24)		39 : 61 (14)	27 : 73 (19)	52 : 48 (15)	45 : 55 (10)

mOCR-Myo. H93G, H64A- 2-OMe, COOMe							
7H	68V	V68A	V68G	V68F	V68Y	V68S	V68T
43F	58 : 42 (19)	44 : 56 (28)		50 : 50 (9)	54 : 47 (11)		
F43Y	51 : 49 NA	65 : 35 (15)	39 : 61 (18)				
F43W	52 : 48 (7)						
F43L	56 : 44 (8)	52 : 48 NA	42 : 58 (17)				
F43I	54 : 46 (6)	44 : 56 (13)			50 : 50 (8)		
F43T	47 : 53 (7)	35 : 65 (26)	44 : 56 NA	49 : 51 NA			
F43H	51 : 49 (7)	53 : 47 (22)	42 : 58 (22)	48 : 52 NA			
F43V	51 : 49 (5)	45 : 55 (12)	39 : 61 (14)	40 : 60 (4)			

Table 6A-BB continued from previous page.

mOCR-Myo 93A, 64L, 43Y, 68A				
7I	L32X	F33X	H97X	I99X
V		38:62 (11)		
L			61:39 (15)	
I				
F			44:56 (23)	
H				
W			38:62 (29)	
Y			36:64 (30)	

mOCR-Myo 93A, 64L, 43L, 68A				
7J	L32X	F33X	H97X	I99X
V		39:61 (18)	69:31 (24)	
L		35:65 (21)		
I	38:62 (25)	39:61 (15)	68:32 (23)	
F	37:63 (22)			
H	48:52 (9)			
W	45:55 (13)	45:55 (18)	42:58 (30)	
Y	48:52 (32)	43:57 (17)	41:59 (33)	

mOCR-Myo 93G, 64L, 68A				
7K	L32X	F33X	H97X	I99X
V	64:36 (17)	61:39 (5)		71:29 (6)
L		66:34 (13)	69:31 (12)	62:38 (10)
I		63:37 (7)	71:29 (24)	
F	67:33 (20)			64:36 (4)
H	59:41 (7)			73:27 (9)
W	56:44 (10)	62:38 (8)		
Y		61:39 (15)	54:46 (3)	70:30 (8)

mOCR-Myo 93G, 64I, 68A				
7L	L32X	F33X	H97X	I99X
V	53:47 (15)	61:39 (9)		
L		59:41 (12)		
I	58:42 (33)			
F	55:45 (21)			
H				
W				
Y	57:43 (10)	53:47 (10)		

mOCR-Myo 93A, 64L, 43W, 68A				
7M	L32X	F33X	H97X	I99X
V		38:62 (13)	71:29 (38)	
L			41:59 (32)	
I		35:65 (16)		
F			31:69 (29)	
H		43:57 (16)		
W		40:60 (14)	27:73 (51)	
Y		42:58 (12)	25:75 (34)	

mOCR-Myo 93A, 64V, 68A, 103C, 108C				
7N	L32X	F33X	H97X	I99X
V			51:49 (28)	55:45 (12)
L		53:47 (9)	56:44 (22)	
I	57:43 (12)		56:44 (25)	
F	54:46 (12)			
H		53:47 (5)		62:38 (10)
W	54:46 (8)	57:43 (22)	40:60 (30)	45:55 (6)
Y	55:45 (36)	58:42 (22)	46:54 (46)	53:47 (8)

mOCR-Myo 93G, 64L, 43V				
7P	L32X	F33X	H97X	I99X
V		71:29 (11)		87:13 (58)
L				
I				
F				
H				
W			72:28 (51)	
Y		77:23 (30)	80:20 (51)	

mOCR-Myo 93G, 64L, 43L				
7Q	L32X	F33X	H97X	I99X
V	79:21 (20)		89:11 (58)	90:10 (64)
L			89:11 (64)	83:17 (39)
I	82:18 (37)			
F	76:24 (11)		86:14 (40)	92:8 (46)
H	83:17 (18)			
W	58:42 (5)		80:20 (27)	
Y	72:28 (15)		86:14 (38)	

Table 6A-BB continued from previous page.

mOCR-Myo 93A, 64I, 43H, 68A				
7R	L32X	F33X	H97X	I99X
V		44:56 (17)	52:48 (12)	41:59 (20)
L			52:48 (11)	
I		40:60 (9)		
F	45:55 (71)		47:53 (14)	40:60 (34)
H				
W			37:63 (24)	
Y	38:62 (15)	42:58 (28)	38:62 (21)	

mOCR-Myo 93A, 64L, 68A				
7S	L32X	F33X	H97X	I99X
V		39:61 (16)	46:54 (53)	44:56 (58)
L			51:49 (68)	
I	42:58 (37)		51:49 (54)	
F			51:49 (16)	
H				
W			45:55 (55)	
Y		46:54 (34)		

mOCR-Myo 93A, 64V, 43Y, 68A				
7T	L32X	F33X	H97X	I99X
V	44:56 (33)	56:44 (66)	59:41 (56)	39:61 (28)
L		36:64 (65)	50:50 (43)	52:48 (5)
I	38:62 (43)	44:56 (17)	56:44 (44)	40:60 (31)
F	33:67 (33)		46:54 (41)	
H		41:59 (23)		
W	39:61 (16)	44:56 (34)	33:67 (61)	55:45 (6)
Y		35:65 (57)	57:43 (52)	

mOCR-Myo 93A, 64L, 43L, 33V				
7U	L32X	F33X	H97X	I99X
V			60:40 (29)	41:59 (20)
L				
I			60:40 (36)	
F			42:58 (38)	53:47 (6)
H				
W			39:61 (24)	
Y			38:62 (38)	

mOCR-Myo 93A, 64V, 68S				
7V	L32X	F33X	H97X	I99X
V	55:45 (48)			
L			40:60 (58)	
I			58:42 (69)	
F			55:45 (69)	
H				
W			47:53 (61)	
Y	53:47 (13)	51:49 (28)		

mOCR-Myo 93A, 64L, 43W, 68A, 97Y				
7W	L32X	F33X	H97X	I99X
V	32:68 (42)	33:67 (43)		
L		29:71 (43)		
I	29:71 (44)	31:69 (63)		
F	29:71 (47)			
H	30:70 (55)	38:62 (67)		
W	42:58 (65)	80:20 (56)		
Y	41:59 (43)	36:64 (36)		

mOCR-Myo 93A, 64V, 68A				
7X	L32X	F33X	H97X	I99X
V				53:47 (33)
L		55:45 (28)		
I				
F				
H				
W				
Y		49:51 (37)		

mOCR-Myo 93G, 64L, 68A, 32F				
7Y	L32X	F33X	H97X	I99X
V			59:41 (36)	63:37 (35)
L			57:43 (59)	48:52 (16)
I			59:41 (49)	
F				79:21 (20)
H				63:37 (11)
W			56:44 (63)	
Y			61:39 (54)	59:41 (35)

Table 6A-BB continued from previous page.

mOCR-Myo 93G, 64L, 43L, 99V				
7Z	L32X	F33X	H97X	I99X
V	80:20 (35)	78:22 (37)		
L		88:12 (50)		
I	84:16 (58)	86:14 (43)		
F	78:22 (27)			
H	79:21 (22)			
W	62:38 (14)	85:15 (44)		
Y	72:28 (36)	82:18 (59)		

mOCR-Myo 93G, 64L, 43L, 99F				
7AA	L32X	F33X	H97X	I99X
V	74:26 (17)	65:35 (21)		
L				
I	86:14 (31)			
F	88:12 (25)			
H	58:42 (13)	57:43 (12)		
W	53:47 (22)	84:16 (28)		
Y	61:39 (14)	81:19 (31)		

mOCR-Myo 93A, 64V, 43Y, 68A, L32I				
7BB	L32X	F33X	H97X	I99X
V				39:61 (57)
L				46:54 (20)
I				
F				79:21 (41)
H				
W				
Y				62:38 (11)

Table 7A-BB. Complete, tabulated results for the directed evolution of Ir(Me)-PIX-mOCR-Myo for the C-H insertion of substrate **7** under the standard, screening reactions conditions. Mutants are designated by the substitutions listed in the table header plus additional mutations indicated in the row and column headers of each table. Data are presented as: enantiomeric ratio (GC yield).

mOCR-Myo. H93G, H64A- 2-OMe, COOMe							
8A	68V	V68A	V68G	V68F	V68Y	V68S	V68T
43F	58 : 42 (40)	69 : 31 (5)	60 : 40 (32)	49 : 51 (26)		63 : 37 (21)	55 : 45 (18)
F43Y	54 : 46 (19)	80 : 20 (38)	68 : 32 (61)			49 : 51 (25)	
F43W	52 : 48 (20)	70 : 30 (32)	67 : 33 (53)	47 : 53 (7)			
F43L	53 : 47 (19)	69 : 31 (24)	51 : 49 (55)	55 : 45 (37)	52 : 48 (42)	71 : 29 (27)	
F43I	54 : 46 (20)	71 : 29 (33)	49 : 51 (88)	48 : 52 (27)			
F43T					45 : 55 (38)		
F43H	53 : 47 (19)	55 : 45 (37)		51 : 49 (19)	47 : 53 (21)	55 : 45 (18)	
F43V			55 : 45 (25)	46 : 54 (43)		52 : 48 (13)	

mOCR-Myo. H93G, H64V- 2-OMe, COOMe							
8B	68V	V68A	V68G	V68F	V68Y	V68S	V68T
43F	60 : 40 (15)	54 : 46 NA	49 : 51 (51)	65 : 35 (16)	50 : 50 0	53 : 47 NA	51 : 49 NA
F43Y	54 : 46 NA						
F43W	52 : 48 NA	59 : 41 (33)					
F43L	53 : 47 (19)	60 : 40 (29)					
F43I	55 : 45 NA	60 : 40 (40)					
F43T	53 : 47 NA		54 : 46 (45)				
F43H		67 : 33 (41)					
F43V							

mOCR-Myo. H93G, H64L- 2-OMe, COOMe							
8C	68V	V68A	V68G	V68F	V68Y	V68S	V68T
43F	59 : 41 (13)	55 : 45 (21)	51 : 49 NA	56 : 44 NA	65 : 36 (32)		51 : 50 (21)
F43Y		67 : 33 (27)		50 : 50 0			
F43W	52 : 48 (21)	64 : 36 (29)	55 : 45 NA		54 : 46 (23)	58 : 42 (22)	46 : 54 (19)
F43L	54 : 46 (36)	90 : 10 (54)	57 : 43 (42)	64 : 36 (19)	78 : 22 (53)		
F43I	51 : 49 (42)	61 : 39 NA		50 : 50 0			
F43T		63 : 37 NA		55 : 45 (21)			
F43H	64 : 36 (52)	66 : 34 NA	53 : 47 (28)	47 : 53 (39)			
F43V	61 : 39 (25)		60 : 40 (26)	62 : 38 (17)			

mOCR-Myo. H93G, H64I- 2-OMe, COOMe							
8D	68V	V68A	V68G	V68F	V68Y	V68S	V68T
43F	69 : 31 (46)	64 : 36 (17)	56 : 44 (45)	54 : 46 (34)			
F43Y		70 : 30 (43)					
F43W	57 : 43 (19)	69 : 31 (29)					
F43L	58 : 42 (15)		71 : 29 NA				
F43I	61 : 39 (14)	65 : 35 (28)			49 : 51 (21)		
F43T		71 : 29 NA		54 : 46 (14)			
F43H	58 : 42 (18)	70 : 30 NA					
F43V	60 : 40 (25)		55 : 45 (26)				

Table 7A-BB continued from previous page.

mOCR-Myo. H93A, H64A- 2-OMe, COOMe							
8E	68V	V68A	V68G	V68F	V68Y	V68S	V68T
43F	69 : 31 (26)	48 : 52 (31)	73 : 27 (38)	45 : 55 (9)	56 : 44 (65)	71 : 29 (34)	64 : 36 (48)
F43Y	63 : 37 (20)	83 : 18 (61)		51 : 49 (15)	56 : 44 (21)		
F43W			71 : 29 (55)	53 : 47 (14)	54 : 46 (24)		55 : 45 (31)
F43L							
F43I						63 : 38 (30)	
F43T	65 : 35 (17)	74 : 26 (56)					
F43H	44 : 56 (23)	78 : 22 (25)	78 : 22 (55)				
F43V	68 : 32 (26)	72 : 28 (64)	72 : 28 (41)				

mOCR-Myo. H93A, H64V- 2-OMe, COOMe							
8F	68V	V68A	V68G	V68F	V68Y	V68S	V68T
43F	80 : 20 (19)	86 : 14 (36)		63 : 37 (28)	66 : 34 (71)	88 : 12 (20)	
F43Y	54 : 46 (12)	89 : 11 (50)	61 : 39 (23)		55 : 45 (21)	80 : 20 (51)	49 : 51 (14)
F43W	65 : 35 (12)			61 : 39 (10)	52 : 48 (26)	75 : 25 (34)	
F43L	54 : 46 (18)	82 : 18 (37)	65 : 35 (46)	52 : 48 (6)			
F43I	55 : 45 (14)	76 : 24 (31)	60 : 40 (42)	36 : 64 (7)			31 : 69 (22)
F43T	52 : 48 (12)					62 : 38 (21)	
F43H	66 : 34 (12)		80 : 20 (41)			81 : 19 (50)	38 : 62 (33)
F43V							

mOCR-Myo. H93A, H64L- 2-OMe, COOMe							
8G	68V	V68A	V68G	V68F	V68Y	V68S	V68T
43F	83 : 17 (74)	84 : 16 (36)		79 : 21 NA	63 : 37 (43)	64 : 36 (13)	57 : 43 (28)
F43Y	76 : 24 (33)	85 : 15 (66)	81 : 19 (55)		57 : 43 (27)	83 : 17 (40)	
F43W	60 : 40 (17)	78 : 22 NA	76 : 24 (39)	54 : 46 (26)	53 : 47 (16)	65 : 35 (29)	23 : 77 (82)
F43L		83 : 17 (35)	76 : 24 (55)	76 : 24 (73)			
F43I	51 : 49 (23)	73 : 27 NA	60 : 40 (22)	58 : 42 (31)	56 : 44 (8)	33 : 67 (52)	
F43T	52 : 48 (30)	75 : 25 NA	51 : 49 (19)	51 : 49 (8)	56 : 44 NA		
F43H	70 : 30 (49)		73 : 27 (39)	60 : 40 (24)	50 : 50 (13)		
F43V	67 : 33 (12)	76 : 24 (62)		45 : 55 (49)	45 : 55 NA	64 : 36 (30)	79 : 21 (26)

mOCR-Myo. H93G, H64A- 2-OMe, COOMe							
8H	68V	V68A	V68G	V68F	V68Y	V68S	V68T
43F	68 : 32 (51)	84 : 16 (56)	84 : 16 (76)	57 : 43 (27)	61 : 40 (48)		
F43Y	50 : 50 (46)		72 : 28 (56)				
F43W	68 : 32 (15)	60 : 40 (29)					
F43L	54 : 46 (18)	54 : 46 NA	67 : 33 (42)				
F43I	67 : 33 (13)	67 : 33 (51)			48 : 52 (16)		
F43T	35 : 65 (23)	74 : 26 (53)	63 : 37 NA	50 : 50 (46)			
F43H	65 : 35 (14)	80 : 20 (82)	73 : 27 (36)	54 : 46 (34)			
F43V		53 : 47 (33)	70 : 30 (38)	51 : 49 (13)			

Table 7A-BB continued from previous page.

mOCR-Myo 93A, 64L, 43Y, 68A				
8I	L32X	F33X	H97X	I99X
V		74:26 (39)		
L			66:34 (32)	
I				
F		77:23 (26)	76:24 (38)	
H				
W			73:27 (58)	
Y			85:15 (76)	

mOCR-Myo 93A, 64L, 43L, 68A				
8J	L32X	F33X	H97X	I99X
V		80:20 (33)	65:35 (37)	
L		82:18 (34)		
I	76:24 (44)	74:26 (34)	64:36 (24)	
F	77:23 (40)			
H	64:36 (23)			
W	65:35 (28)	72:28 (32)	81:19 (61)	
Y	72:28 (63)	79:21 (32)	81:19 (66)	

mOCR-Myo 93G, 64L, 68A				
8K	L32X	F33X	H97X	I99X
V	58:42 (30)	59:41 (12)		41:59 (10)
L		58:42 (28)	61:39 (23)	61:39 (11)
I		63:37 (14)	65:35 (46)	
F	57:43 (42)			53:47 (6)
H	58:42 (11)			46:54 (12)
W	51:49 (20)	54:46 (19)		
Y		54:46 (31)	52:48 (5)	57:43 (13)

mOCR-Myo 93G, 64I, 68A				
8L	L32X	F33X	H97X	I99X
V	61:39 (43)	63:37 (17)		
L		60:40 (42)		
I	67:33 (71)			
F	66:34 (64)			
H				
W				
Y	64:36 (26)	58:42 (32)		

mOCR-Myo 93A, 64L, 43W, 68A				
8M	L32X	F33X	H97X	I99X
V		72:28 (43)		
L			67:33 (90)	
I		71:29 (53)		
F			76:24 (57)	
H		71:29 (58)		
W		69:31 (61)	79:21 (92)	
Y		73:27 (53)	78:22 (57)	

mOCR-Myo 93A, 64V, 68A, 103C, 108C				
8N	L32X	F33X	H97X	I99X
V			69:31 (61)	81:19 (52)
L		77:23 (31)	62:38 (71)	
I	73:27 (37)		65:35 (74)	
F	73:27 (27)			
H		73:27 (23)		52:48 (17)
W	53:47 (17)	78:22 (38)	76:24 (75)	65:35 (16)
Y	76:24 (69)	78:22 (30)	81:19 (71)	52:48 (12)

mOCR-Myo 93G, 64L, 43V				
8P	L32X	F33X	H97X	I99X
V		56:44 (13)		55:45 (38)
L				
I				
F				
H				
W			60:40 (61)	
Y		57:43 (33)	60:40 (63)	

mOCR-Myo 93G, 64L, 43L				
8Q	L32X	F33X	H97X	I99X
V	57:43 (21)		56:44 (56)	47:53 (28)
L			55:45 (44)	52:48 (28)
I	58:42 (37)			
F	61:39 (13)		58:42 (47)	45:55 (15)
H	61:39 (16)			
W	52:48 (14)		56:44 (35)	
Y	67:33 (21)		55:45 (37)	

Table 7A-BB continued from previous page.

mOCR-Myo 93A, 64I, 43H, 68A				
8R	L32X	F33X	H97X	I99X
V		75:25 (43)	72:28 (43)	85:15 (57)
L			68:32 (40)	
I		81:19 (28)		
F	76:24 (96)		84:16 (48)	87:13 (95)
H				
W			88:12 (82)	
Y	74:26 (43)	78:22 (71)	89:11 (58)	

mOCR-Myo 93A, 64L, 68A				
8S	L32X	F33X	H97X	I99X
V		83:17 (46)	79:21 (80)	84:16 (66)
L			77:23 (55)	
I	81:19 (62)		80:20 (72)	
F			55:45 (34)	
H				
W			83:17 (94)	
Y		86:14 (67)		

mOCR-Myo 93A, 64V, 43Y, 68A				
8T	L32X	F33X	H97X	I99X
V	78:22 (57)	65:35 (89)	61:39 (53)	81:19 (72)
L			66:34 (76)	73:27 (15)
I	76:24 (81)	80:20 (44)	64:36 (83)	84:16 (72)
F	83:17 (63)		80:20 (47)	
H		83:17 (53)		
W	77:23 (40)	81:19 (40)	84:16 (60)	58:42 (15)
Y		35:65 (57)	64:36 (50)	

mOCR-Myo 93A, 64L, 43L, 33V				
8U	L32X	F33X	H97X	I99X
V			70:30 (60)	78:22 (51)
L				
I			67:33 (58)	
F			81:19 (76)	55:45 (17)
H				
W			82:18 (76)	
Y			80:20 (95)	

mOCR-Myo 93A, 64V, 68S				
8V	L32X	F33X	H97X	I99X
V	83:17 (75)			
L			85:15 (55)	
I			77:23 (103)	
F			81:19 (107)	
H				
W			76:24 (105)	
Y	62:38 (27)	85:15 (63)		

mOCR-Myo 93A, 64L, 43W, 68A, 97Y				
8W	L32X	F33X	H97X	I99X
V	75:25 (84)	78:22 (86)		
L		79:21 (99)		
I	73:27 (85)	80:20 (58)		
F	70:30 (86)			
H	78:22 (104)	82:18 (54)		
W	62:38 (104)			
Y	53:47 (89)	85:21.5 (77)		

mOCR-Myo 93A, 64V, 68A				
8X	L32X	F33X	H97X	I99X
V				53:47 (33)
L		55:45 (28)		
I				
F				
H				
W				
Y		49:51 (37)		

mOCR-Myo 93G, 64L, 68A, 32F				
8Y	L32X	F33X	H97X	I99X
V			59:41 (83)	62:38 (58)
L			54:46 (72)	61:39 (20)
I			59:41 (81)	
F				53:47 (27)
H				50:50 (21)
W			59:41 (80)	
Y			52:48 (88)	61:39 (63)

Table 7A-BB continued from previous page.

mOCR-Myo 93G, 64L, 43L, 99V				
8Z	L32X	F33X	H97X	I99X
V	54:46 (37)	47:53 (22)		
L		49:51 (26)		
I	53:47 (48)	52:48 (28)		
F	57:43 (27)			
H	54:46 (24)			
W	51:49 (55)	49:51 (30)		
Y	68:32 (48)	51:49 (52)		

mOCR-Myo 93G, 64L, 43L, 99F				
8AA	L32X	F33X	H97X	I99X
V	49:51 (21)	49:51 (23)		
L				
I	47:53 (21)			
F	46:54 (21)			
H	49:51 (34)	50:50 (11)		
W	51:49 (24)	48:52 (24)		
Y	52:48 (39)	49:51 (19)		

mOCR-Myo 93A, 64V, 43Y, 68A, L32I				
8BB	L32X	F33X	H97X	I99X
V				79:21 (58)
L				68:32 (45)
I				
F				58:42 (50)
H				
W				
Y				55:45 (33)

Table 8A-BB. Complete, tabulated results for the directed evolution of Ir(Me)-PIX-mOCR-Myo for the C-H insertion of substrate **8** under the standard, screening reactions conditions. Mutants are designated by the substitutions listed in the table header plus additional mutations indicated in the row and column headers of each table. Data are presented as: enantiomeric ratio (GC yield).

mOCR7Myo.4H93G,4H64A72DMe,-COOMe							
9A	68V	V68A	V68G	V68F	V68Y	V68S	V68T
43F	36 : 64 (7)	21 : 79 (5)	34 : 66 (6)	43 : 57 (2)		22 : 78 (9)	41 : 59 (4)
F43Y		23 : 77 (11)	29 : 71 (13)			47 : 53 (3)	
F43W		27 : 73 (8)	64 : 36 (19)	45 : 55 (3)			
F43L		51 : 49 (25)	30 : 70 (16)	47 : 53 (3)	51 : 49 (4)	47 : 53 (13)	
F43I		28 : 72 (9)	38 : 62 (20)	47 : 53 (3)			
F43T	47 : 53 (2)				50 : 50 (3)		
F43H		50 : 50 0		45 : 55 (3)	48 : 52 (2)	37 : 63 (2)	
F43V			41 : 59 (7)	42 : 58 (5)		42 : 58 (1)	

mOCR7Myo.4H93G,4H64V72DMe,-COOMe							
9B	68V	V68A	V68G	V68F	V68Y	V68S	V68T
43F	34 : 66 (3)			36 : 64 (4)			
F43Y							
F43W		44 : 56 NA					
F43L		32 : 68 NA					
F43I		33 : 68 NA					
F43T			35 : 65 NA				
F43H		41 : 60 NA					
F43V							

mOCR7Myo.4H93G,4H64L72DMe,-COOMe							
9C	68V	V68A	V68G	V68F	V68Y	V68S	V68T
43F	35 : 65 (3)	20 : 80 (5)	30 : 70 (15)	48 : 52 (7)	53 : 47 (6)		33 : 67 (5)
F43Y	71 : 29 (51)	26 : 74 (11)		48 : 52 NA			
F43W		38 : 62 (16)		25 : 75 (5)	43 : 57 (23)	41 : 59 (5)	44 : 56 (3)
F43L	31 : 69 (5)	37 : 63 (15)	40 : 60 (25)	45 : 55 (4)	68 : 32 (32)		
F43I	49 : 51 NA	31 : 69 (8)		42 : 58 (1)			
F43T		39 : 61 (4)		49 : 51 (4)			
F43H	50 : 50 NA	32 : 68 (7)	38 : 62 (19)	49 : 51 (6)			
F43V	32 : 68 (4)		35 : 65 (15)	57 : 43 (4)			

mOCR7Myo.4H93G,4H64I72DMe,-COOMe							
9D	68V	V68A	V68G	V68F	V68Y	V68S	V68T
43F	34 : 66 (7)	20 : 80 (14)	29 : 71 (22)				
F43Y		27 : 73 NA					
F43W	43 : 57 (5)	41 : 59 NA					
F43L							
F43I	38 : 62 (2)	26 : 74 NA					
F43T							
F43H	44 : 56 (2)						
F43V	29 : 71 (15)		27 : 73 (10)				

Table 8A-BB continued from previous page.

mOCR7Myo.4H93A,4H64A72OMe,-COOMe							
9E	68V	V68A	V68G	V68F	V68Y	V68S	V68T
43F	47 : 53 (4)	49 : 51 (5)	60 : 40 (8)	53 : 47 (3)	38 : 62 (6)	63 : 37 (12)	42 : 58 (6)
F43Y	56 : 44 (0)	79 : 21 (29)		55 : 45 (4)	49 : 51 (3)		
F43W			93 : 7 (71)	72 : 28 (7)	48 : 52 (4)		55 : 45 (8)
F43L							
F43I							
F43T	57 : 43 (3)	67 : 33 (18)					
F43H	55 : 45 (3)	22 : 78 (7)	53 : 47 (14)				
F43V	52 : 48 (6)	63 : 37 (32)	66 : 34 (8)				

mOCR7Myo.4H93A,4H64V72OMe,-COOMe							
9F	68V	V68A	V68G	V68F	V68Y	V68S	V68T
43F	45 : 55 (2)	49 : 51 (13)		57 : 43 (2)	47 : 53 (14)	43 : 57 (4)	
F43Y		70 : 30 (29)	41 : 59 (3)		61 : 39 (3)	67 : 33 (14)	52 : 49 (1)
F43W	57 : 43 (3)			80 : 20 (7)	61 : 39 NA	81 : 19 (22)	52 : 49 (3)
F43L	61 : 39 (17)		55 : 45 (24)	53 : 47 (1)			
F43I	59 : 41 (14)	55 : 45 (22)		53 : 47 (1)			46 : 54 (1)
F43T							
F43H	52 : 48 (1)		53 : 47 (31)				45 : 55 (1)
F43V							

mOCR7Myo.4H93A,4H64L72OMe,-COOMe							
9G	68V	V68A	V68G	V68F	V68Y	V68S	V68T
43F	39 : 61 (19)	49 : 51 (8)	46 : 54 (7)	53 : 47 (9)	49 : 51 (17)	42 : 58 (2)	37 : 63 (3)
F43Y	47 : 53 (9)	61 : 39 (33)	65 : 35 (17)		47 : 53 (4)	56 : 44 (14)	
F43W	52 : 48 NA	77 : 23 (26)	76 : 24 (29)	60 : 40 (12)	47 : 53 (2)	69 : 31 (27)	39 : 61 (7)
F43L		54 : 46 (11)	32 : 68 (14)	54 : 46 (23)			
F43I	52 : 48 NA	46 : 54 (4)	53 : 47 (6)	53 : 47 (6)	52 : 48 (4)	41 : 59 (5)	
F43T	52 : 48 NA	52 : 48 (34)	49 : 51 (2)	54 : 46 (1)	52 : 48 (4)		
F43H	47 : 53 (10)		56 : 45 (12)	57 : 43 (5)			
F43V	52 : 48 (2)	62 : 38 (23)		53 : 47 (4)	55 : 45 (8)	50 : 50 (3)	54 : 46 (6)

mOCR7Myo.4H93G,4H64A72OMe,-COOMe							
9H	68V	V68A	V68G	V68F	V68Y	V68S	V68T
43F	41 : 59 (8)	52 : 48 (25)	55 : 45 (21)				
F43Y		46 : 54 (6)					
F43W	54 : 46 (13)						
F43L							
F43I		57 : 43 NA					
F43T	48 : 52 (2)	55 : 45 (17)					
F43H	49 : 51 (11)	34 : 66 (5)					
F43V	49 : 51 (14)	41 : 59 (10)	55 : 45 (18)				

Table 8A-BB continued from previous page.

mOCR-Myo 93A, 64L, 43Y, 68A				
9I	L32X	F33X	H97X	I99X
V		57:43 (6)		
L			47:53 (4)	
I				
F			59:41 (12)	
H				
W			74:26 (18)	
Y			68:32 (13)	

mOCR-Myo 93A, 64L, 43L, 68A				
9J	L32X	F33X	H97X	I99X
V		57:43 (3)	46:54 (10)	
L		55:45 (10)		
I	70:30 (26)	54:46 (11)	48:52 (6)	
F	53:47 NA			
H	49:51 (6)			
W	45:55 (3)	60:40 (18)	58:42 (35)	
Y	52:48 (10)	55:45 (13)	54:46 (49)	

mOCR-Myo 93G, 64L, 68A				
9K	L32X	F33X	H97X	I99X
V	21:79 (12)	25:75 (3)		28:72 (2)
L		24:76 (8)	26:74 (4)	37:63 (6)
I		24:76 (4)	43:57 (12)	
F	15:85 (16)			41:59 (2)
H	31:69 (2)			45:55 (1)
W	24:76 (5)	25:75 (3)		
Y		30:70 (7)	43:57 (3)	43:57 (3)

mOCR-Myo 93G, 64I, 68A				
9L	L32X	F33X	H97X	I99X
V	22:78 (18)	23:77 (5)		
L		23:77 (13)		
I	30:70 (61)			
F	18:82 (44)			
H				
W				
Y	22:78 (11)	35:65 (6)		

mOCR-Myo 93A, 64L, 43W, 68A				
9M	L32X	F33X	H97X	I99X
V				
L			67:33 (23)	
I		65:35 (17)		
F			75:25 (54)	
H		58:42 (10)		
W		61:39 (15)	82:18 (100)	
Y		57:43 (6)	79:21 (56)	

mOCR-Myo 93A, 64V, 68A, 103C, 108C				
9N	L32X	F33X	H97X	I99X
V			51:49 (19)	46:54 (12)
L		57:43 (10)	46:54 (28)	
I	49:51 (11)		48:52 (15)	
F	46:54 (8)			
H		44:56 (8)		52:48 (4)
W	51:49 (6)	49:51 (12)	56:44 (59)	53:47 (3)
Y	51:49 (24)	49:51 (6)	53:47 (86)	49:51 (2)

mOCR-Myo 93G, 64L, 43V				
9P	L32X	F33X	H97X	I99X
V		48:52 (2)		40:60 (11)
L				
I				
F				
H				
W			37:63 (16)	
Y		42:58 (6)	32:68 (14)	

mOCR-Myo 93G, 64L, 43L				
9Q	L32X	F33X	H97X	I99X
V	46:54 (8)		44:56 (17)	35:65 (8)
L			43:57 (11)	44:56 (13)
I	44:56 (18)			
F	47:53 (20)		41:59 (17)	41:59 (4)
H	47:53 (9)			
W	49:51 (1)		45:55 (19)	
Y	47:53 (13)		42:58 (14)	

Table 8A-BB continued from previous page.

mOCR-Myo 93A, 64I, 43H, 68A				
9R	L32X	F33X	H97X	I99X
V		50:50 (23)	48:52 (9)	47:53 (19)
L			61:39 (6)	
I		53:47 (10)		
F	51:49 (57)		40:60 (14)	40:60 (41)
H				
W			44:56 (33)	
Y	53:47 (6)	54:46 (27)	52:48 (26)	

mOCR-Myo 93A, 64L, 68A				
9S	L32X	F33X	H97X	I99X
V		47:53 (11)	44:56 -12	41:59 (21)
L			51:49 (23)	
I	40:60 (29)		43:57 (33)	
F			49:51 (12)	
H				
W			37:63 (39)	
Y		28:72 (17)		

mOCR-Myo 93A, 64V, 43Y, 68A				
9T	L32X	F33X	H97X	I99X
V	71:29 (57)	62:38 (81)	59:41 (28)	64:36 (35)
L		76:24 (93)	60:40 (39)	53:47 (3)
I	83:17 (81)	65:35 (16)	60:40 (28)	72:28 (49)
F	73:27 (63)		58:42 (41)	
H		56:44 (18)		
W	62:38 (6)	53:47 (46)	73:27 (54)	51:49 (1)
Y		71:29 (89)	59:41 (49)	

mOCR-Myo 93A, 64L, 43L, 33V				
9U	L32X	F33X	H97X	I99X
V			50:50 (18)	42:58 (11)
L				
I			51:49 (11)	
F			56:44 (44)	49:51 (18)
H				
W			59:41 (37)	
Y			57:43 (68)	

mOCR-Myo 93A, 64V, 68S				
9V	L32X	F33X	H97X	I99X
V	39:61 (9)			
L			36:64 (32)	
I			38:62 (35)	
F			48:52 (53)	
H				
W			51:49 (57)	
Y	47:53 (4)	46:54 (18)		

mOCR-Myo 93A, 64L, 43W, 68A, 97Y				
9W	L32X	F33X	H97X	I99X
V				40:60 (33)
L		50:50 (19)		
I				
F				
H				
W				
Y		48:52 (30)		

mOCR-Myo 93A, 64V, 68A				
9X	L32X	F33X	H97X	I99X
V				53:47 (33)
L		55:45 (28)		
I				
F				
H				
W				
Y		49:51 (37)		

mOCR-Myo 93G, 64L, 68A, 32F				
9Y	L32X	F33X	H97X	I99X
V			36:64 (15)	13:87 (13)
L			19:81 (20)	45:55 (30)
I			40:60 (20)	
F				47:53 (24)
H				49:51 (17)
W			16:84 (62)	
Y			13:87 (63)	46:54 (28)

Table 8A-BB continued from previous page.

mOCR-Myo 93G, 64L, 43L, 99V				
9Z	L32X	F33X	H97X	I99X
V	31:69 (6)	46:54 (1)		
L		32:68 (5)		
I	27:73 (11)	33:67 (4)		
F	35:65 (4)			
H	47:53 (28)			
W	47:53 (20)	33:67 (5)		
Y	42:58 (11)	29:71 (4)		

mOCR-Myo 93G, 64L, 43L, 99F				
9AA	L32X	F33X	H97X	I99X
V	41:59 (4)	49:51 (1)		
L				
I	39:61 (4)			
F	39:61 (4)			
H	49:51 (4)	50:50 (2)		
W	50:50 (27)	48:52 (4)		
Y	51:49 (34)	49:51 (12)		

mOCR-Myo 93A, 64V, 43Y, 68A, L32I				
9BB	L32X	F33X	H97X	I99X
V				82:18 (74)
L				59:41 (15)
I				
F				40:60 (19)
H				
W				
Y				49:51 (16)

Table 9A-BB. Complete, tabulated results for the directed evolution of Ir(Me)-PIX-mOCR-Myo for the C-H insertion of substrate **9** under the standard, screening reactions conditions. Mutants are designated by the substitutions listed in the table header plus additional mutations indicated in the row and column headers of each table. Data are presented as: enantiomeric ratio (GC yield).

mOCR7Myo.4H93G,4H64A7270Me,-COOMe							
10A	68V	V68A	V68G	V68F	V68Y	V68S	V68T
43F	49 : 51 (20)	48 : 52 (18)	48 : 52 (18)	43 : 57 (19)		46 : 54 (NA)	46 : 54 (NA)
F43Y	49 : 51 (15)	41 : 59 (27)	70 : 30 (56)			46 : 54 (NA)	
F43W	50 : 50 (15)	63 : 37 (NA)	62 : 38 (48)	49 : 52 (23)			
F43L	50 : 50 (15)	61 : 39 (NA)	67 : 33 (62)	49 : 51 (41)	49 : 52 (NA)	58 : 42 (NA)	
F43I	51 : 49 (15)	57 : 43 (NA)	65 : 35 (NA)	44 : 56 (39)			
F43T		60 : 40			44 : 57 (NA)		
F43H	50 : 50 (16)	51 : 49 (16)		47 : 53 (22)	50 : 51 (NA)	53 : 47 (NA)	
F43V		52 : 48	71 : 29 (NA)	38 : 62 (NA)		51 : 50 (NA)	

mOCR7Myo.4H93G,4H64V7270Me,-COOMe							
10B	68V	V68A	V68G	V68F	V68Y	V68S	V68T
43F	47 : 53 (14)	47 : 53 NA	47 : 53 NA	NA (9)	48 : 52 NA	46 : 54 NA	48 : 52 NA
F43Y	51 : 49 NA						
F43W	48 : 52 NA	NA (33)					
F43L	51 : 49 NA	NA (25)					
F43I	50 : 50 NA	56 : 44 (40)					
F43T	50 : 50 NA		NA (43)				
F43H		NA (33)					
F43V							

mOCR7Myo.4H93G,4H64L7270Me,-COOMe							
10C	68V	V68A	V68G	V68F	V68Y	V68S	V68T
43F	47 : 53 (28)	31 : 69 (21)	46 : 54 (31)	49 : 51 (7)	50 : 50 (25)		34 : 66 (20)
F43Y	77 : 23 (38)			47 : 53 NA	45 : 55 (18)		
F43W		52 : 48 (27)	51 : 49 NA		48 : 52 (21)	49 : 51 (24)	48 : 52 (18)
F43L	42 : 58 (31)	80 : 20 (34)	54 : 46 (28)	61 : 39 (4)	72 : 28 (43)		
F43I	NA (24)	53 : 47 (26)		54 : 46 (1)			
F43T		59 : 41 (8)		50 : 50 (4)			
F43H	NA (45)	57 : 43 (21)	57 : 43 (28)	NA (6)			49 : 51 (16)
F43V	50 : 50 (22)		31 : 69 (23)	51 : 49 (4)			

mOCR7Myo.4H93G,4H64I7270Me,-COOMe							
10D	68V	V68A	V68G	V68F	V68Y	V68S	V68T
43F	48 : 52 (36)	46 : 54 (18)	NA (26)	48 : 52 (30)			
F43Y		55 : 45 NA					
F43W	49 : 51 (14)	55 : 45 (24)					
F43L	NA (10)		65 : 35 NA				
F43I	49 : 51 (11)	53 : 47 NA			55 : 45 (18)		
F43T		58 : 42 NA		50 : 50 (14)			
F43H	51 : 49 (15)	56 : 44 NA					
F43V	51 : 49 (25)		52 : 48 (25)				

Table 9A-BB continued from previous page.

mOCR7Myo.4H93A,4H64A72DMe,-COOMe							
10E	68V	V68A	V68G	V68F	V68Y	V68S	V68T
43F	52 : 48 (14)	48 : 52 (NA)	49 : 51 (26)	48 : 52 (7)		47 : 53 (NA)	54 : 46 (NA)
F43Y	52 : 48 (NA)	60 : 40 (NA)				59 : 41 (NA)	39 : 61 (NA)
F43W	52 : 48 (NA)		67 : 33 (NA)				
F43L	55 : 45 (13)						
F43I							
F43T	53 : 47 (NA)						
F43H	57 : 43 (NA)		57 : 43 (NA)			61 : 40 (NA)	
F43V	51 : 49 (NA)	54 : 46 (NA)			37 : 63 (NA)		

mOCR7Myo.4H93A,4H64V72DMe,-COOMe							
10F	68V	V68A	V68G	V68F	V68Y	V68S	V68T
43F	53 : 47 (14)	71 : 29 (39)		73 : 27 (14)	57 : 43 (36)	69 : 31 (26)	
F43Y	55 : 45 (8)	76 : 24 (29)	57 : 43 (29)		55 : 45 (17)	70 : 30 (21)	54 : 46 (8)
F43W	49 : 51 (12)			56 : 44 (5)	48 : 52 (10)	65 : 35 (13)	52 : 48 (11)
F43L	48 : 52 (10)	64 : 36 (36)	55 : 45 (43)	54 : 46 (4)			
F43I	56 : 44 (11)	60 : 40 (37)	53 : 47 (41)	50 : 50 (7)			45 : 55 (11)
F43T	49 : 51 (10)					48 : 52 (11)	
F43H			68 : 32 (34)			69 : 31 (23)	54 : 46 (12)
F43V							

mOCR7Myo.4H93A,4H64L72DMe,-COOMe							
10G	68V	V68A	V68G	V68F	V68Y	V68S	V68T
43F	68 : 32 (52)	71 : 29 (26)	62 : 38 (44)	64 : 36 (29)	27 : 73 (17)		42 : 58 (20)
F43Y	61 : 39 (27)	70 : 30 (37)	67 : 33 (32)		51 : 49 (27)	65 : 35 (28)	
F43W	53 : 47 (24)	63 : 37 (20)	64 : 36 (39)	48 : 52 (18)	47 : 53 (11)	51 : 49 (20)	44 : 57 (21)
F43L		69 : 31 (27)	62 : 38 (29)	63 : 37 (47)			
F43I	NA (20)	73 : 27 (16)	55 : 45 (29)	61 : 39 (23)	62 : 38 (15)	48 : 52 (30)	
F43T	NA (18)	66 : 34 (41)	56 : 44 (25)	47 : 53 (6)	52 : 48 (27)		
F43H	59 : 41 (37)		63 : 37 (32)	61 : 39 (24)	51 : 49 (9)		
F43V	53 : 47 (10)	66 : 34 (44)		51 : 49 (38)	56 : 44 (39)	59 : 41 (26)	63 : 37 (20)

mOCR7Myo.4H93G,4H64A72DMe,-COOMe							
10H	68V	V68A	V68G	V68F	V68Y	V68S	V68T
43F	65 : 35 (24)	65 : 35 (47)	65 : 35 (33)	48 : 52 (16)	49 : 52 (19)		
F43Y	51 : 49 (30)	41 : 59 (20)	60 : 40 (49)				
F43W	NA (11)						
F43L	51 : 49 (14)	46 : 54 (NA)	52 : 48 (33)				
F43I	54 : 46 (8)	58 : 42 (27)			52 : 48 (14)		
F43T	47 : 53 (15)	68 : 32 (50)		49 : 51 (29)			
F43H	56 : 44 (9)	33 : 67 (41)	51 : 49 (24)	52 : 48 (32)			
F43V	NA (10)	61 : 39 (40)	59 : 41 (43)	48 : 52 (11)			

Table 9A-BB continued from previous page.

mOCR-Myo 93A, 64L, 43Y, 68A				
10I	L32X	F33X	H97X	I99X
V		75:25 NA		
L			58:42 NA	
I				
F		67:33 NA	66:34 NA	
H				
W			70:30 NA	
Y			76:24 NA	

mOCR-Myo 93A, 64L, 43L, 68A				
10J	L32X	F33X	H97X	I99X
V		76:24 (36)	55:45 (42)	
L		76:24 (34)		
I	62:38 (42)	72:28 NA	62:38 (37)	
F	71:29 (41)			
H	58:42 NA			
W	66:34 NA	66:34 NA	60:40 (52)	
Y	50:50 (0)	69:31 (35)	68:32 (54)	

mOCR-Myo 93G, 64L, 68A				
10K	L32X	F33X	H97X	I99X
V	34:66 (29)	41:59 (10)		26:74 (11)
L		39:61 (29)	35:65 (19)	62:38 (16)
I		41:59 (13)	43:57 (43)	
F	42:58 (35)			54:46 (6)
H	46:54 (9)			53:47 (6)
W		65:35 (15)		
Y		35:65 (25)	43:57 NA	54:46 (10)

mOCR-Myo 93G, 64I, 68A				
10L	L32X	F33X	H97X	I99X
V	46:54 NA	50:50 (12)		
L		51:49 NA		
I	54:46 NA			
F	59:41 NA			
H				
W				
Y	64:36 NA	51:49 NA		

mOCR-Myo 93A, 64L, 43W, 68A				
10M	L32X	F33X	H97X	I99X
V		67:33 NA		
L			56:44 NA	
I		69:31 NA		
F			55:45 (53)	
H		67:33 NA		
W		66:34 NA	59:41 (56)	
Y		70:30 NA	60:40 (54)	

mOCR-Myo 93A, 64V, 68A, 103C, 108C				
10N	L32X	F33X	H97X	I99X
V			59:41 NA	65:35 NA
L		63:37 NA	58:42 NA	
I	62:38 NA		60:40 NA	
F	61:39 NA			
H		57:43 NA		52:48 (11)
W	55:45 (25)	60:40 NA	65:35 NA	64:36 (13)
Y	64:36 (57)	63:37 (19)	66:34 NA	52:48 NA

mOCR-Myo 93G, 64L, 43V				
10P	L32X	F33X	H97X	I99X
V		48:52 (9)		43:57 (43)
L				
I				
F				
H				
W			55:45 (31)	
Y		55:45 (21)	47:53 (38)	

mOCR-Myo 93G, 64L, 43L				
10Q	L32X	F33X	H97X	I99X
V	45:55 (12)		60:40 (29)	27:73 (23)
L			52:48 (23)	62:38 (14)
I	48:52 (19)			
F	52:48 (19)		43:57 (28)	33:67 (11)
H	50:50 (10)			
W	49:51 (6)		45:55 (23)	
Y	61:39 (12)		37:63 (21)	

Table 9A-BB continued from previous page.

mOCR-Myo 93A, 64I, 43H, 68A				
10R	L32X	F33X	H97X	I99X
V		70:30 (25)	62:38 (29)	73:27 (44)
L			53:47 (31)	
I		72:28 (20)		
F	53:47 (23)		69:31 (39)	71:29 (98)
H				
W			74:26 (61)	
Y	80:20 (33)	71:29 (45)	74:26 (50)	

mOCR-Myo 93A, 64L, 68A				
10S	L32X	F33X	H97X	I99X
V		70:30 (27)	71:29 (93)	76:24 (65)
L			56:44 (100)	
I	66:34 (45)		68:32 (78)	
F			59:41 (11)	
H				
W			63:37 (105)	
Y		73:27 (71)		

mOCR-Myo 93A, 64V, 43Y, 68A				
10T	L32X	F33X	H97X	I99X
V	73:27 (36)	58:42 (75)	55:45 (63)	79:21 (38)
L		77:23 (59)	56:44 (57)	61:39 (8)
I	67:33 (68)	71:29 (25)	56:44 (56)	77:23 (41)
F	79:21 (43)		72:28 (40)	
H		71:29 (29)		
W	74:26 (32)	69:31 (36)	81:19 (64)	55:45 (5)
Y		77:23 (66)	60:40 (54)	

mOCR-Myo 93A, 64L, 43L, 33V				
10U	L32X	F33X	H97X	I99X
V			64:36 (71)	5:28.5 (41)
L				
I			62:38 (61)	
F			67:33 (81)	61:39 (6)
H				
W			NA (87)	
Y			66:34 (102)	

mOCR-Myo 93A, 64V, 68S				
10V	L32X	F33X	H97X	I99X
V	64:36 (93)			
L			71:29 (59)	
I			61:39 (58)	
F			61:39 (59)	
H				
W			62:38 (65)	
Y	63:37 (37)	65:35 (60)		

mOCR-Myo 93A, 64L, 43W, 68A, 97Y				
10W	L32X	F33X	H97X	I99X
V	51:49 (91)	68:32 (89)		
L		63:37 (80)		
I	49:51 (91)	67:33 (NA)		
F	63:37 (95)			
H	66:34 (61)	64:36 (NA)		
W	64:36 (70)	64:36		
Y	72:28 (86)	66:34 (81)		

mOCR-Myo 93A, 64V, 68A				
10X	L32X	F33X	H97X	I99X
V				65:35 (84)
L		53:47 (72)		
I				
F				
H				
W				
Y		64:36 (73)		

mOCR-Myo 93G, 64L, 68A, 32F				
10Y	L32X	F33X	H97X	I99X
V			51:49 (62)	39:61 (30)
L			42:58 (67)	55:45 (22)
I			52:48 (67)	
F				49:51 (17)
H				46:54 (8)
W			55:45 (91)	
Y			43:57 (73)	53:47 (41)

Table 9A-BB continued from previous page.

mOCR-Myo 93G, 64L, 43L, 99V				
10Z	L32X	F33X	H97X	I99X
V	NA (45)	47:53 (11)		
L		NA (39)		
I	NA (57)	NA (31)		
F	48:52 (32)			
H	53:47 (19)			
W	46:54 (24)	NA (43)		
Y	56:44 (49)	42:58 (20)		

mOCR-Myo 93G, 64L, 43L, 99F				
10AA	L32X	F33X	H97X	I99X
V	NA (22)	51:49 (7)		
L				
I	NA (4)			
F	NA (4)			
H	48:52 (4)	51:49 (44)		
W	50:50 (27)	NA (35)		
Y	51:49 (34)	49:51 (14)		

mOCR-Myo 93A, 64V, 43Y, 68A, L32I				
10BB	L32X	F33X	H97X	I99X
V				58:42 (74)
L				54:46 (15)
I				
F				42:58 (19)
H				
W				50:50 0
Y				55:45 (14)

Table 10A-BB. Complete, tabulated results for the directed evolution of Ir(Me)-PIX-mOCR-Myo for the C-H insertion of substrate **10** under the standard, screening reactions conditions. Mutants are designated by the substitutions listed in the table header plus additional mutations indicated in the row and column headers of each table. Data are presented as: enantiomeric ratio (GC yield).

mOCR-Myo. H93G, H64A- 2-OMe, COOMe							
11A	68V	V68A	V68G	V68F	V68Y	V68S	V68T
43F	48 : 52 (32)	60 : 40 (7)	59 : 41 (30)	43 : 57 (21)		63 : 37 (16)	58 : 42 (13)
F43Y	53 : 47 (22)	74 : 26 (35)	72 : 28 (65)			48 : 52 NA	
F43W	56 : 44 NA	65 : 35 (31)	65 : 35 (55)	48 : 52 (29)			
F43L	55 : 45 (1)	62 : 38 (25)	48 : 52 (57)	48 : 52 (43)	51 : 49 (41)	64 : 36 (23)	
F43I	56 : 44 (0)	67 : 33 (38)	48 : 52 (NA)	42 : 58 (44)			
F43T	61 : 40 NA	60 : 40			45 : 55 (31)		
F43H	56 : 44 NA	55 : 45 (15)		46 : 54 (27)	54 : 46 (15)	60 : 40 (14)	
F43V			54 : 46 (34)	45 : 55 (31)		61 : 39 (14)	

mOCR-Myo. H93G, H64V- 2-OMe, COOMe							
11B	68V	V68A	V68G	V68F	V68Y	V68S	V68T
43F	47 : 53 (12)	51 : 49 NA	52 : 48 NA	52 : 48 (7)	52 : 48 NA	51 : 49 NA	47 : 53 NA
F43Y	47 : 53 NA						
F43W	51 : 49 NA	55 : 45 (44)					
F43L	53 : 47 NA	60 : 40 (38)					
F43I	53 : 47 NA	59 : 41 (52)					
F43T	51 : 49 NA		55 : 45 (49)				
F43H		61 : 39 (52)					
F43V							

mOCR-Myo. H93G, H64L- 2-OMe, COOMe							
11C	68V	V68A	V68G	V68F	V68Y	V68S	V68T
43F	50 : 50 (38)	50 : 50 (20)	52 : 48 (18)	52 : 48 (12)	49 : 51 (33)		47 : 53 (23)
F43Y	84 : 16 (50)			52 : 48 (50)	50 : 50 (20)		
F43W		56 : 44 (32)	49 : 51 NA		49 : 51 (27)	54 : 46 (28)	46 : 54 (21)
F43L	54 : 46 (36)	82 : 18 (25)	50 : 51 (42)	51 : 49 (21)	77 : 23 (51)		
F43I	57 : 43 (37)	54 : 46 (20)		57 : 43 (15)			
F43T		60 : 40 (5)		71 : 29 (6)			
F43H	60 : 40 (65)	60 : 40 (17)	52 : 48 (39)	41 : 59 (42)			53 : 47 (0)
F43V	57 : 43 (32)		52 : 48 (28)	50 : 50 (20)			

mOCR-Myo. H93G, H64I- 2-OMe, COOMe							
11D	68V	V68A	V68G	V68F	V68Y	V68S	V68T
43F	49 : 51 (44)	NA (18)	54 : 46 (34)	49 : 51 (43)			
F43Y		61 : 39 (43)					
F43W	55 : 45 (20)	58 : 42 (45)					
F43L	57 : 43 (18)		60 : 41 NA				
F43I	59 : 41 (18)	63 : 37 (32)			52 : 48 (26)		
F43T		62 : 38 NA		59 : 41 NA			
F43H	57 : 43 (20)	60 : 40 NA					
F43V	60 : 40 (44)		48 : 52 (33)				

Table 10A-BB continued from previous page.

mOCR-Myo. H93A, H64A- 2-OMe, COOMe							
11E	68V	V68A	V68G	V68F	V68Y	V68S	V68T
43F	50 : 50 (20)	47 : 53 (26)	64 : 36 (18)	41 : 59 (6)	49 : 51 (43)	63 : 38 (19)	55 : 45 (30)
F43Y	64 : 36 (18)	75 : 25 (42)		53 : 47 (14)	51 : 49 (27)	68 : 32 (27)	52 : 48 (43)
F43W	60 : 40 (30)		63 : 37 (33)	51 : 49 (3)	52 : 48 (25)		52 : 48 (40)
F43L	55 : 45 (18)						
F43I							
F43T	66 : 34 (NA)	64 : 36 (48)					
F43H	65 : 35 (13)	74 : 26 (33)	74 : 26 (55)			72 : 28 (29)	
F43V	57 : 43 (27)	61 : 39 (NA)	49 : 51 (25)				

mOCR-Myo. H93A, H64V- 2-OMe, COOMe							
11F	68V	V68A	V68G	V68F	V68Y	V68S	V68T
43F	54 : 46 (22)	72 : 28 (30)		52 : 48 (18)	NA (42)	78 : 22 (25)	
F43Y	53 : 47 (16)	80 : 20 (31)	53 : 47 (25)		47 : 53 (19)	59 : 41 (37)	55 : 45 (9)
F43W	53 : 47 (12)			51 : 49 (6)	48 : 52 (16)	67 : 33 (20)	51 : 49 (16)
F43L	52 : 48 (13)	67 : 33 (38)	58 : 42 (49)	NA (6)			
F43I	51 : 49 (20)	64 : 36 (31)	52 : 48 (38)	39 : 61 (9)			33 : 67 (31)
F43T	51 : 49 (16)					55 : 45 (20)	
F43H	59 : 41 (11)		69 : 31 (38)			78 : 22 (37)	49 : 51 (26)
F43V							

mOCR-Myo. H93A, H64L- 2-OMe, COOMe							
11G	68V	V68A	V68G	V68F	V68Y	V68S	V68T
43F	69 : 31 (58)	72 : 28 (28)	62 : 38 (13)	62 : 38 (24)	54 : 46 (23)		51 : 50 (25)
F43Y	63 : 37 (30)	75 : 25 (39)	70 : 30 (57)		51 : 49 (32)	64 : 36 (33)	
F43W	52 : 48 (30)	66 : 34 (22)	66 : 34 (43)	41 : 59 (27)	48 : 52 (11)	47 : 53 (21)	32 : 68 (38)
F43L		65 : 35 (30)	60 : 40 (46)	59 : 41 (51)			
F43I	51 : 49 (22)	68 : 32 (14)	52 : 48 (36)	45 : 55 (33)	43 : 57 (20)	37 : 63 (45)	
F43T	58 : 42 (24)	62 : 38 (28)	50 : 50 (31)	63 : 37 (6)	40 : 60 (35)		
F43H	61 : 39 (44)		63 : 37 (35)	NA (28)	NA (0)		
F43V	53 : 47 (14)	71 : 29 (46)		38 : 62 (26)	39 : 61 (47)	56 : 44 (31)	74 : 26 (26)

mOCR-Myo. H93G, H64A- 2-OMe, COOMe							
11H	68V	V68A	V68G	V68F	V68Y	V68S	V68T
43F	59 : 41 (41)	71 : 29 (41)	55 : 45 (41)	52 : 48 (23)	53 : 47 (33)		
F43Y	51 : 49 (56)	62 : 38 (23)	66 : 34 (44)				
F43W	55 : 45 (12)						
F43L		47 : 53 (NA)	59 : 41 (44)				
F43I	72 : 28 (17)	58 : 42 (41)			49 : 51 (25)		
F43T	42 : 58 (22)	62 : 38 (48)	54 : 46 (NA)	49 : 51 (46)			
F43H	56 : 44 (13)	25 : 75 (69)	63 : 37 (34)	52 : 48 (51)			
F43V	57 : 43 (19)	52 : 48 (46)	58 : 42 (15)	47 : 53 (16)			

Table 10A-BB continued from previous page.

mOCR-Myo 93A, 64L, 43Y, 68A				
11I	L32X	F33X	H97X	I99X
V		72:28 (45)		
L			56:44 (33)	
I				
F		69:31 (20)	68:32 (27)	
H				
W			71:29 (52)	
Y			75:25 (79)	

mOCR-Myo 93A, 64L, 43L, 68A				
11J	L32X	F33X	H97X	I99X
V		64:36 (42)	54:46 (53)	
L		69:31 (38)		
I	62:38 (80)	65:35 (34)	53:47 (44)	
F	68:32 (44)			
H	60:40 (30)			
W	63:37 (38)	59:41 (32)	65:35 (68)	
Y	73:27 (50)	66:34 (44)	63:37 (55)	

mOCR-Myo 93G, 64L, 68A				
11K	L32X	F33X	H97X	I99X
V	53:47 (31)	55:45 (13)		42:58 (11)
L		54:46 (34)	56:44 -23	51:49 (19)
I		57:43 (17)	41:59 -43	
F	61:39 (49)			52:48 (8)
H	59:41 (14)			52:48 (10)
W		52:48 (13)		
Y		52:48 (27)	44:56 -6	55:45 (12)

mOCR-Myo 93G, 64I, 68A				
11L	L32X	F33X	H97X	I99X
V	68:32 (24)	60:40 (18)		
L		61:39 (24)		
I	63:37 (51)			
F	51:49 (47)			
H				
W				
Y	69:31 (33)	57:43 (24)		

mOCR-Myo 93A, 64L, 43W, 68A				
11M	L32X	F33X	H97X	I99X
V		67:33 (41)		
L			59:41 (80)	
I		85:15 (43)		
F			62:38 (64)	
H		71:29 (48)		
W		70:30 (38)	69:31 (76)	
Y		73:27 (33)	62:38 (63)	

mOCR-Myo 93A, 64V, 68A, 103C, 108C				
11N	L32X	F33X	H97X	I99X
V			61:39 (69)	69:31 (38)
L		67:33 (31)	59:41 (76)	
I	63:37 (42)		61:39 (76)	
F	67:33 (36)			
H		65:35 (22)		48:52 (16)
W	51:49 (16)	71:29 (29)	64:36 (64)	59:41 (18)
Y	64:36 (66)	61:39 (25)	71:29 (88)	52:48 (16)

mOCR-Myo 93G, 64L, 43V				
11P	L32X	F33X	H97X	I99X
V		52:48 (12)		66:34 (20)
L				
I				
F				
H				
W			65:35 (52)	
Y		59:41 (26)	61:39 (59)	

mOCR-Myo 93G, 64L, 43L				
11Q	L32X	F33X	H97X	I99X
V	56:44 (73)		53:47 (55)	
L			53:47 (64)	53:47 (18)
I	56:44 (64)			
F	59:41 (58)		54:46 (56)	49:51 (14)
H	65:35 (59)			
W	55:45 (51)		56:44 (64)	
Y	73:27 (74)		55:45 (58)	

Table 10A-BB continued from previous page.

mOCR-Myo 93A, 64I, 43H, 68A				
11R	L32X	F33X	H97X	I99X
V		74:26 (35)	66:34 (4)	76:24 (4)
L			67:33 (5)	
I		75:25 (3)		
F	71:29 (102)		78:22 (52)	81:19 (70)
H				
W			84:16 (77)	
Y	79:21 (4)	76:24 (53)	77:23 (59)	

mOCR-Myo 93A, 64L, 68A				
11S	L32X	F33X	H97X	I99X
V		70:30 (28)	76:24 (68)	82:18 (65)
L			71:29 (87)	
I	70:30 (54)		72:28 (64)	
F			65:35 (27)	
H				
W			72:28 (83)	
Y		81:19 (68)		

mOCR-Myo 93A, 64V, 43Y, 68A				
11T	L32X	F33X	H97X	I99X
V	73:27 (54)	59:41 (66)	59:41 (97)	61:39 (61)
L		78:22 (59)	58:42 (99)	54:46 (16)
I	66:34 (78)	68:32 (47)	57:43 (95)	74:26 (68)
F	79:21 (74)		78:22 (60)	
H		71:29 (65)		
W	72:28 (47)	78:22 (62)	79:21 (99)	52:48 (21)
Y		75:25 (104)	60:40 (91)	

mOCR-Myo 93A, 64L, 43L, 33V				
11U	L32X	F33X	H97X	I99X
V			60:40 (64)	72:28 (42)
L				
I			65:35 (66)	
F			69:31 (83)	NA (6)
H				
W			71:29 (83)	
Y			66:34 (94)	

mOCR-Myo 93A, 64V, 68S				
11V	L32X	F33X	H97X	I99X
V	79:21 (53)			
L			78:22 (53)	
I			67:33 (92)	
F			74:26 (94)	
H				
W			70:30 (91)	
Y	67:33 (15)	82:18 (32)		

mOCR-Myo 93A, 64L, 43W, 68A, 97Y				
11W	L32X	F33X	H97X	I99X
V	58:42 (8)	67:33 (8)		
L		64:36 (8)		
I	57:43 (8)	72:28 (53)		
F	62:38 (8)			
H	69:31 (79)	73:27 (76)		
W	61:39 (67)	73:27		
Y	60:40 (9)	72:28 (46)		

mOCR-Myo 93A, 64V, 68A				
11X	L32X	F33X	H97X	I99X
V				70:30 (63)
L		71:29 (56)		
I				
F				
H				
W			61:39 (59)	
Y		74:26 (56)		

mOCR-Myo 93G, 64L, 68A, 32F				
11Y	L32X	F33X	H97X	I99X
V			56:44 (67)	73:27 (39)
L			54:46 (66)	56:44 (26)
I			56:44 (69)	
F				61:39 (16)
H				46:54 (8)
W			65:35 (77)	
Y			60:40 (71)	57:43 (58)

Table 10A-BB continued from previous page.

mOCR-Myo 93G, 64L, 43L, 99V				
11Z	L32X	F33X	H97X	I99X
V	56:44 (39)	50:50 (16)		
L		53:47 (28)		
I	56:44 (54)	53:47 (34)		
F	58:42 (34)			
H	59:41 (26)			
W	53:47 (32)	5:38.5 (36)		
Y	75:25 (58)	64:36 (25)		

mOCR-Myo 93G, 64L, 43L, 99F				
11AA	L32X	F33X	H97X	I99X
V	52:48 (24)	51:49 (14)		
L				
I	54:46 (22)			
F	52:48 (23)			
H	53:47 (17)	55:45 (15)		
W	49:51 (18)	51:49 (40)		
Y	58:42 (35)	51:49 (18)		

mOCR-Myo 93A, 64V, 43Y, 68A, L32I				
11BB	L32X	F33X	H97X	I99X
V				67:33 (73)
L				61:39 (36)
I				
F				61:39 (52)
H				
W				
Y				57:43 (16)

Table 11A-BB. Complete, tabulated results for the directed evolution of Ir(Me)-PIX-mOCR-Myo for the C-H insertion of substrate **11** under the standard, screening reactions conditions. Mutants are designated by the substitutions listed in the table header plus additional mutations indicated in the row and column headers of each table. Data are presented as: enantiomeric ratio (GC yield).

mOCR7Myo.4H93G,4H64A7270Me,-COOMe							
12A	68V	V68A	V68G	V68F	V68Y	V68S	V68T
43F	49 : 51 (14)	33 : 67 (5)	44 : 56 (18)	53 : 47 (5)		49 : 51 (8)	52 : 48 (5)
F43Y		33 : 67 (10)	76 : 24 (15)			53 : 47 (8)	
F43W	53 : 47 (22)	68 : 32 (16)	54 : 46 (21)	56 : 44 (10)			
F43L	52 : 48 (23)	51 : 49 (8)	43 : 57 (24)	56 : 44 (15)	50 : 50 (12)	58 : 42 (10)	
F43I	53 : 47 (22)	52 : 48 (12)	47 : 53 (14)	57 : 43 (15)			
F43T		57 : 43			50 : 50 (13)		
F43H	53 : 47 (27)	64 : 36 (12)		63 : 37 (10)	51 : 49 (6)	53 : 47 (6)	
F43V		65 : 35	51 : 49 (0)	60 : 40 (30)		51 : 49 (0)	

mOCR7Myo.4H93G,4H64V7270Me,-COOMe							
12B	68V	V68A	V68G	V68F	V68Y	V68S	V68T
43F	48 : 52 (14)	50 : 50 NA	50 : 50 NA	51 : 49 (3)	47 : 53 NA	47 : 53 NA	47 : 53 NA
F43Y	48 : 53 NA						
F43W	49 : 51 NA	49 : 51 (17)					
F43L		46 : 54 (17)					
F43I	49 : 51 NA	48 : 52 (14)					
F43T	50 : 50 NA		47 : 53 (20)				
F43H		53 : 47 (21)					
F43V							

mOCR7Myo.4H93G,4H64L7270Me,-COOMe							
12C	68V	V68A	V68G	V68F	V68Y	V68S	V68T
43F	49 : 51 (14)	NA (20)	44 : 56 (18)	53 : 47 (7)	47 : 53 (13)		46 : 54 NA
F43Y				51 : 49 (26)	51 : 49 (10)		
F43W	51 : 49 (12)	45 : 55 (17)	42 : 58 NA		54 : 46 NA	45 : 55 (15)	49 : 51 (12)
F43L	53 : 47 (17)	36 : 64 (15)	33 : 67 (21)	46 : 54 (10)	76 : 24 (28)		
F43I	49 : 51 (13)	39 : 61 (12)		45 : 55 (0)			
F43T		45 : 55 (6)		53 : 47 (12)			
F43H	51 : 49 (22)	53 : 47 (10)	44 : 56 (12)	51 : 49 (0)			52 : 48 (25)
F43V	60 : 40 (11)		49 : 51 (6)	45 : 55 (11)			

mOCR7Myo.4H93G,4H64I7270Me,-COOMe							
12D	68V	V68A	V68G	V68F	V68Y	V68S	V68T
43F	49 : 51 (19)	42 : 58 (18)	47 : 53 (15)	50 : 50 (23)			
F43Y		51 : 49 (19)					
F43W	53 : 47 (6)	48 : 52 (17)	49 : 51 (13)				
F43L			47 : 53 NA				
F43I	66 : 34 (9)	48 : 52 (16)			56 : 44 NA		
F43T		53 : 47 NA		57 : 43 (15)			
F43H	53 : 47 (9)	54 : 46 NA					
F43V	57 : 43 (15)		33 : 67 (13)				

Table 11A-BB continued from previous page.

mOCR7Myo.4H93A,4H64A72DMe,-COOMe							
12E	68V	V68A	V68G	V68F	V68Y	V68S	V68T
43F	49 : 51 (11)	20 : 80 (10)	36 : 64 (6)	50 : 50 (6)	53 : 47 (6)	48 : 52 (9)	51 : 49 (9)
F43Y	51 : 49 (0)	59 : 41 (14)		59 : 41 (5)	56 : 44 (9)	65 : 35 (9)	51 : 49 (10)
F43W			42 : 58 (13)	55 : 45 (4)	52 : 48 (13)		53 : 47 (11)
F43L							
F43I							
F43T	51 : 49 (4)	50 : 50 (18)					
F43H	57 : 43 (5)	65 : 35 (14)	52 : 48 (14)			70 : 30 (11)	
F43V	52 : 48 (12)	52 : 48 (NA)	51 : 49 (10)		47 : 53 (13)		

mOCR7Myo.4H93A,4H64V72DMe,-COOMe							
12F	68V	V68A	V68G	V68F	V68Y	V68S	V68T
43F	51 : 49 (8)	34 : 66 (14)		50 : 50 (2)	49 : 51 (14)	46 : 54 (10)	
F43Y	50 : 50 (5)	69 : 31 (13)	44 : 56 (27)		57 : 43 (5)	66 : 34 (22)	47 : 53 (4)
F43W	51 : 49 (4)			56 : 44 (6)	53 : 47 (5)	68 : 32 (8)	49 : 51 (6)
F43L	51 : 49 (7)	69 : 31 (13)	44 : 56 (13)	50 : 50 (1)			
F43I	51 : 49 (9)	54 : 46 (24)	47 : 53 (17)	50 : 50 (3)			50 : 50 (11)
F43T	50 : 50 (8)					63 : 37 (16)	
F43H			61 : 39 (15)			77 : 23 (22)	55 : 45 (11)
F43V							

mOCR7Myo.4H93A,4H64L72DMe,-COOMe							
12G	68V	V68A	V68G	V68F	V68Y	V68S	V68T
43F	58 : 42 (19)	44 : 56 (15)	52 : 48 (8)	38 : 62 (15)	53 : 47 (12)		49 : 51 (8)
F43Y	54 : 46 (15)	55 : 45 (17)	57 : 43 (22)		52 : 48 (16)	57 : 43 (13)	
F43W		46 : 54 (11)	69 : 31 (15)	59 : 41 (7)	53 : 47 (0)	57 : 43 (8)	39 : 61 (20)
F43L		43 : 57 (12)	39 : 61 (18)	41 : 59 (21)			
F43I	51 : 49 (13)	60 : 40 (5)	41 : 59 (18)	45 : 55 (13)	52 : 48 (5)	49 : 51 (16)	
F43T	49 : 51 (22)	44 : 56 (18)	50 : 50 (8)	52 : 48 (5)	49 : 51 (8)		
F43H	41 : 59 (31)		56 : 44 (16)	60 : 40 (11)	52 : 48 (0)		
F43V	64 : 36 (7)	58 : 42 (36)		49 : 51 (15)	47 : 53 (25)	61 : 39 (19)	63 : 37 (19)

mOCR7Myo.4H93G,4H64A72DMe,-COOMe							
12H	68V	V68A	V68G	V68F	V68Y	V68S	V68T
43F	52 : 48 (12)	40 : 60 (21)	52 : 48 (16)	52 : 48 (10)	51 : 49 (8)		
F43Y	50 : 50 (22)	60 : 40 (17)	54 : 46 (26)				
F43W	41 : 59 (4)						
F43L		54 : 46 NA	51 : 49 (13)				
F43I	51 : 49 (13)	51 : 49 (15)			50 : 50 (10)		
F43T	39 : 61 (6)	69 : 31 (26)	43 : 57 NA	52 : 48 (16)			
F43H	51 : 49 (4)	44 : 56 (27)	43 : 57 (16)	53 : 47 (22)			
F43V	56 : 44 (7)	53 : 47 (11)	47 : 53 (17)	58 : 42 (4)			

Table 11A-BB continued from previous page.

mOCR-Myo 93A, 64L, 43Y, 68A				
12I	L32X	F33X	H97X	I99X
V		48:52 (16)		
L			41:59 (10)	
I				
F		51:49 (12)	57:43 (18)	
H				
W			62:38 (24)	
Y			74:26 (22)	

mOCR-Myo 93A, 64L, 43L, 68A				
12J	L32X	F33X	H97X	I99X
V		31:69 (16)	37:63 (18)	
L		41:59 (15)		
I	32:68 (15)	29:71 (18)	35:65 (16)	
F	39:61 (15)			
H	55:45 (13)			
W	56:44 (14)	34:66 (14)	59:41 (26)	
Y	35:65 (15)	39:61 (17)	55:45 (20)	

mOCR-Myo 93G, 64L, 68A				
12K	L32X	F33X	H97X	I99X
V	40:60 (21)	32:68 (8)		45:55 (4)
L		41:59 (22)	35:65 -8	47:53 (10)
I		37:63 (9)	45:55 -16	
F	34:66 (25)			47:53 (3)
H	42:58 (7)			45:55 (3)
W		42:58 (7)		
Y		44:56 (17)	50:50 -3	43:57 (7)

mOCR-Myo 93G, 64L, 68A				
12L	L32X	F33X	H97X	I99X
V	40:60 (11)	41:59 (8)		
L		45:55 (14)		
I	35:65 (15)			
F	36:64 (14)			
H				
W				
Y	32:68 (13)	46:54 (11)		

mOCR-Myo 93A, 64L, 43W, 68A				
12M	L32X	F33X	H97X	I99X
V		46:54 (16)		
L			43:57 (18)	
I		51:49 (12)		
F			55:45 (26)	
H		44:56 (18)		
W		46:54 (16)	63:37 (41)	
Y		46:54 (5)	59:41 (38)	

mOCR-Myo 93A, 64V, 68A, 103C, 108C				
12N	L32X	F33X	H97X	I99X
V			41:59 (32)	38:62 (21)
L		60:40 (23)	41:59 (37)	
I	31:69 (28)		42:58 (33)	
F	30:70 (24)			
H		55:45 (17)		48:52 (8)
W	46:54 (16)	44:56 (22)	37:63 (42)	51:49 (8)
Y	42:58 (24)	52:48 (9)	29:71 (52)	47:53 (7)

mOCR-Myo 93G, 64L, 43V				
12P	L32X	F33X	H97X	I99X
V		53:47 (8)		61:39 (58)
L				
I				
F				
H				
W			62:38 (22)	
Y		59:41 (9)	66:34 (29)	

mOCR-Myo 93G, 64L, 43L				
12Q	L32X	F33X	H97X	I99X
V	55:45 (73)		52:48 (12)	66:34 (11)
L			46:54 (10)	43:57 (10)
I	55:45 (64)			
F	48:52 (58)		57:43 (41)	54:46 (6)
H	5:42.5 (59)			
W	48:52 (51)		53:47 (40)	
Y	38:62 (74)		55:45 (34)	

Table 11A-BB continued from previous page.

mOCR-Myo 93A, 64I, 43H, 68A				
12R	L32X	F33X	H97X	I99X
V		55:45 (15)	65:35 (15)	61:39 (16)
L			51:49 (16)	
I		62:38 (7)		
F	42:58 (NA)		65:35 (23)	
H				
W			74:26 (28)	
Y	47:53 (14)	60:40 (21)	77:23 (20)	

mOCR-Myo 93A, 64L, 68A				
12S	L32X	F33X	H97X	I99X
V		24:76 (15)	32:68 (NA)	35:65 (NA)
L			57:43 (NA)	
I	21:79 (22)		29:71 (NA)	
F			45:55 (NA)	
H				
W			47:53 (NA)	
Y		37:63 (NA)		

mOCR-Myo 93A, 64V, 43Y, 68A				
12T	L32X	F33X	H97X	I99X
V	53:47 (11)		46:54 (43)	63:37 (15)
L		69:31 (48)	52:48 (22)	50:50 (11)
I	40:60 (16)	58:42 (16)	54:46 (25)	64:36 (18)
F	55:45 (15)		69:31 (27)	
H		53:47 (24)		
W	52:48 (13)	72:28 (20)	73:27 (38)	48:52 (5)
Y		71:29 (61)	55:45 (38)	

mOCR-Myo 93A, 64L, 43L, 33V				
12U	L32X	F33X	H97X	I99X
V			26:74 (30)	37:63 (17)
L				
I			27:73 (20)	
F			39:61 (35)	52:48 (7)
H				
W			56:44 (42)	
Y			38:62 (46)	

mOCR-Myo 93A, 64V, 68S				
12V	L32X	F33X	H97X	I99X
V	33:67 (8)			
L			47:53 (17)	
I			41:59 (15)	
F			40:60 (20)	
H				
W			54:46 (28)	
Y	43:57 (5)	61:39 (9)		

mOCR-Myo 93A, 64L, 43W, 68A, 97Y				
12W	L32X	F33X	H97X	I99X
V	58:42 (23)	57:43 (18)		
L		58:42 (26)		
I	45:55 (27)	64:36 (41)		
F	51:49 (34)			
H	69:31 (27)	54:46 (33)		
W	59:41 (30)	55:45 (43)		
Y	48:52 (42)	52:48 (29)		

mOCR-Myo 93A, 64V, 68A				
12X	L32X	F33X	H97X	I99X
V				33:67 (33)
L		29:71 (31)		
I				
F				
H				
W			59:41 (23)	
Y		35:65 (4%)		

mOCR-Myo 93G, 64L, 68A, 32F				
12Y	L32X	F33X	H97X	I99X
V			33:67 (6)	39:61 (7)
L			22:78 (9)	38:62 (17)
I			34:66 (5)	
F				49:51 (21)
H				46:54 (8)
W			21:79 (15)	
Y			21:79 (7)	45:55 (23)

Table 11A-BB continued from previous page.

mOCR-Myo 93G, 64L, 43L, 99V				
12Z	L32X	F33X	H97X	I99X
V	54:46 (13)	51:49 (4)		
L		53:47 (7)		
I	53:47 (18)	54:46 (10)		
F	55:45 (11)			
H	49:51 (13)			
W	52:48 (12)	54:46 (9)		
Y	52:48 (10)	60:40 (3)		

mOCR-Myo 93G, 64L, 43L, 99F				
12AA	L32X	F33X	H97X	I99X
V	49:51 (8)	52:48 (1)		
L				
I	53:47 (10)			
F	54:46 (9)			
H	53:47 (9)	48:52 (4)		
W	55:45 (12)	50:50 (7)		
Y	57:43 (16)	53:47 (2)		

mOCR-Myo 93A, 64V, 43Y, 68A, L32I				
12BB	L32X	F33X	H97X	I99X
V				27:73 (7)
L				31:69 (34)
I				
F				63:37 (14)
H				
W				50:50 0
Y				41:59 (8)

Table 12. Cyclopropanation of 1-octene with EDA with Ir(Me)-PIX-mCOR-Myo (H93A, H64A, V68F) – different conditions.

a. Effect of substrate stoichiometry

Entry	[1-octene]	[EDA]	TON
A	10 mM	100 mM	42
B	10 mM	60 mM	40
C	10 mM	30 mM	20
D	10 mM	10 mM	11
E	30 mM	10 mM	24
F	60 mM	10 mM	23
G	100 mM	10 mM	21

b. Effect of rate of EDA addition

Entry	[1-octene]	[EDA]	Method	TON	er
A	10 mM	60 mM	Standard Method	20	85:15
B	10 mM	60 mM	Syringe Pump Addition of EDA (1 hr)	40	88:12
C	10 mM	60 mM	Syringe Pump Addition of EDA (12 hr)	20	91:9

Table 13. Results from screening for enantioselective Ir(Me)-PIX-mCOR-Myo's for cyclopropanation of 1-octene with EDA. Data are presented as: enantiomeric ratio (GC yield).

mOCR-Myo. H93G, H64A- 2-OMe, COOMe							
14A	68V	V68A	V68G	V68F	V68Y	V68S	V68T
43F	44 : 56 (1)	58 : 42 (3)					
F43Y							
F43W							
F43L							
F43I							
F43T							
F43H							
F43V							

mOCR-Myo. H93G, H64V- 2-OMe, COOMe							
14B	68V	V68A	V68G	V68F	V68Y	V68S	V68T
43F	51 : 49 (1)						
F43Y							
F43W							
F43L							
F43I							
F43T							
F43H							
F43V							

mOCR-Myo. H93G, H64L- 2-OMe, COOMe							
14C	68V	V68A	V68G	V68F	V68Y	V68S	V68T
43F	49 : 51 (19)				49 : 51 (3)		48 : 52 (1)
F43Y							
F43W	46 : 54 (2)	52 : 48 (3)			49 : 51 (4)	50 : 50 (4)	51 : 49 (2)
F43L			56 : 44 (2)	54 : 46 (3)			
F43I				52 : 48 (3)			
F43T				49 : 51 (3)			
F43H			52 : 48 (7)	49 : 51 (4)			
F43V			47 : 53 (3)	48 : 52 (4)			

mOCR-Myo. H93G, H64I- 2-OMe, COOMe							
14D	68V	V68A	V68G	V68F	V68Y	V68S	V68T
43F	48 : 52 (2)						
F43Y							
F43W							
F43L							
F43I	49 : 51 (4)						
F43T							
F43H	49 : 51 (4)						
F43V	50 : 50 (4)		54 : 46 (5)				

Table 13 Continued

mOCR-Myo. H93A, H64A- 2-OMe, COOMe							
14E	68V	V68A	V68G	V68F	V68Y	V68S	V68T
43F	54 : 46 (12)		49 : 51 (16)	83 : 17 (11)			
F43Y							
F43W							
F43L							
F43I							
F43T							
F43H							
F43V							

mOCR-Myo. H93A, H64V- 2-OMe, COOMe							
14F	68V	V68A	V68G	V68F	V68Y	V68S	V68T
43F	49 : 51 (1)			58 : 42 (3)	51 : 49 (3)	51 : 49 (2)	
F43Y					50 : 50 (5)	50 : 50 (6)	
F43W	49 : 51 (1)			52 : 48 (3)	52 : 48 (5)	50 : 50 (6)	50 : 50 (5)
F43L		48 : 52 (4)	54 : 46 (4)	47 : 53 (9)			
F43I		50 : 50 (4)	58 : 42 (4)	51 : 49 (3)			51 : 49 (5)
F43T							
F43H	49 : 51 (5)		52 : 48 (5)			51 : 49 (5)	
F43V							

mOCR-Myo. H93A, H64L- 2-OMe, COOMe							
14G	68V	V68A	V68G	V68F	V68Y	V68S	V68T
43F	55 : 45 (2)						50 : 50 (4)
F43Y	49 : 51 (5)	49 : 51 (2)	54 : 46 (3)		58 : 42 (2)	48 : 52 (3)	
F43W		50 : 50 (0)	56 : 44 (2)	57 : 43 (3)		52 : 48 (3)	47 : 53 (3)
F43L	49 : 51 (4)	59 : 41 (2)	53 : 47 (2)	59 : 41 (2)			
F43I						49 : 51 (3)	
F43T					50 : 50 (6)		
F43H				49 : 51 (4)			
F43V	48 : 52 (4)	50 : 50 (0)					

mOCR-Myo. H93G, H64A- 2-OMe, COOMe							
14H	68V	V68A	V68G	V68F	V68Y	V68S	V68T
43F	49 : 51 (1)		59 : 41 (3)				
F43Y	49 : 51 (6)		49 : 51 (3)				
F43W							
F43L							
F43I	49 : 51 (4)						
F43T	51 : 49 (4)						
F43H	49 : 51 (5)		55 : 45 (3)				
F43V	52 : 48 (4)		56 : 44 (2)	51 : 49 (4)			

Table 13 Continued

mOCR-Myo93G, 14I, 18A				
14I	L32X	F33X	H97X	I99X
V	52:48 (6)			
L		51:49 (5)		
I	52:48 (4)			
F	51:49 (6)			
H				
W				
Y	51:49 (6)	51:49 (5)		

mOCR-Myo93A, 14L, 13W, 18A				
14J	L32X	F33X	H97X	I99X
V		54:46 (5)		
L			60:40 (2)	
I		53:47 (4)		
F				
H		53:47 (4)		
W		52:48 (4)		
Y		53:47 (4)		

Table 14. Results from screening for enantioselective Ir(Me)-PIX-mCOR-Myo's for cyclopropanation of trans- β -methylstyrene **3** with EDA. Data are presented as: enantiomeric ratio of the major diastereomer (GC yield). Diastereomeric ratio > 33 : 1 in all cases.

mOCR-Myo. H93G, H64A- 2-OMe, COOMe							
15A	68V	V68A	V68G	V68F	V68Y	V68S	V68T
43F	48 : 52 (12)	50 : 50 (13)					
F43Y							
F43W							
F43L							
F43I							
F43T							
F43H							
F43V							

mOCR-Myo. H93G, H64V- 2-OMe, COOMe							
15B	68V	V68A	V68G	V68F	V68Y	V68S	V68T
43F	49 : 51 (7)						
F43Y							
F43W							
F43L							
F43I							
F43T							
F43H							
F43V							

mOCR-Myo. H93G, H64L- 2-OMe, COOMe							
15C	68V	V68A	V68G	V68F	V68Y	V68S	V68T
43F	48 : 52 (12)				54 : 46 (11)		48 : 52 (12)
F43Y							
F43W	45 : 55 (10)	50 : 50 (15)			53 : 47 (11)	53 : 47 (12)	51 : 49 (12)
F43L			57 : 43 (7)	51 : 49 (12)			
F43I				51 : 49 (10)			
F43T				52 : 48 (16)			
F43H			52 : 48 (12)	57 : 43 (17)			
F43V			49 : 51 (12)	51 : 49 (13)			

mOCR-Myo. H93G, H64I- 2-OMe, COOMe							
15D	68V	V68A	V68G	V68F	V68Y	V68S	V68T
43F	46 : 54 (7)		50 : 50 (16)				
F43Y							
F43W							
F43L							
F43I	55 : 45 (10)						
F43T							
F43H	50 : 50 (15)						
F43V	51 : 49 (14)		54 : 46 (13)				

Table 14 Continued

mOCR-Myo. H93G, H64A- 2-OMe, COOMe							
15A	68V	V68A	V68G	V68F	V68Y	V68S	V68T
43F	48 : 52 (12)	50 : 50 (13)					
F43Y							
F43W							
F43L							
F43I							
F43T							
F43H							
F43V							

mOCR-Myo. H93G, H64V- 2-OMe, COOMe							
15B	68V	V68A	V68G	V68F	V68Y	V68S	V68T
43F	49 : 51 (7)						
F43Y							
F43W							
F43L							
F43I							
F43T							
F43H							
F43V							

mOCR-Myo. H93G, H64L- 2-OMe, COOMe							
15C	68V	V68A	V68G	V68F	V68Y	V68S	V68T
43F	48 : 52 (12)				54 : 46 (11)		48 : 52 (12)
F43Y							
F43W	45 : 55 (10)	50 : 50 (15)			53 : 47 (11)	53 : 47 (12)	51 : 49 (12)
F43L			57 : 43 (7)	51 : 49 (12)			
F43I				51 : 49 (10)			
F43T				52 : 48 (16)			
F43H			52 : 48 (12)	57 : 43 (17)			
F43V			49 : 51 (12)	51 : 49 (13)			

mOCR-Myo. H93G, H64I- 2-OMe, COOMe							
15D	68V	V68A	V68G	V68F	V68Y	V68S	V68T
43F	46 : 54 (7)		50 : 50 (16)				
F43Y							
F43W							
F43L							
F43I	55 : 45 (10)						
F43T							
F43H	50 : 50 (15)						
F43V	51 : 49 (14)		54 : 46 (13)				

Table 14 Continued

mOCR-Myo93G,94I,98A				
15I	L32X	F33X	H97X	I99X
V	51:49 (17)			
L		49:51 (13)		
I	51:49 (13)			
F	49:51 (16)			
H				
W				
Y	54:46 (13)	51:49 (14)		

mOCR-Myo93A,94L,93W,98A				
15J	L32X	F33X	H97X	I99X
V		49:51 (16)		
L			48:52 (17)	
I		50:50 (13)		
F				
H		51:49 (13)		
W		51:49 (13)		
Y		50:50 (13)		

mOCR-Myo93A,94V,93Y,98A				
15K	L32X	F33X	H97X	I99X
V				
L				
I				
F			40 (15)	
H				
W				
Y				

Table 15. Methods used to separate enantiomers of the generated reaction products.

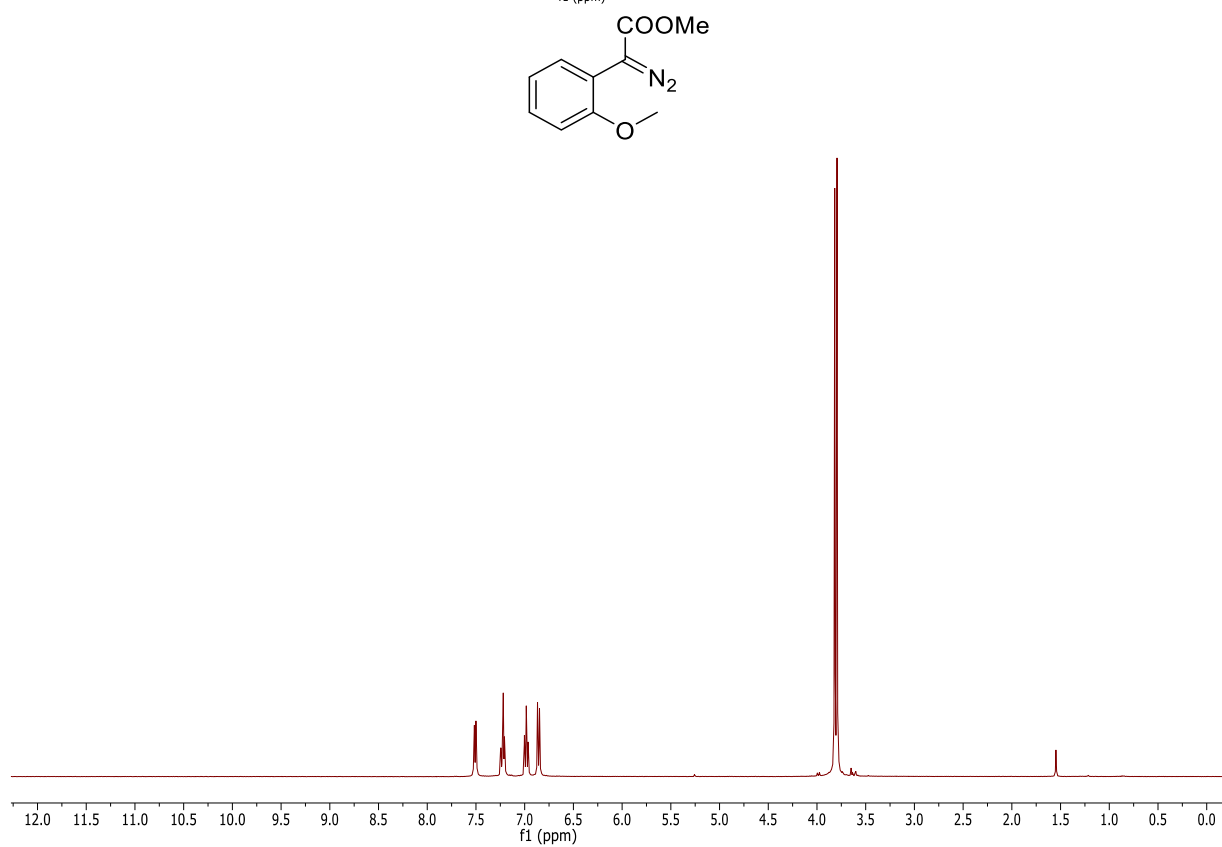
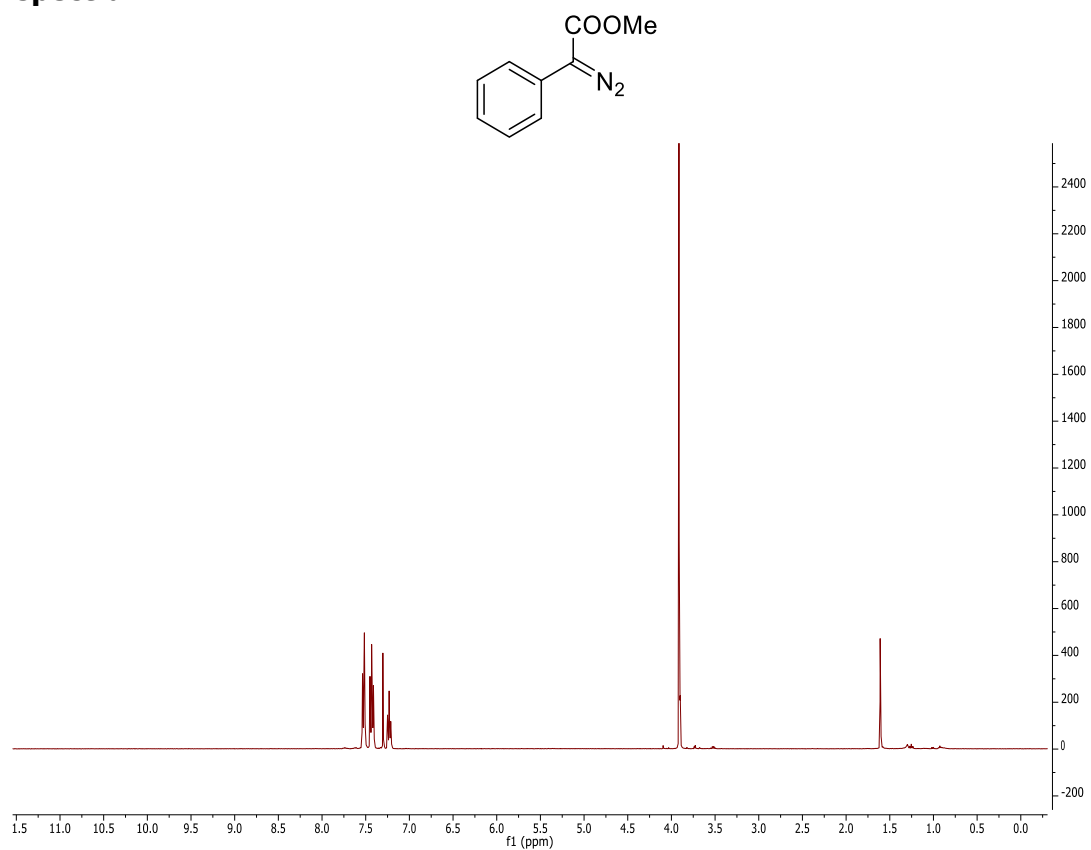
Product	Instrument	Column	Method	Retention Times
2^a	GC	CYCLOSIL-B (30m x 0.25mm x 0.25u)	Isothermal: 150 °C	t1(R)(-)=13.8 min t2(S)(+)=14.0 min
P7	GC	CYCLOSIL-B (30m x 0.25mm x 0.25u)	Isothermal: 145 °C	t1=12.0 min t2=12.3 min
P8	GC	CYCLOSIL-B (30m x 0.25mm x 0.25u)	Isothermal: 145 °C	t1=47.1 min t2=47.9 min
P11	GC	CYCLOSIL-B (30m x 0.25mm x 0.25u)	Isothermal: 170 °C	t1=15.0 min t2=15.3 min
5 (trans- β -methylstyrene + EDA)	GC	CYCLOSIL-B (30m x 0.25mm x 0.25u)	Isothermal: 130 °C	t1=39.1 min t2=39.6 min
P13^a (1-octene+EDA)	GC	CYCLOSIL-B (30m x 0.25mm x 0.25u)	Isothermal: 90 °C	Cis: (1S,2R)(+) t1=81.5 min (1R,2S)(-) t2=82.9 min Trans: (1R,2R)(-) t1=97.4 min (1S,2S)(+) t2=98.8 min
P12^a (styrene+EDA)	GC	CYCLOSIL-B (30m x 0.25mm x 0.25u)	Isothermal: 120 °C	Cis: (1S,2R)(+) t1=37.2 min (1R,2S)(-) t2=39.0 min Trans: (1R,2R)(-) t1=48.3 min (1S,2S)(+) t2=49.2 min
P6	SFC	Chiracel OD-H (Diacel)	Isocratic: 1% MeOH, 4 ml/min flow	t1=1.3 min t2=1.5 min
P9	SFC	Chiracel AD-H (Diacel)	Isocratic: 1% MeOH, 4 ml/min flow	t1=1.6 min t2=2.25 min
P10	SFC	Chiracel AD-H (Diacel)	Isocratic: 4% MeOH, 4 ml/min flow	t1=2.5 min t2=2.75 min

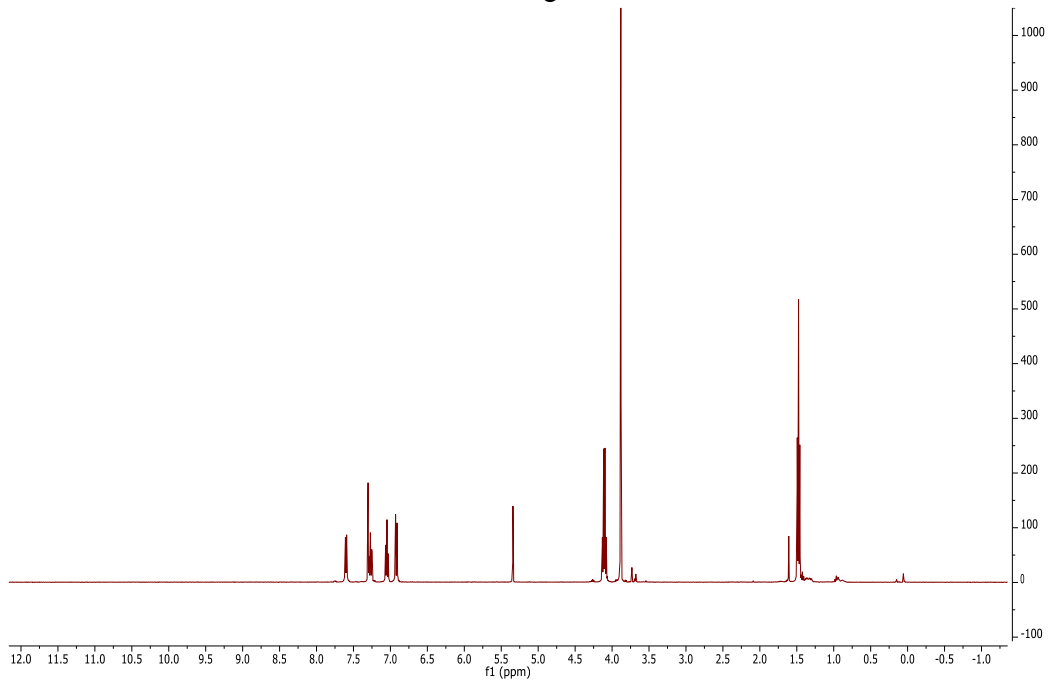
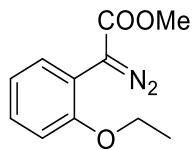
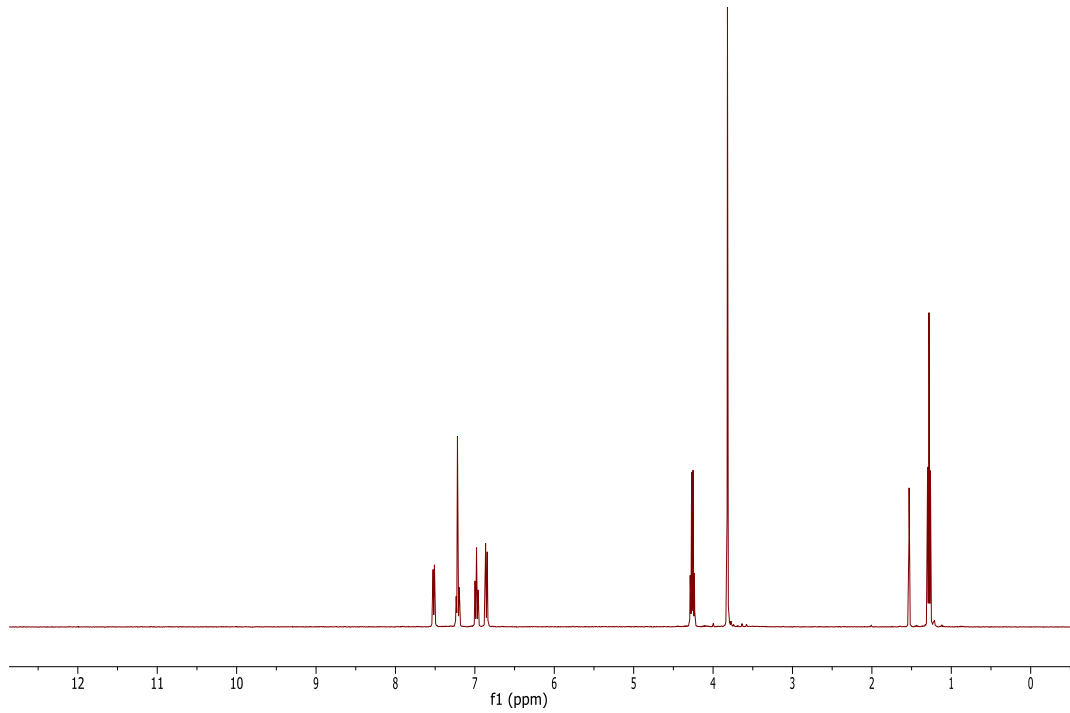
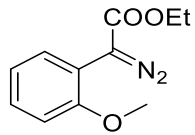
a – absolute geometry assigned based on the reported retention times of enantiomers^{7,8}.

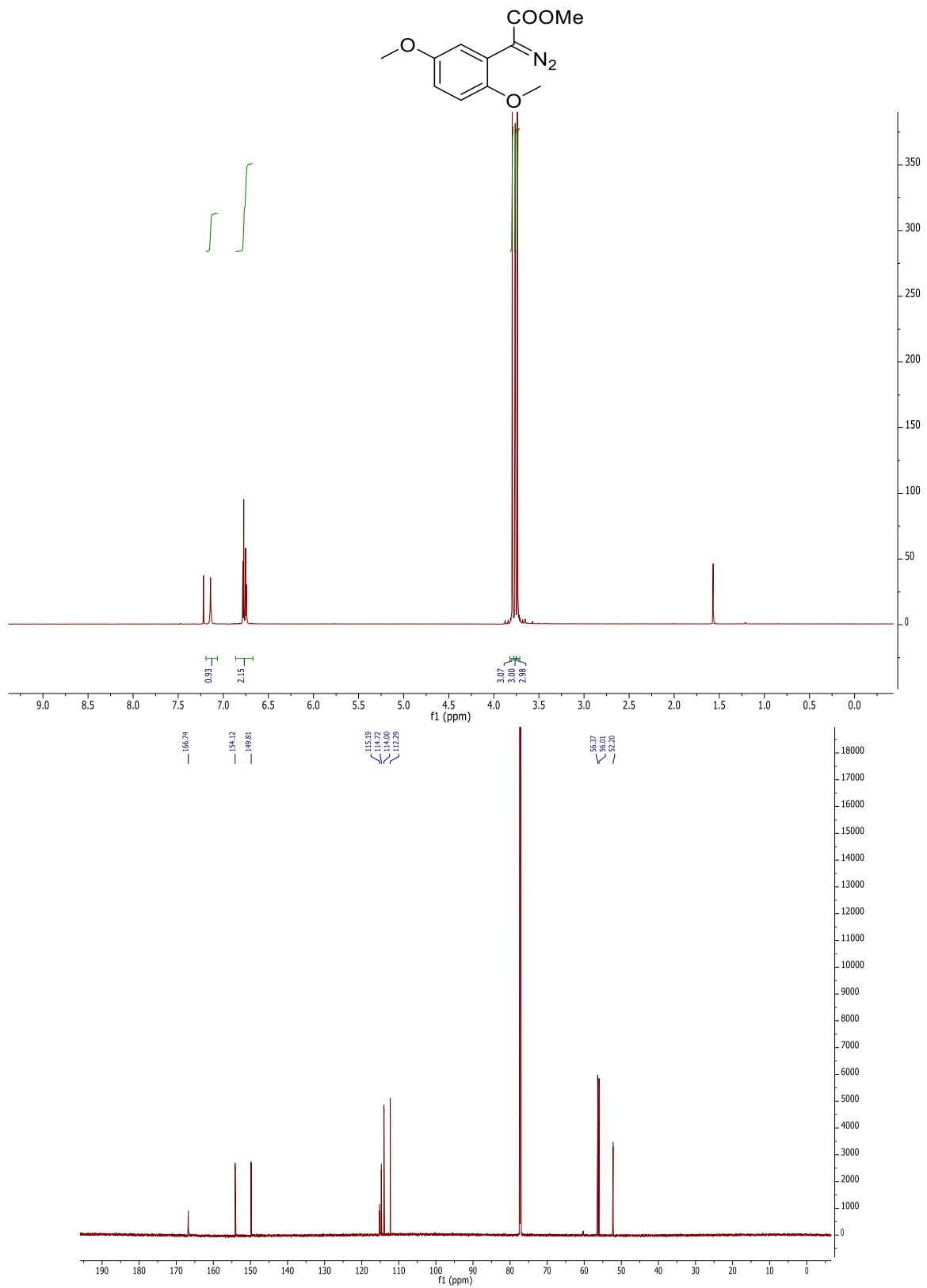
Table 16. Validation of GC yields: Control studies of the extraction of the known amount of the product from the pseudo-reaction mixture.

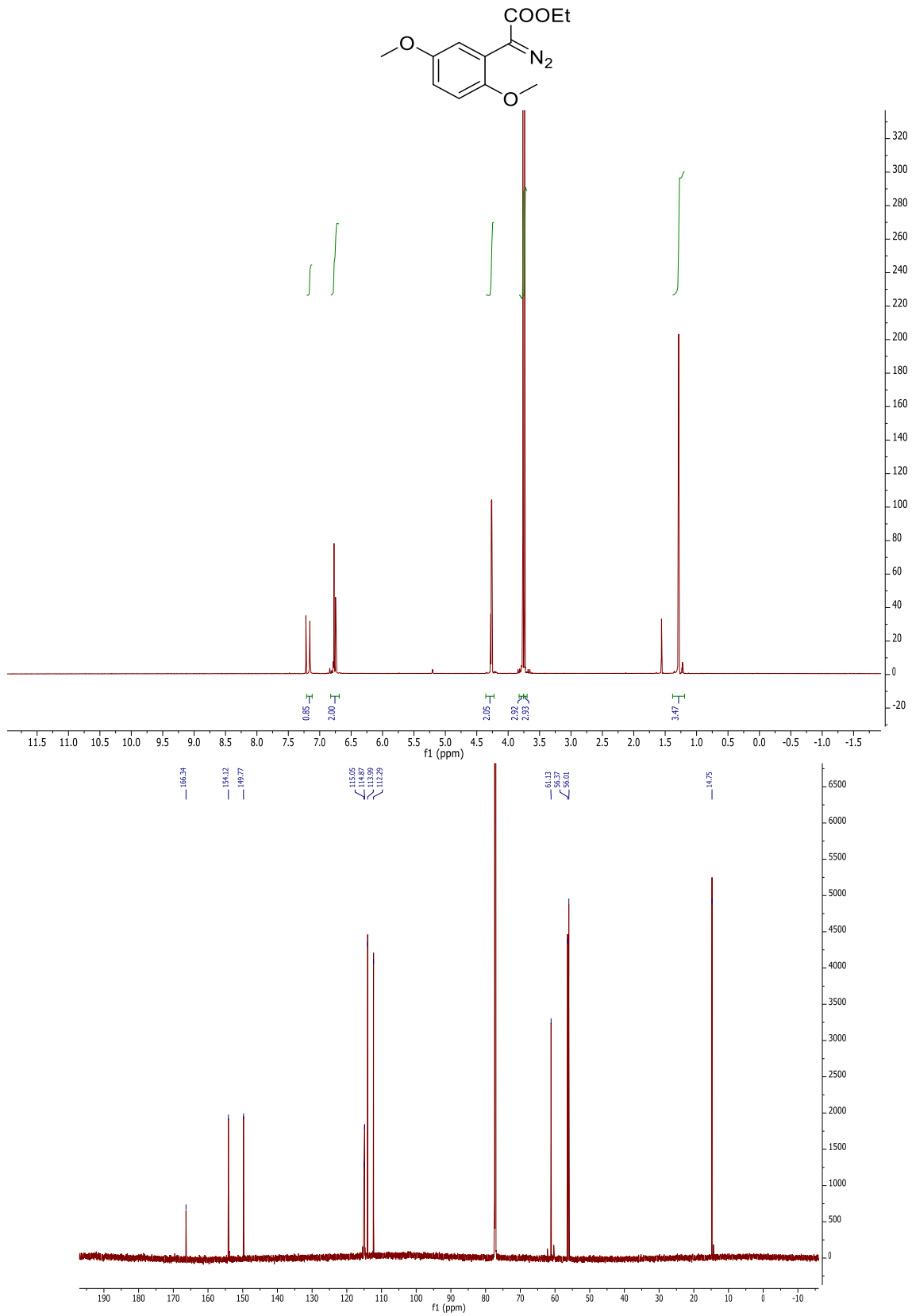
Experiment	1	2	3	4	5	6
extracted product	97.9%	99.6%	97.5%	103.1%	97.9%	100.7%

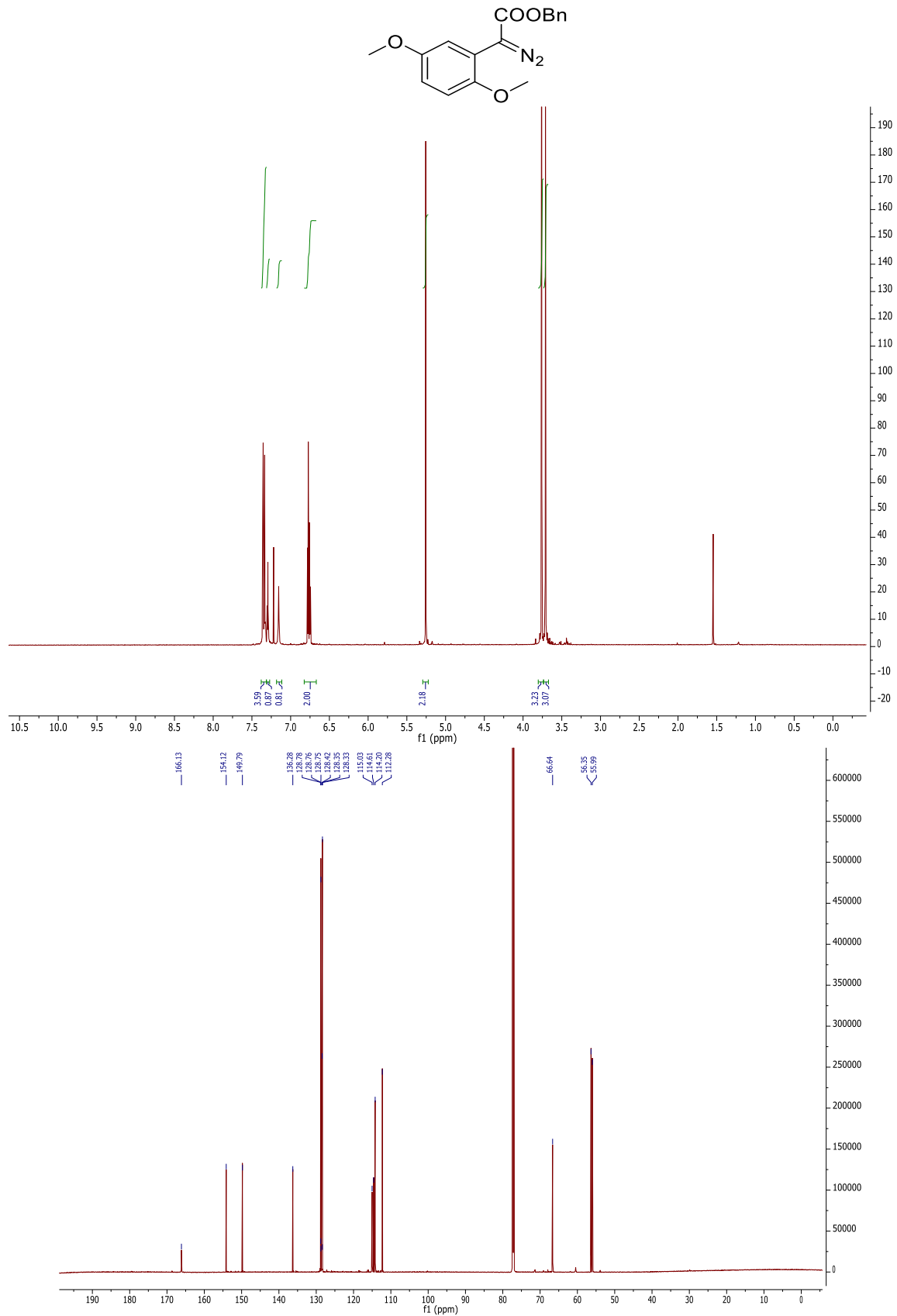
NMR spectra:

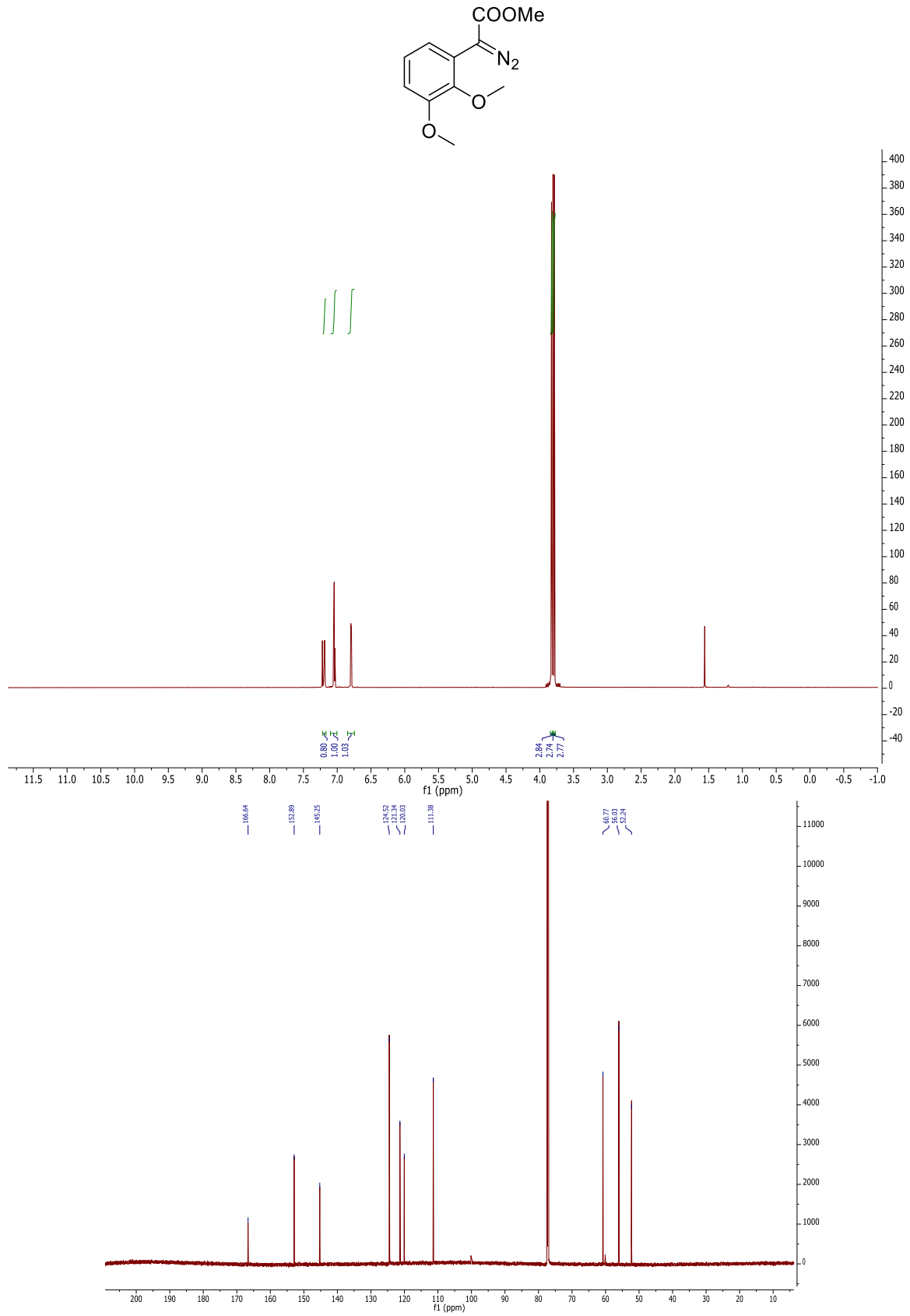


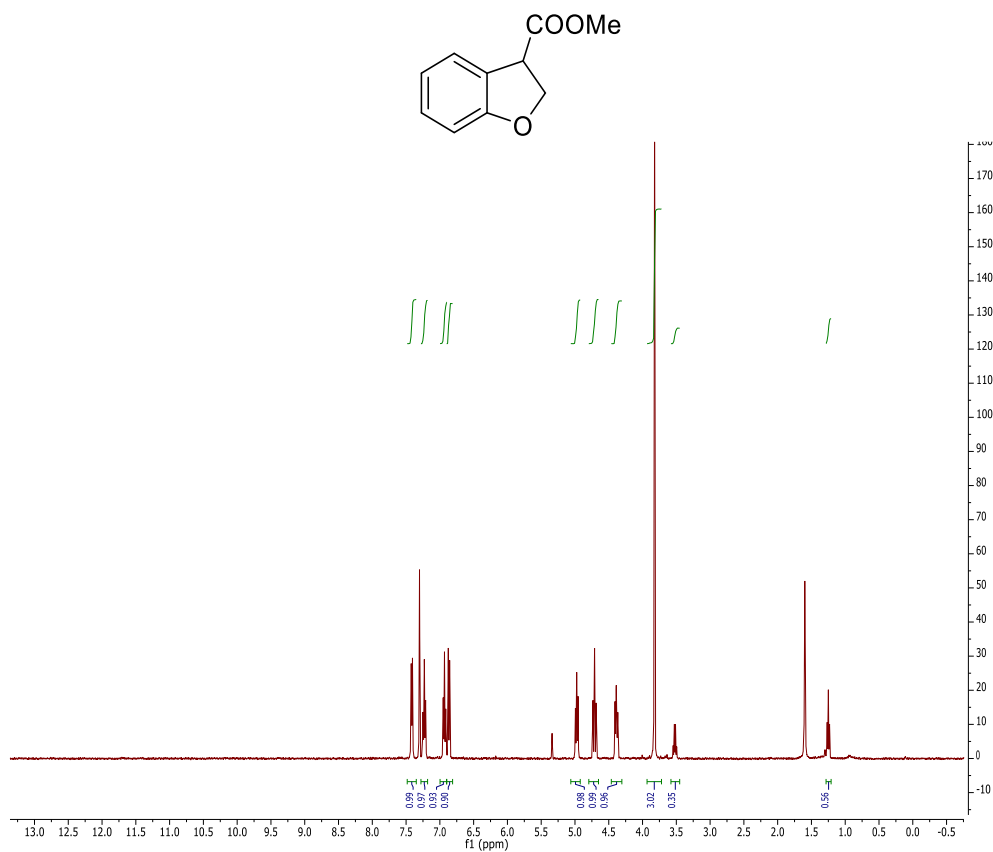


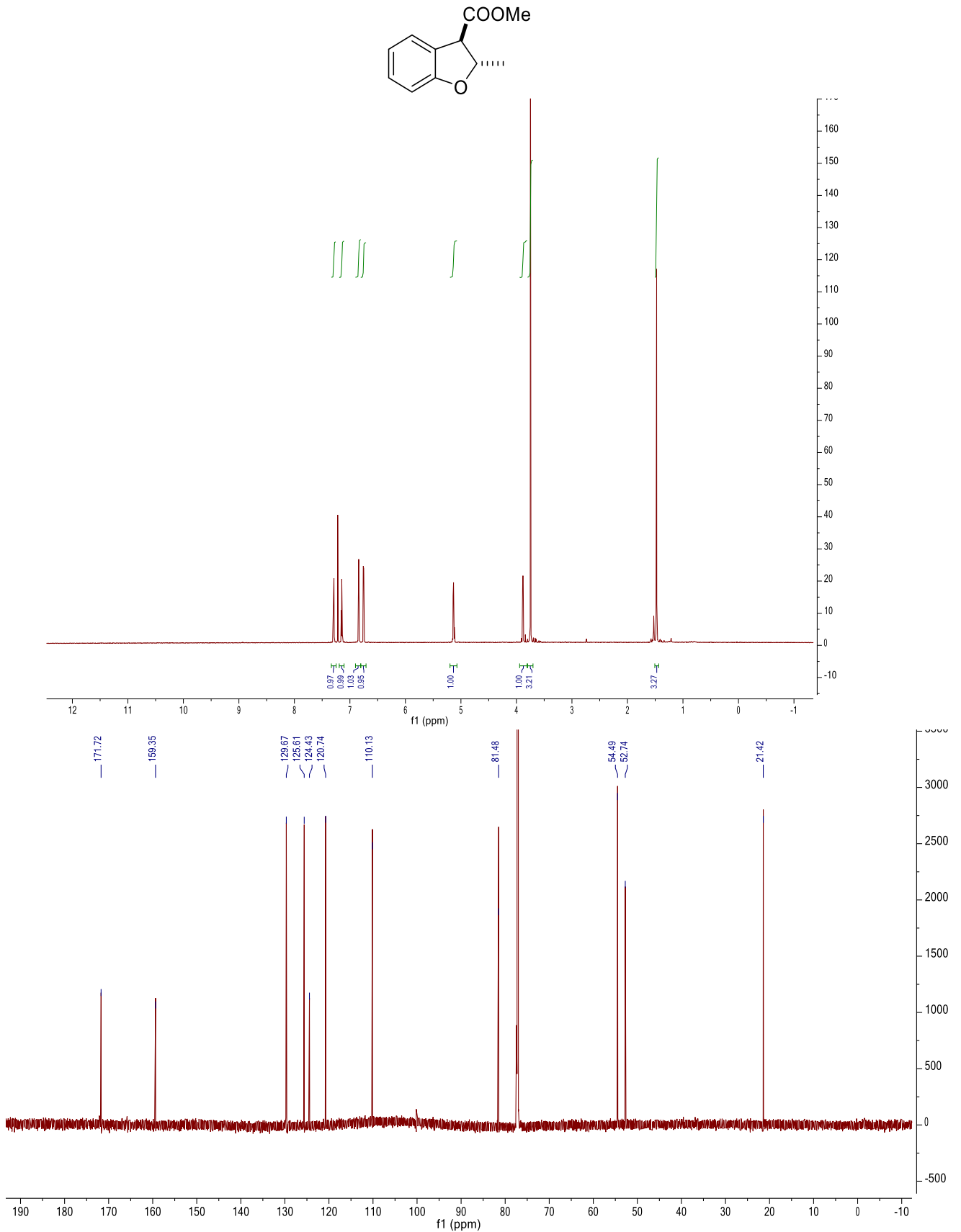


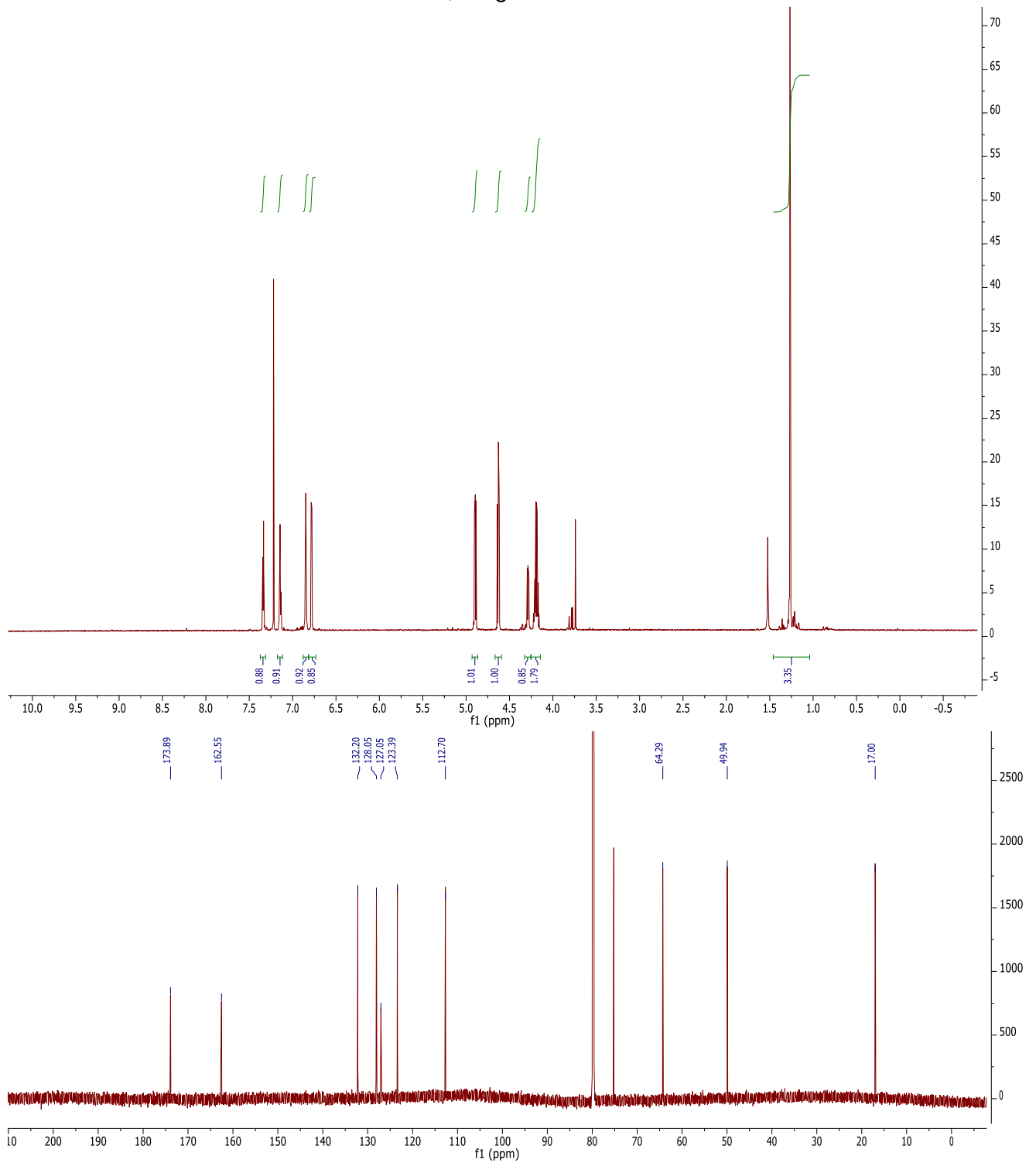
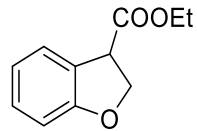


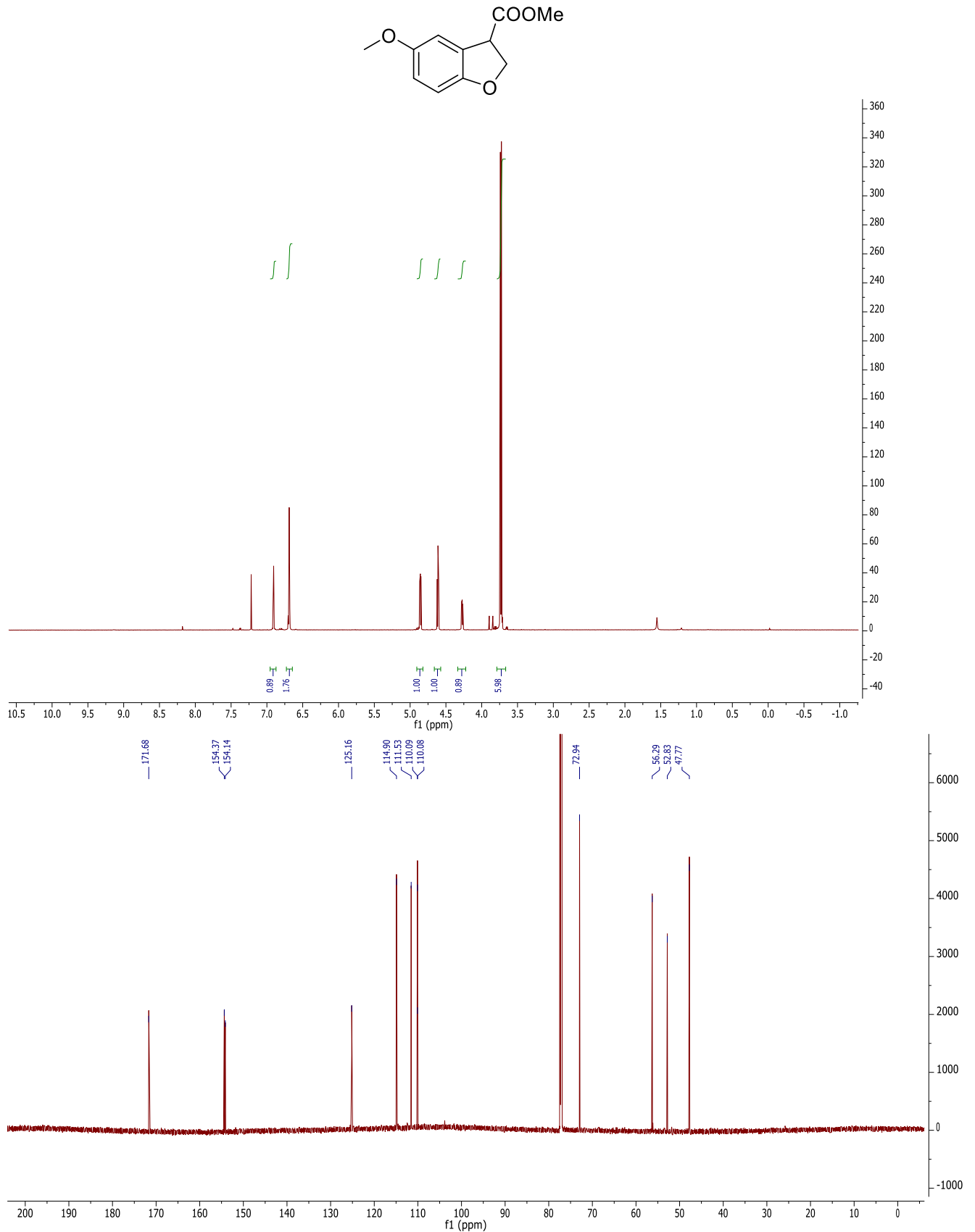


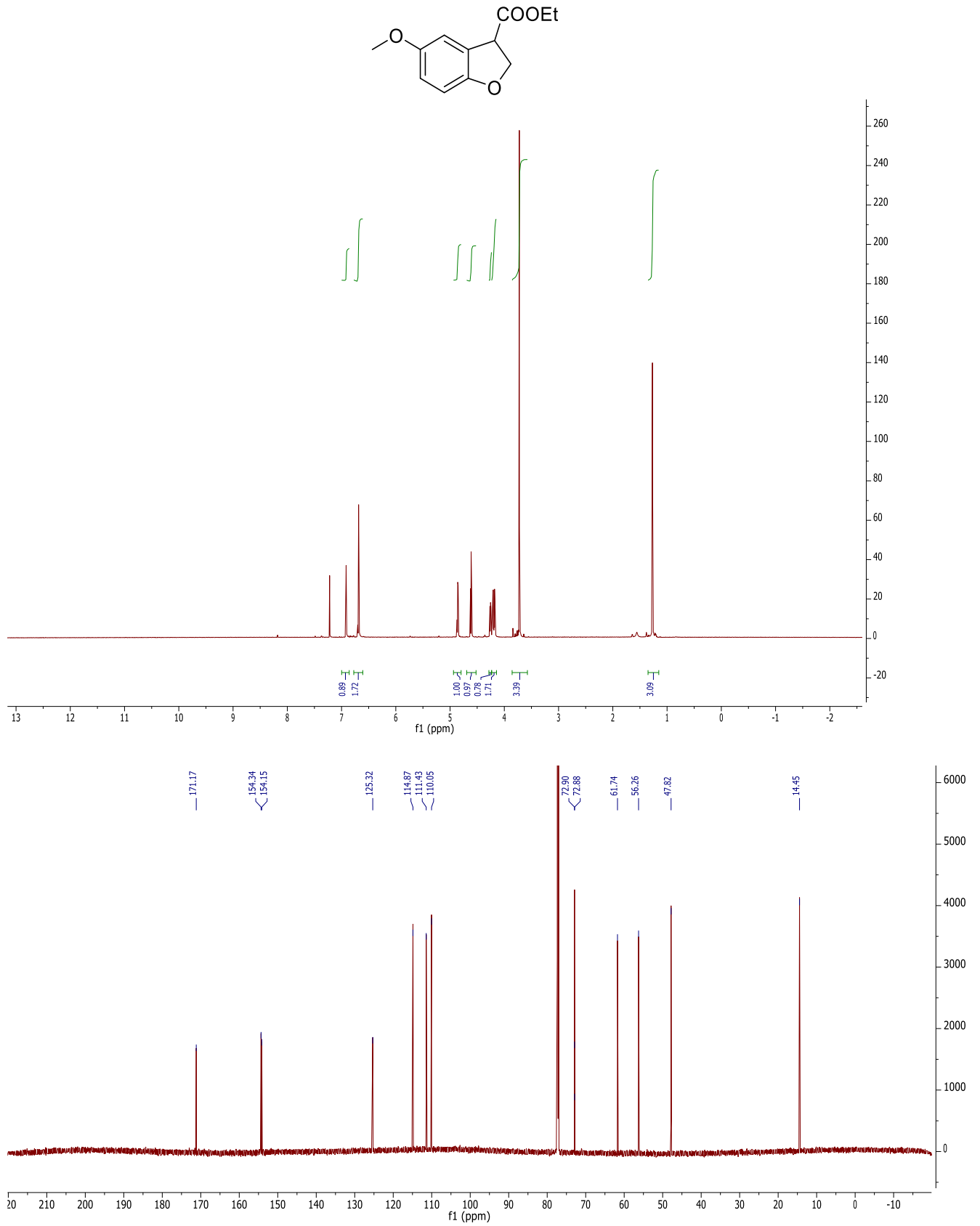


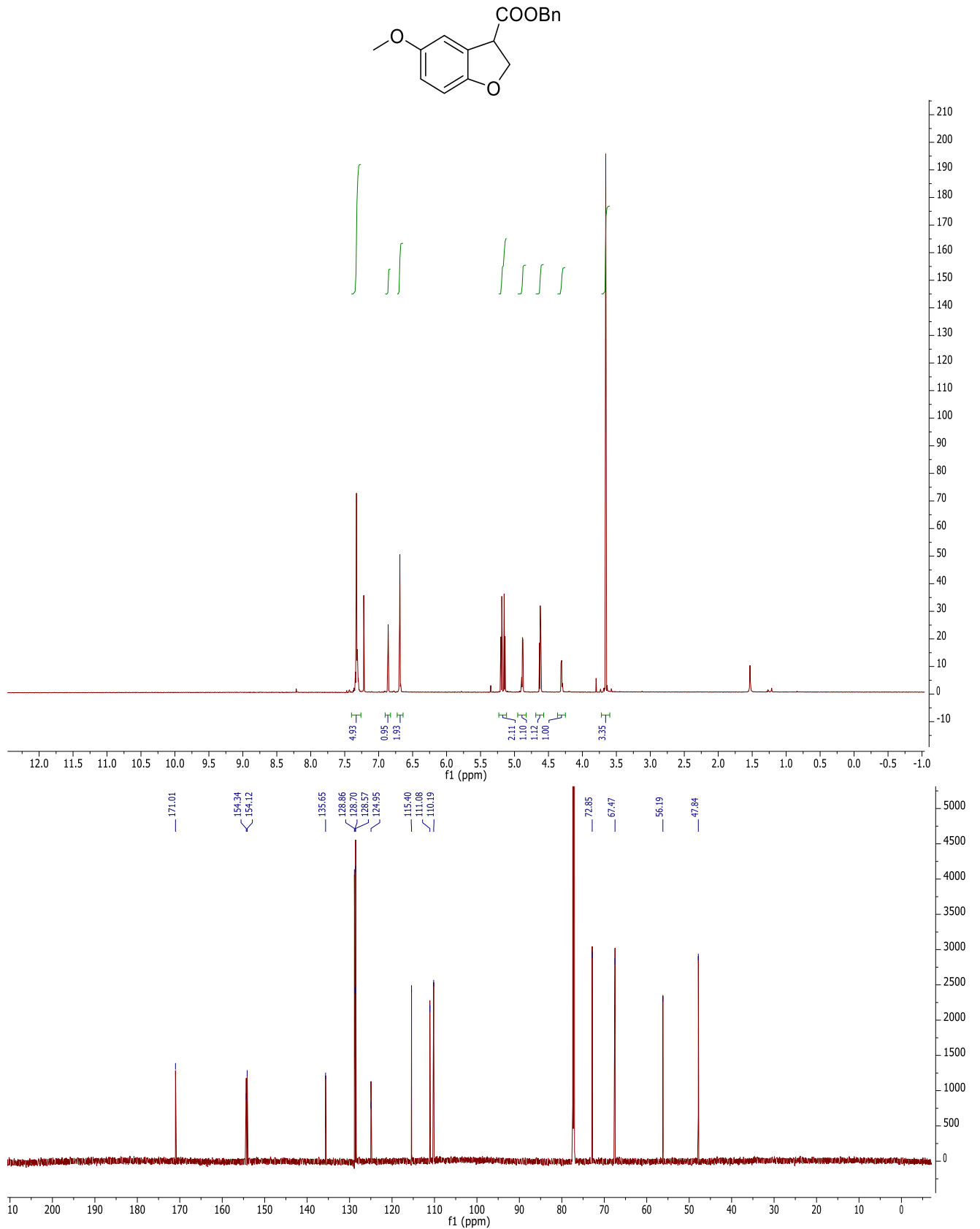


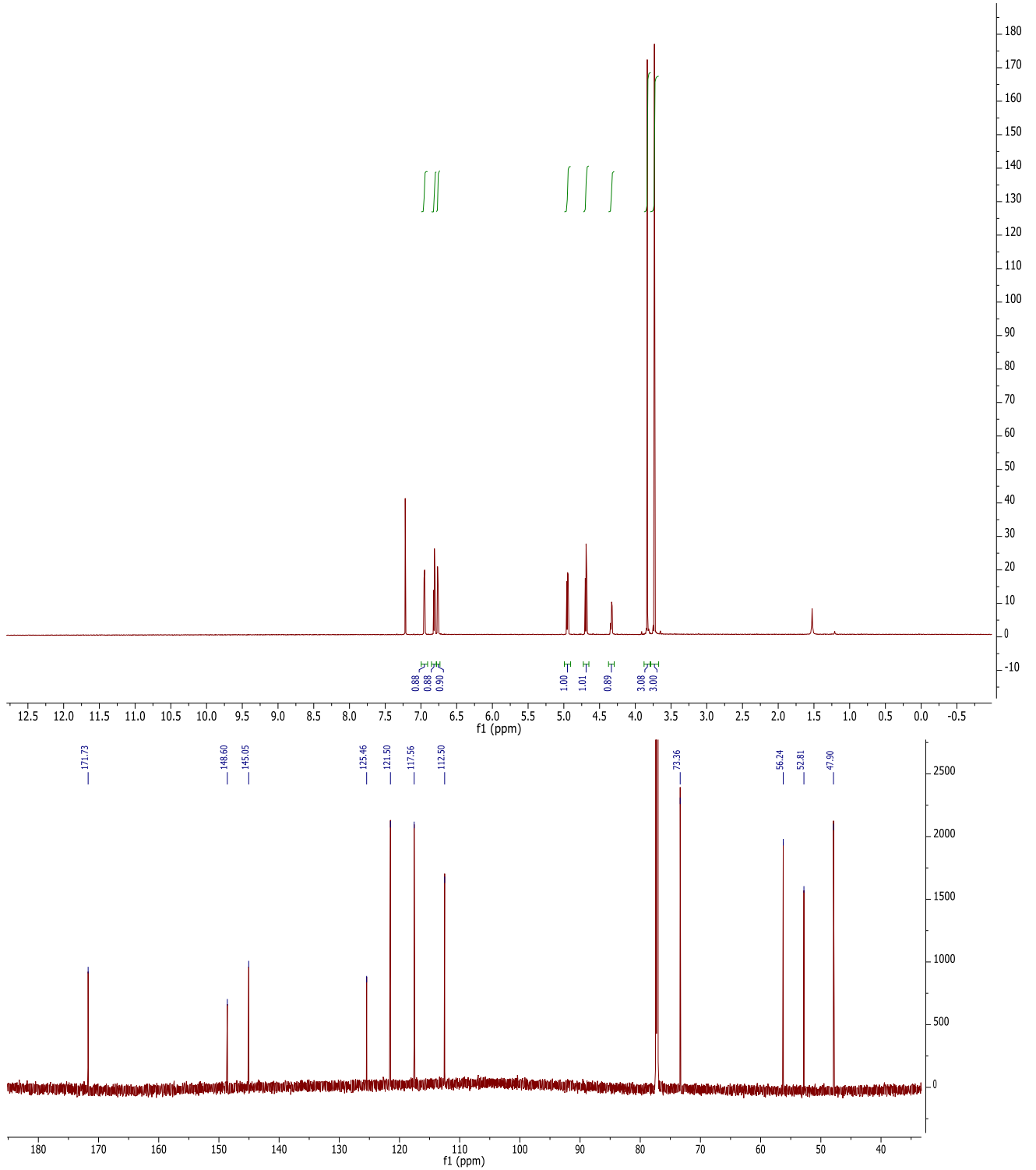
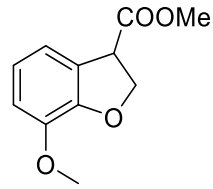


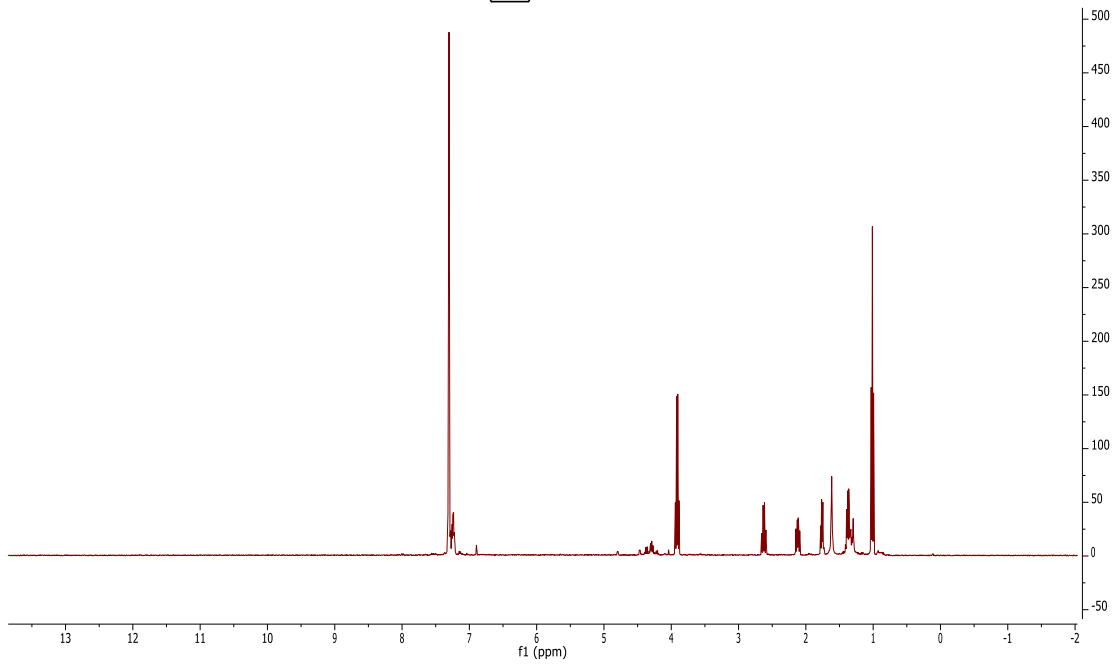
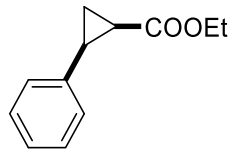
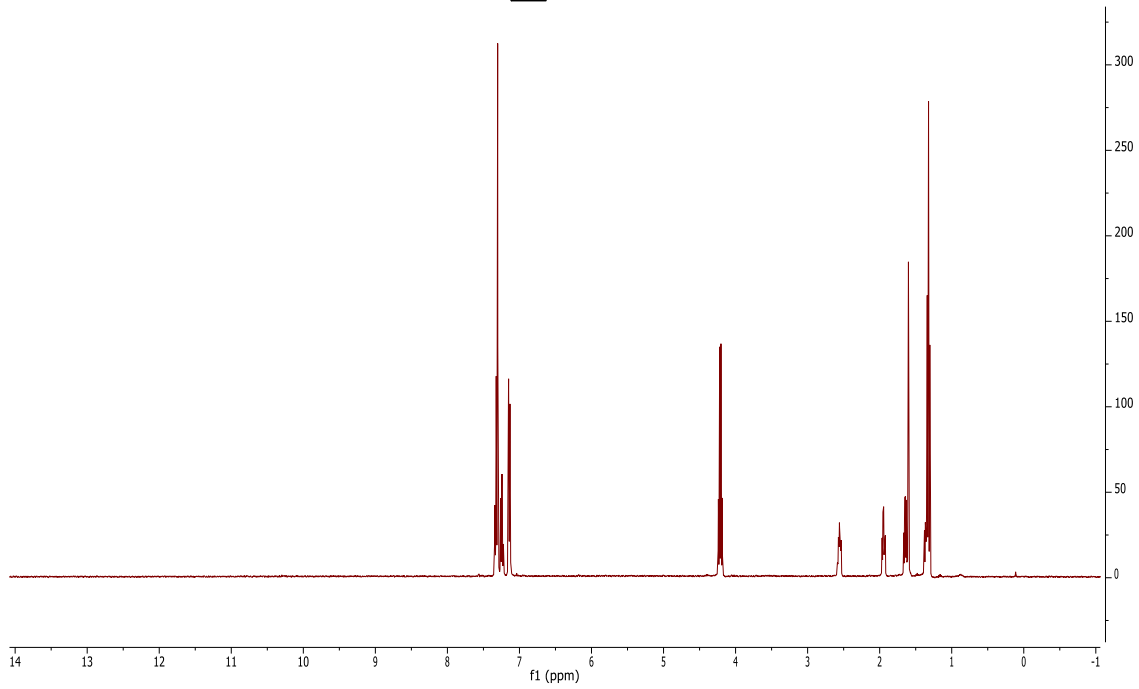
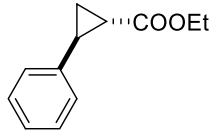


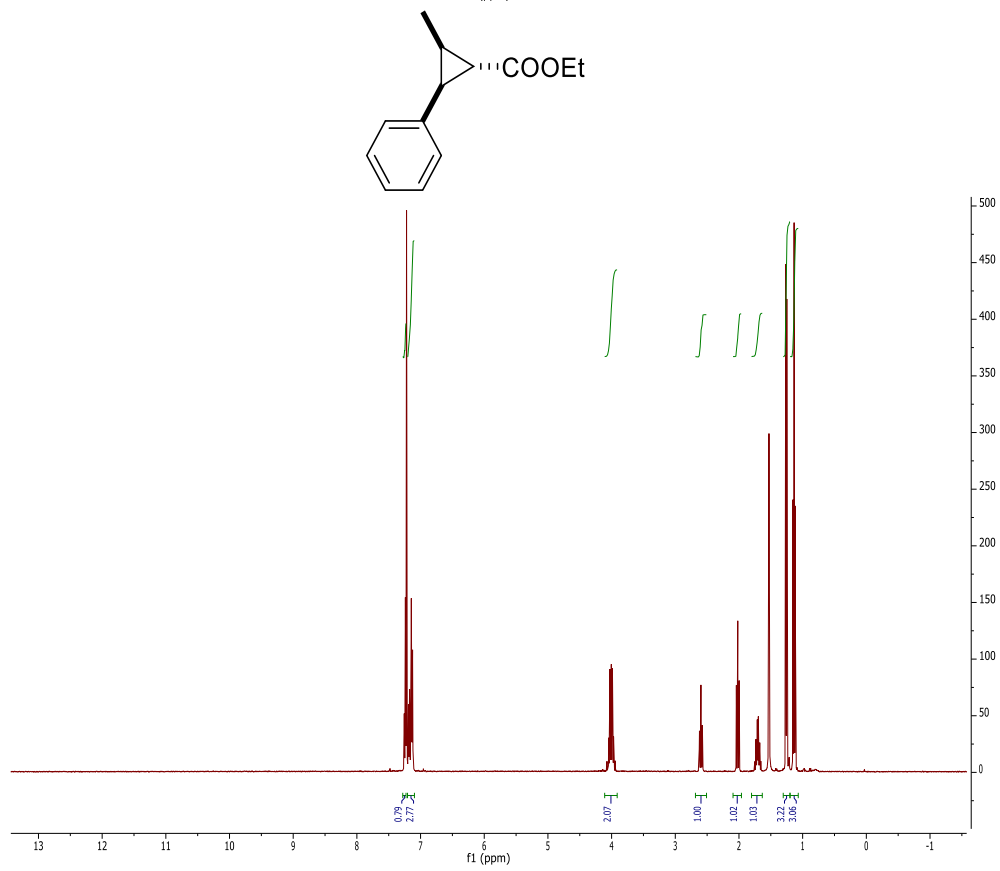
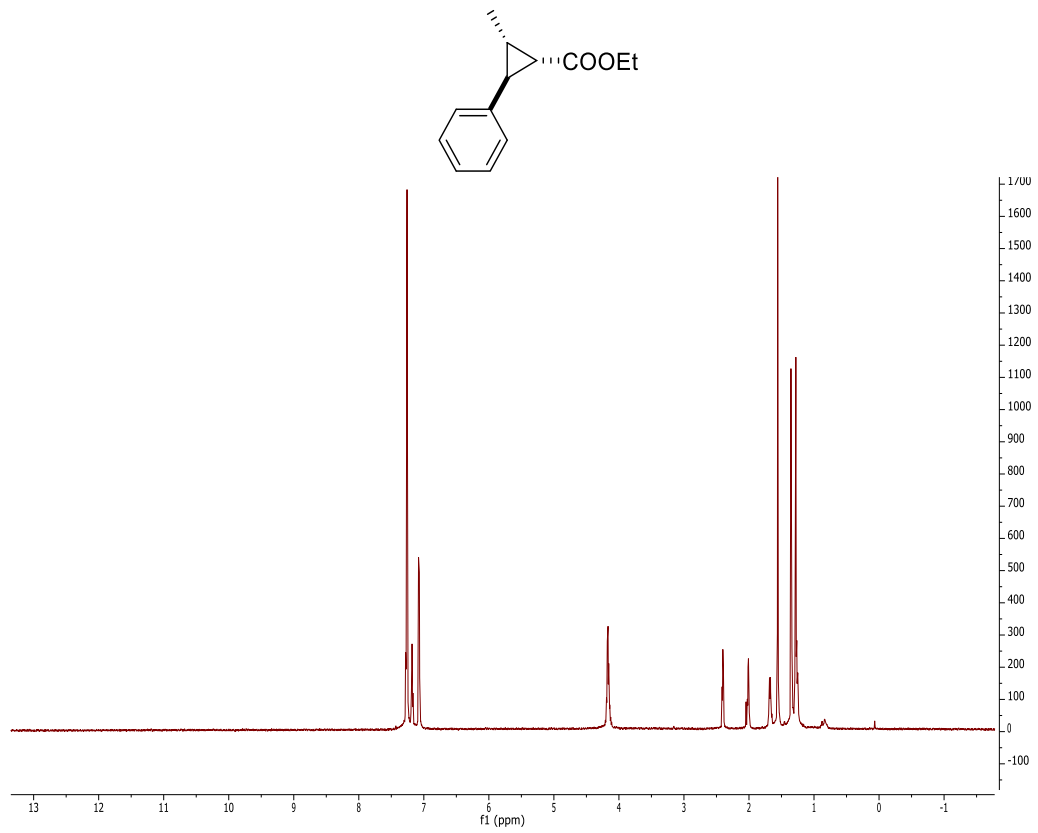


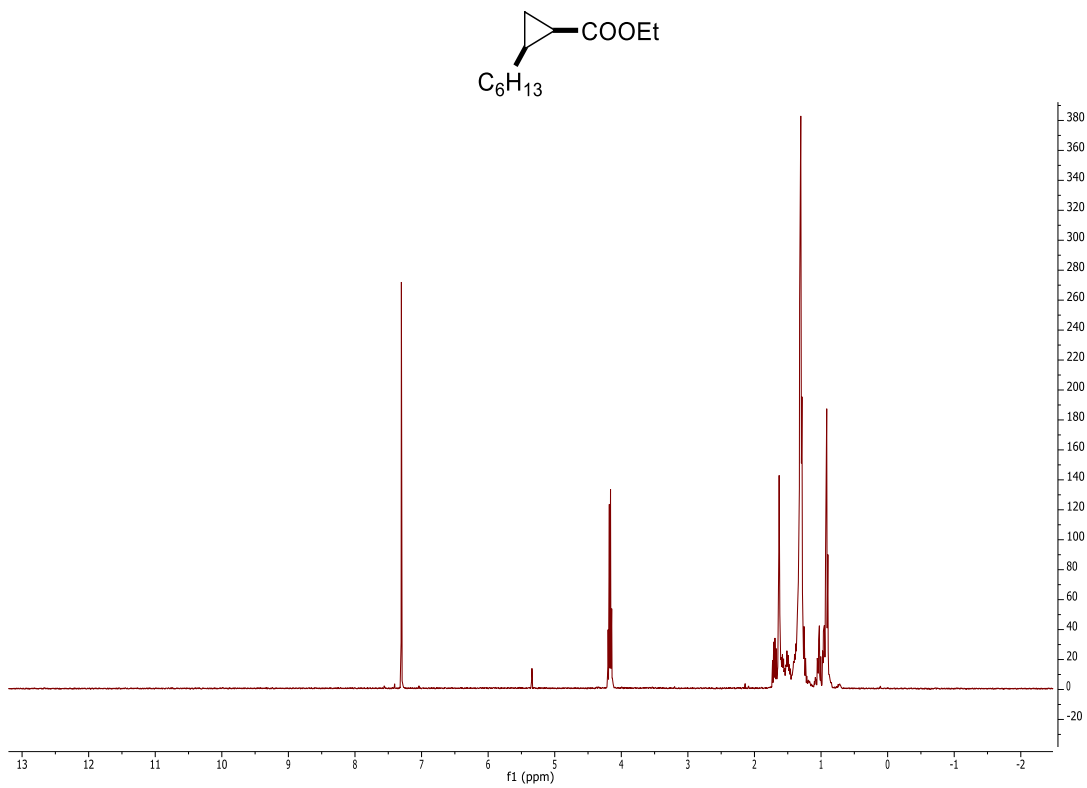
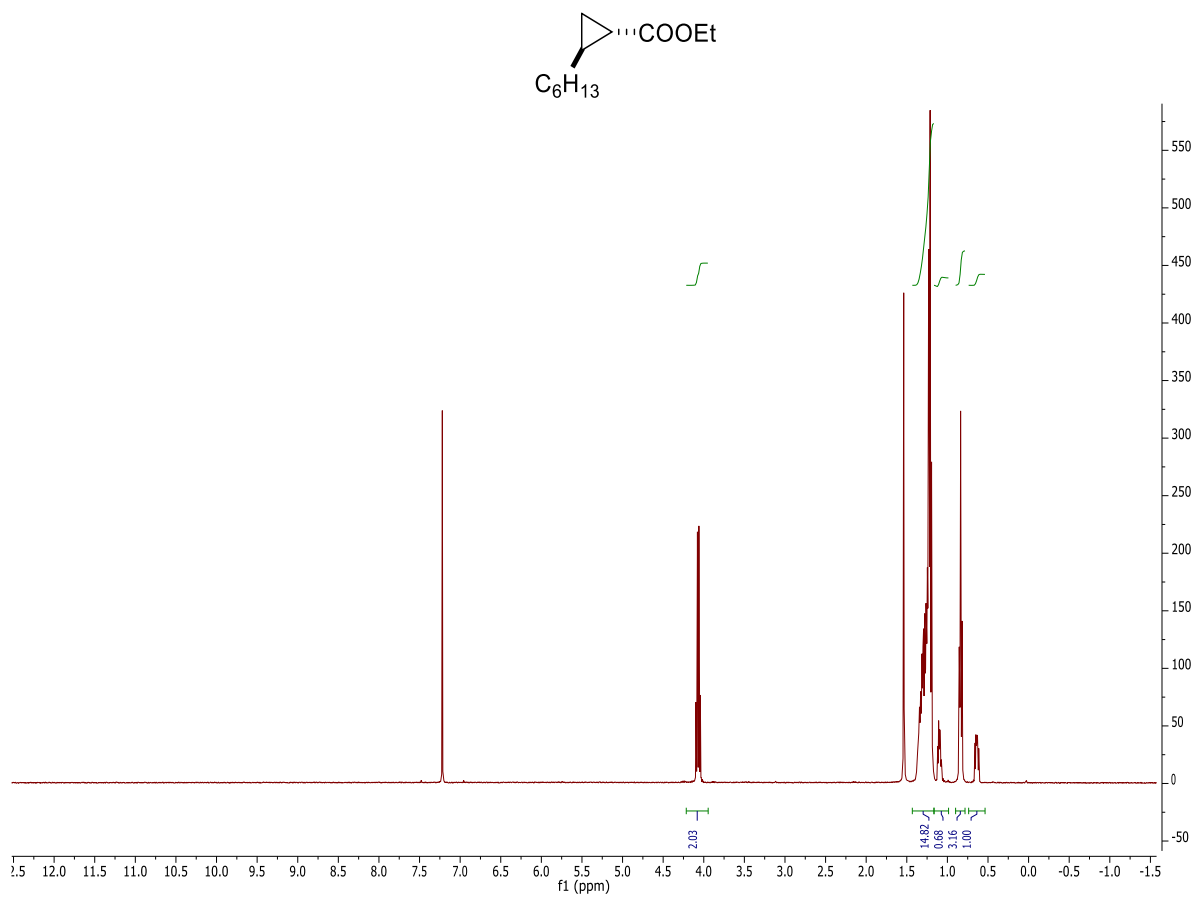


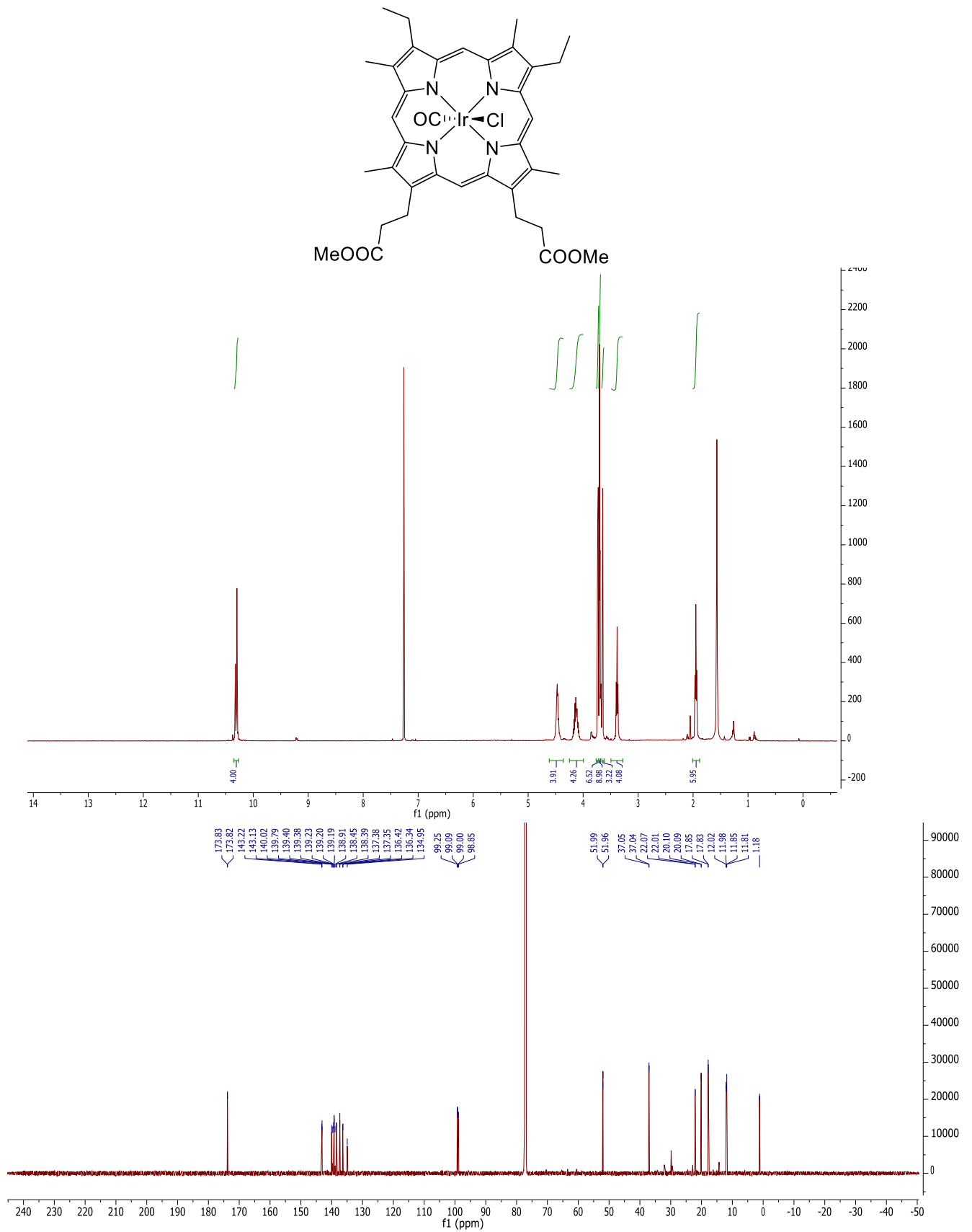


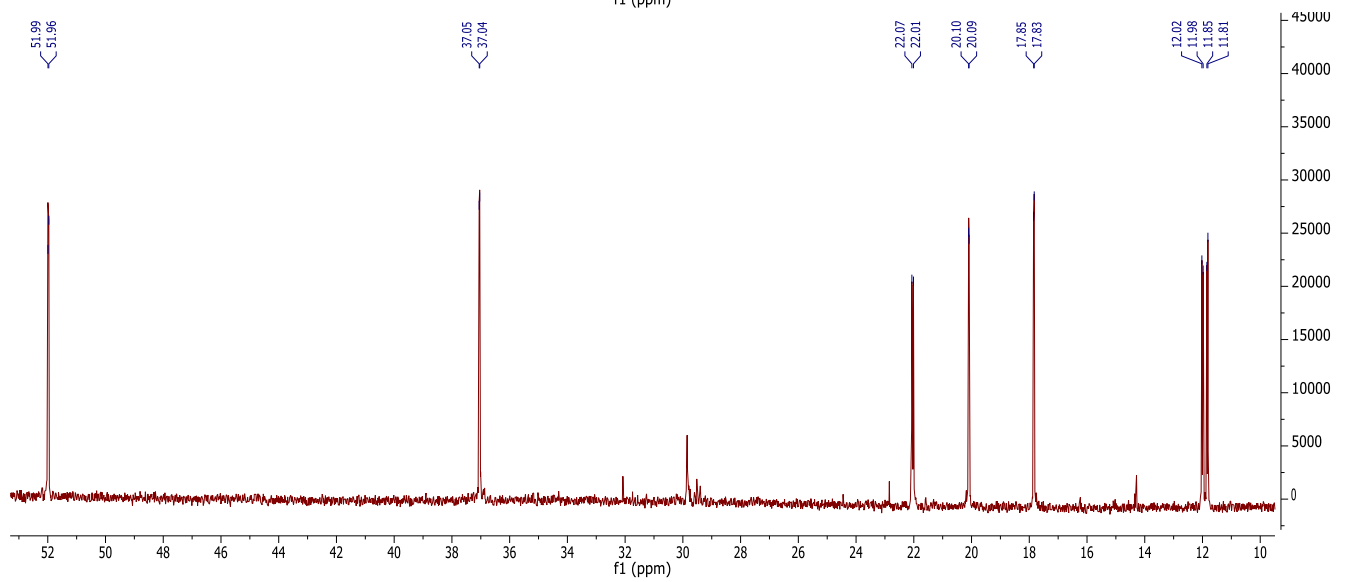
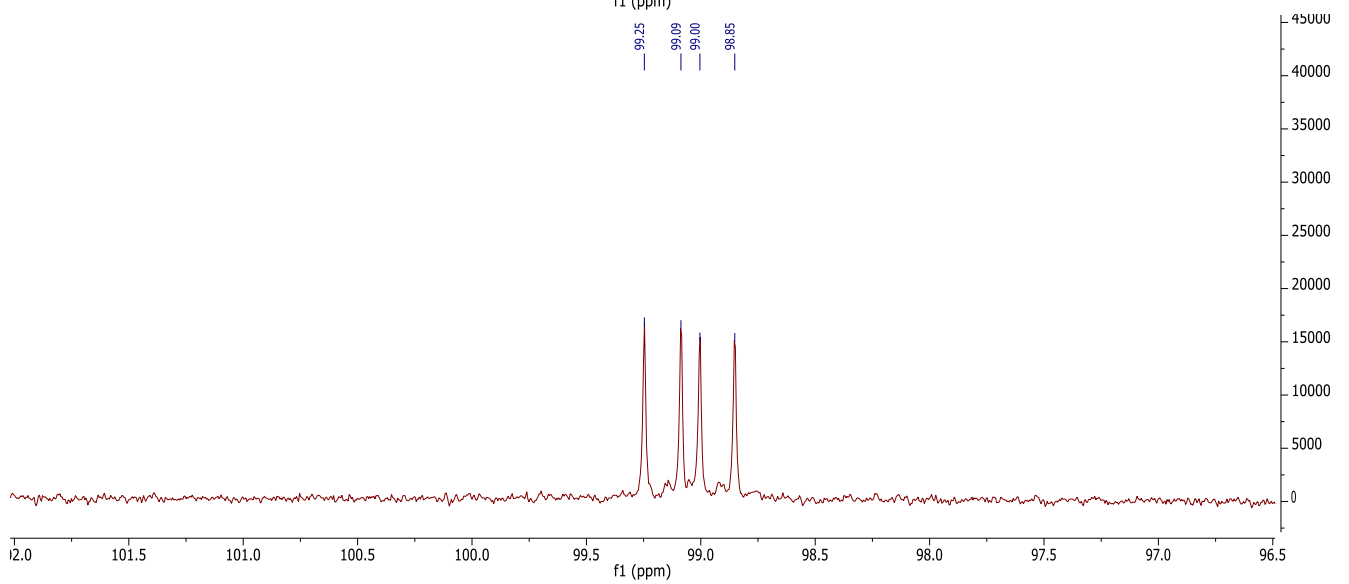
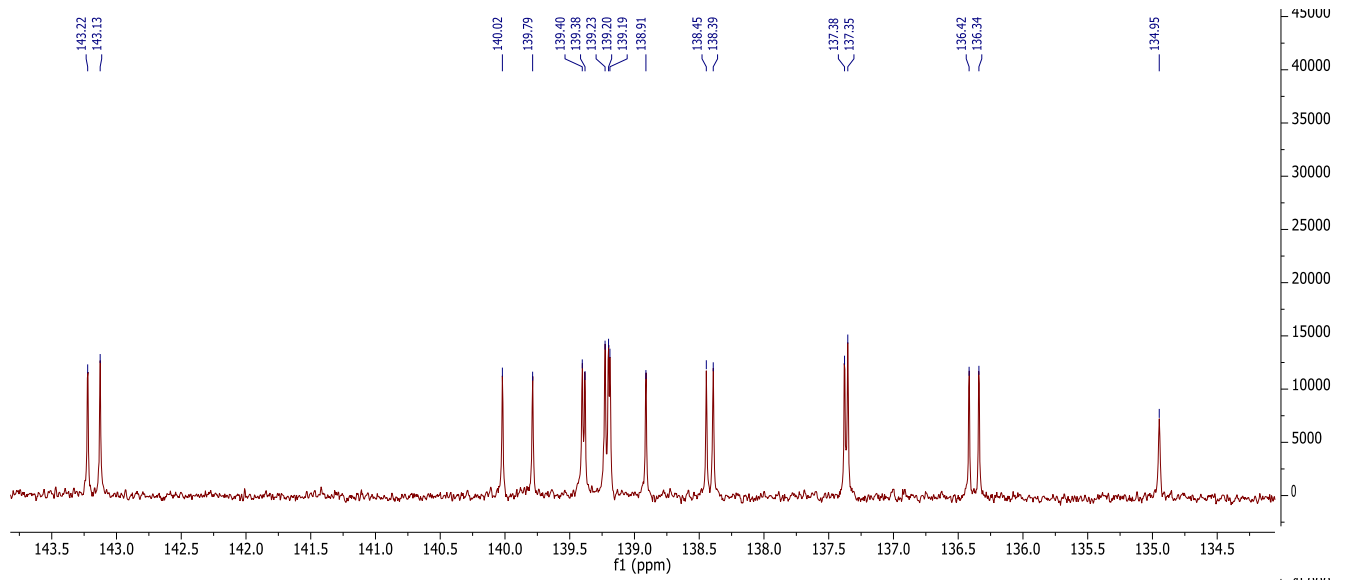


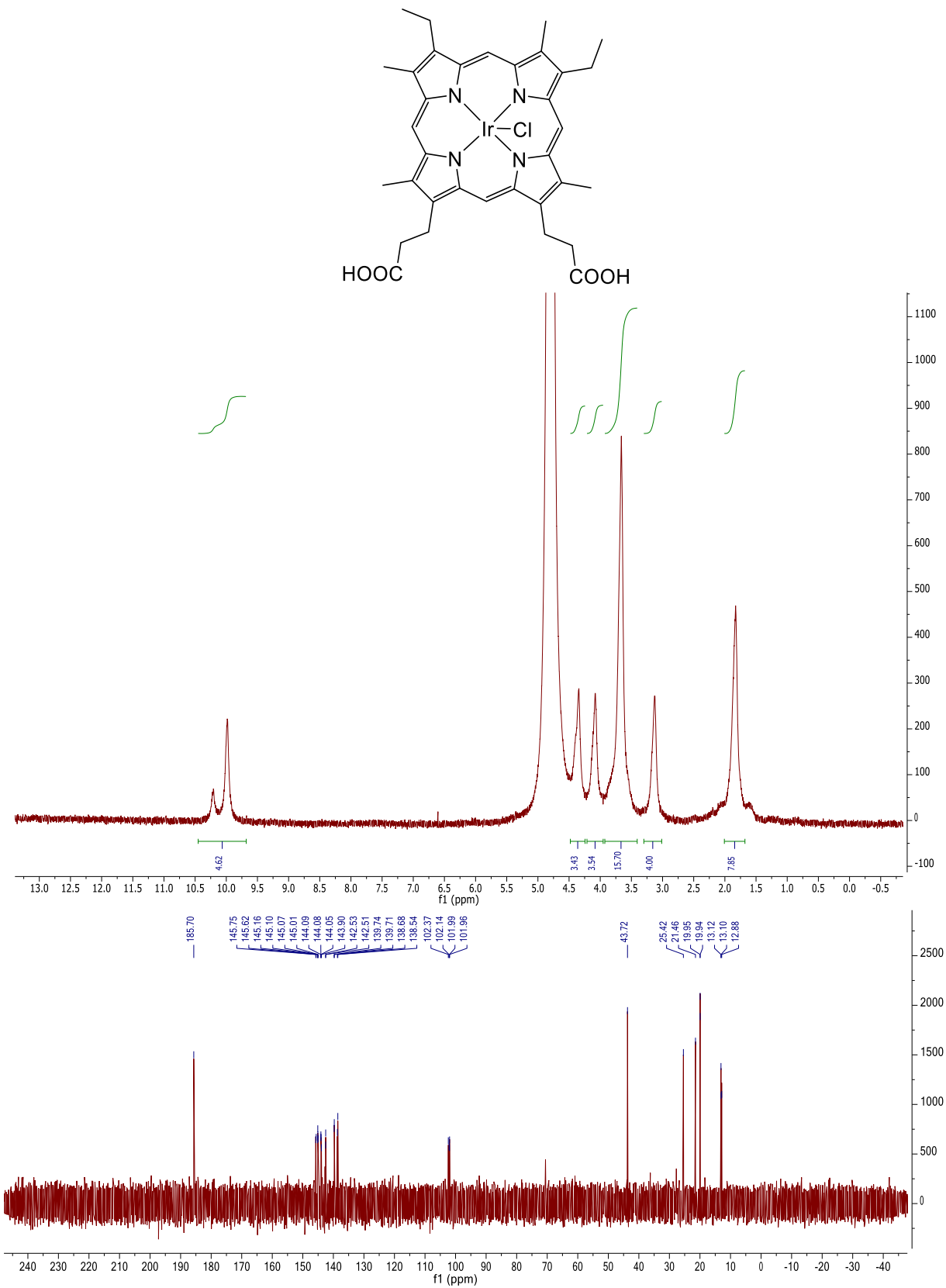


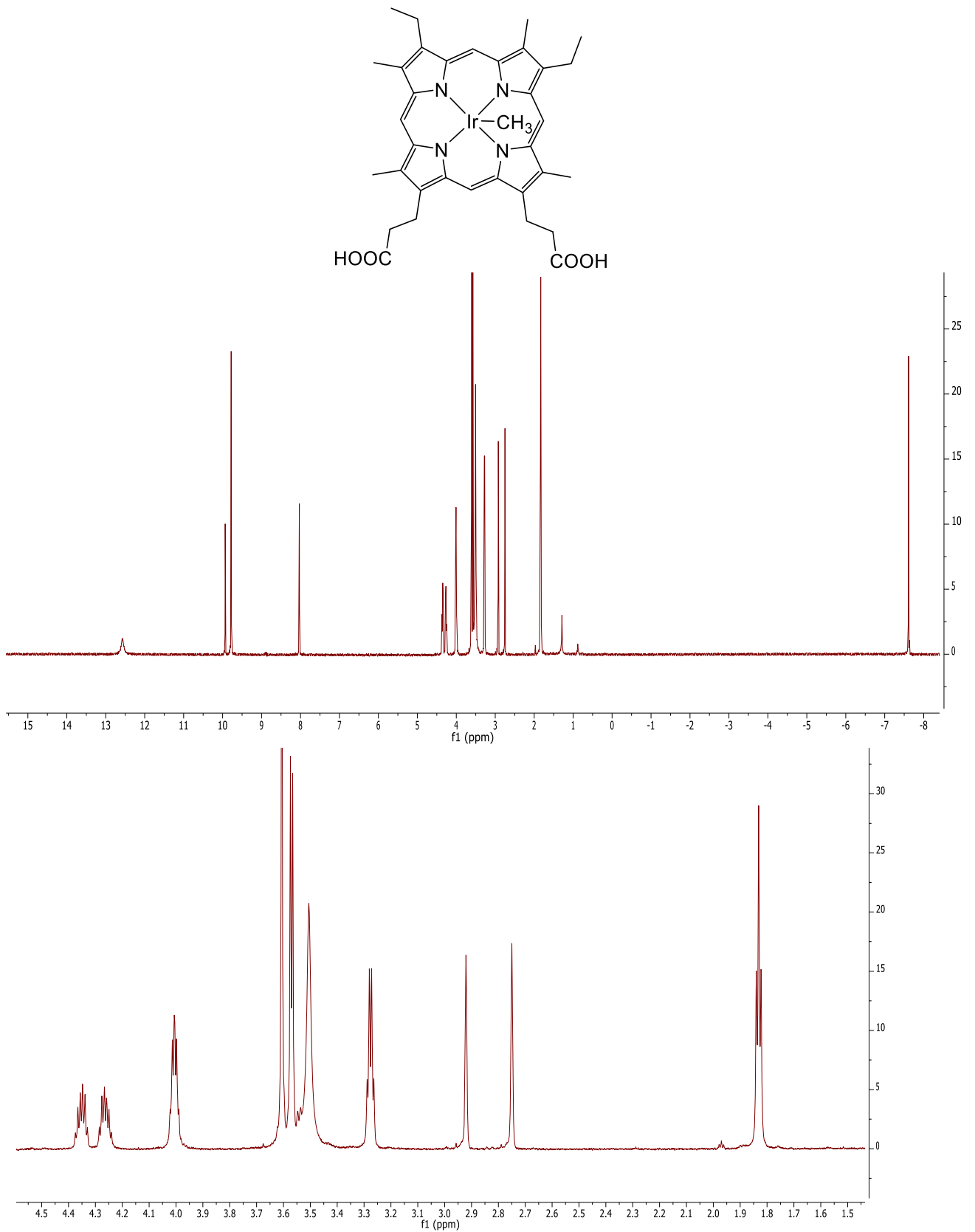


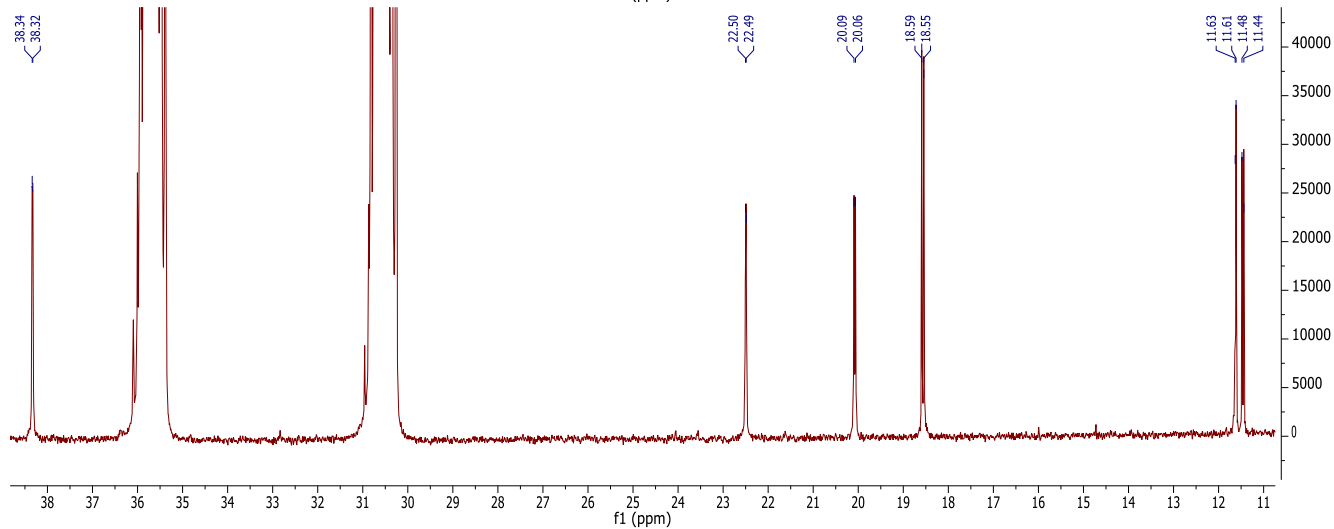
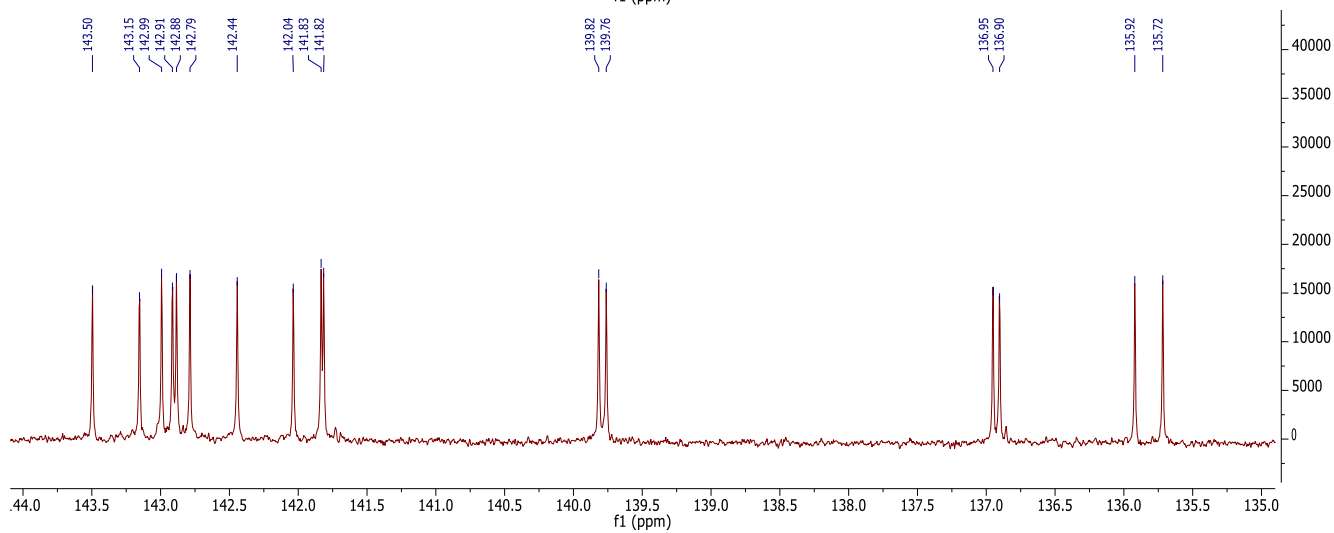
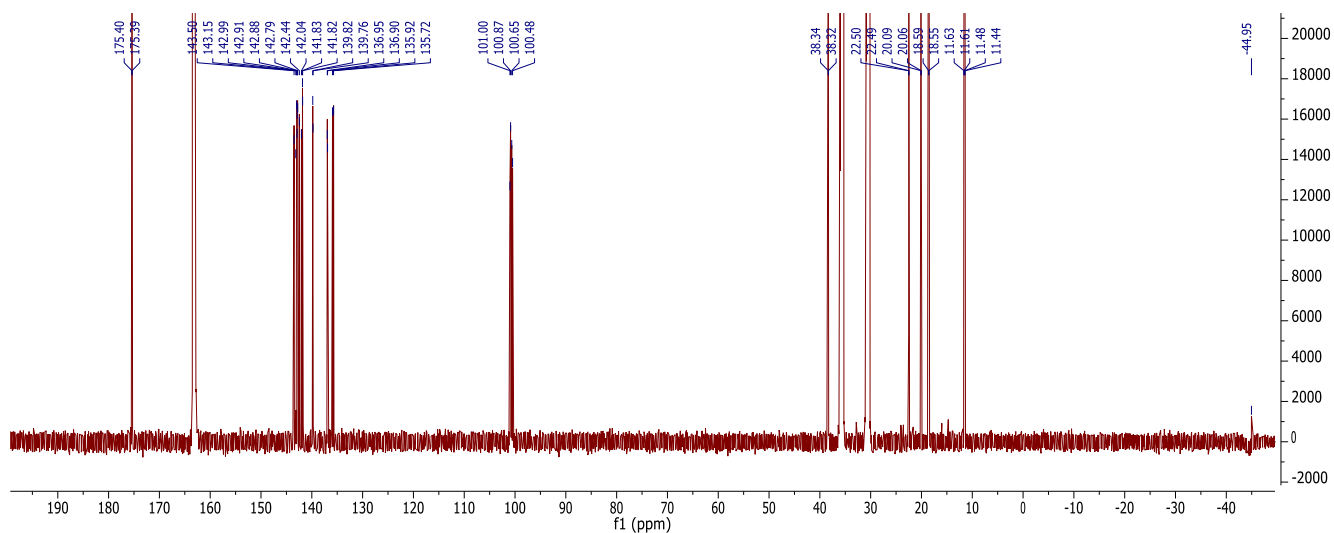












References:

1. Bordeaux, M., Tyagi, V. & Fasan, R. Highly diastereoselective and enantioselective olefin cyclopropanation using engineered myoglobin-based catalysts. *Angew. Chem. Int. Ed.* **54**, 1744–1748 (2015).
2. Fulmer, G. R. *et al.* NMR Chemical Shifts of Trace Impurities: Common Laboratory Solvents, Organics, and Gases in Deuterated Solvents Relevant to the Organometallic Chemist. *Organometallics* **29**, 2176–2179 (2010).
3. Davies, H.M.L., Mônica, V. A., Grazini, A., & Aouad, E. Asymmetric Intramolecular C–H Insertions of Aryldiazoacetates. *Org. Lett.* **3**, 1475–1477 (2001).
4. Nicolle, S. M. & Moody, C. J. Potassium N-Iodo p-Toluenesulfonamide (TsNIK, Iodamine-T): A New Reagent for the Oxidation of Hydrazones to Diazo Compounds. *Chem. Eur. J.* **20**, 4420–4425 (2014).
5. Bongen, P., Pietruszka, J. & Simon, R. C. Dynamic Kinetic Resolution of 2,3-Dihydrobenzo[b]furans: Chemoenzymatic Synthesis of Analgesic Agent BRL 37959. *Chem. Eur. J.* **18**, 11063–11070 (2012).
6. Kamata, K., Kimura, T. & Mizuno, N. Cyclopropanation of Olefins with Diazo Compounds Catalyzed by a Dicopper-substituted Silicotungstate $[\gamma\text{-H}_2\text{SiW}_{10}\text{O}_{36}\text{Cu}_2(\mu\text{-}1,1\text{-N}_3)_2]^{4-}$. *Chem. Lett.* **39**, 702–703 (2010).
7. Bonaccorsi, C. & Mezzetti, A. Optimization or Breakthrough? The First Highly cis- and Enantioselective Asymmetric Cyclopropanation of 1-Octene by ‘Electronic and Counterion’ Tuning of $[\text{RuCl}(\text{PNNP})]^+$ Catalysts. *Organometallics* **24**, 4953–4960 (2005).
8. Coelho, P. S., Brustad, E. M., Kannan, A. & Arnold, F. H. Olefin cyclopropanation via carbene transfer catalyzed by engineered cytochrome P450 enzymes. *Science* **339**, 307–310 (2013).
9. Barrick, D. Replacement of the Proximal Ligand of Sperm Whale Myoglobin with Free Imidazole in the Mutant His93Gly. *Biochemistry* **33**, 6546–6554 (1994).